ROLE OF GABA/GLYCINE DEPOLARIZATION AND HYPERPOLARIZATION IN NEONATAL CIRCUIT DEVELOPMENT

by

Hanmi Lee

BS, Kunkuk University, 1995

MS, Gwangju Institute of Science and Technology, 2000

Submitted to the Graduate Faculty of

School of Medicine in partial fulfillment

of the requirements for the degree of

Doctor of Philosophy

University of Pittsburgh

2007

UNIVERSITY OF PITTSBURGH

SCHOOL OF MEDICINE

This dissertation was presented

by

Hanmi Lee

It was defended on

May 7, 2007

and approved by

Committee Chair: Elias Aizenman, Ph. D.

Guo-Qiang Bi, Ph.D.

H. Richard Koerber, Ph.D.

Nathaniel N. Urban, Ph.D.

Eric Delpire, Ph.D.

Thesis Advisor: Karl Kandler, Ph.D

ROLE OF GABA/GLYCINE DEPOLARIZATION AND HYPERPOLARIZATION IN NEONATAL CIRCUIT DEVELOPMENT

Hanmi Lee, Ph.D.

University of Pittsburgh, 2007

During development, GABA/glycinergic responses switch from depolarizing to hyperpolarizing due to the gradual decrease in chloride equilibrium potential (E_{Cl}) to a more negative value than the resting membrane potential. Depolarizing GABA/glycinergic responses and the developmental switch to hyperpolarization are believed to play a key role in neuronal circuit development, yet a clear demonstration of how and to what degree they are important has not been investigated.

In my dissertation studies, I investigated the functional significance of the developmental switch to hyperpolarizing GABA/glycinergic responses in circuit development. To this end, I compared synaptic strength in a brain slice preparation containing the intact topographic pathway of GABA/glycinergic projections from the Medial Nucleus of Trapezoid Body (MNTB) to the lateral superior olive (LSO) between wild type (WT) and KCC2-knockdown (KD) mice. In KCC2-KD mice, the developmental switch to GABA/glycinergic hyperpolarization was prevented due to reduced expression of the potassium chloride co-transporter 2 (KCC2) (KCC2-KD mice).

I found that the GABA/glycinergic MNTB to LSO synapses in KCC2-KD mice undergo normal refinement through strengthening and elimination during development. Furthermore, the glutamatergic cochlear nucleus (CN) inputs to LSO neurons maintained their normal strength even when depolarizing MNTB synaptic inputs were strengthened, resulting in an abnormally high amount of depolarization. Based on these results, I concluded that the hyperpolarizing switch of GABA/glycinergic responses is not a necessary condition for the refinement of inhibitory synapses during development. Furthermore, homeostatic regulation of excitability in

LSO neurons seemed to be impaired, due to the normal strengthening of depolarizing MNTB synapses together with the unaltered CN synaptic strength in KCC2-KD mice. In addition, my results suggest that GABA/glycinergic synapses can regulate their synaptic strength independently of E_{Cl}, emphasizing the importance of chloride homeostasis when investigating the strength of inhibition.

However, the strength of the CN inputs to the MNTB, the calyx of Held, was reduced in MNTB neurons in KCC2-KD mice at hearing onset, suggesting that the developmental switch to hyperpolarizing GABA/glycine responses is necessary to maintain the normal strength of the calyx of Held synapse. I discuss possible mechanisms of the reduced strength of calyx of Held synapses in the absence of hyperpolarizing GABA/glycinergic responses.

Finally, in immature cortical neuronal cells *in vitro,* I demonstrated that KCC2 overexpression is sufficient to terminate the GABAergic excitatory period earlier than normal development. Based on these results, I generated KCC2OVER mice in which KCC2 can be overexpressed in a temporally regulated, neuronal-specific manner (Appendix) *in vivo*. Overexpression of KCC2 both *in vitro* and *in vivo* will help us to understand the role of excitatory (or depolarizing) GABA and glycine responses in neuronal circuit development.

TABLE OF CONTENTS

LIST OF FIGURES

1.0 GENERAL INTRODUCTION

1.1 GABA AND GLYCINE ARE EXCITATORY NEUROTRANSMITTERS DURING EARLY DEVELOPMENT.

GABA and glycine are the major fast inhibitory neurotransmitters in the adult brain, activating ligand-gated anion channels that lead to membrane hyperpolarization in mature neurons (Bormann et al., 1987). Activation of GABA and glycine receptors inhibits action potential firing by suppressing glutamate-mediated membrane depolarization and exerting shunting inhibition by increasing conductance. However, during early development, GABA also is thought to play a role in establishing neural circuitry, one that is very different from its role as an inhibitory neurotransmitter in the mature brain. For example, in the embryonic spinal cord, GABA application *in- vivo* causes dendritic growth in superior cervical ganglia (SCG) neurons in rat (Wolff et al., 1978). In the presence of GABA, ectopically implanted hypoglossal nerves innervate the SCG neurons, implying GABA could promote synaptogenesis (Dames et al., 1985). These effects seem to be mediated through GABAergic activity because application of a $GABA_A$ receptor antagonist abolishes neurites formation or synaptogenesis.

GABA as a trophic factor also has a role at the early stages of neurogenesis. GABA reduces the number of neurons which synthesize DNA indicated by BrdU incorporation within the ventricular zone (VZ) in rat embryonic neocortex, suggesting that GABAergic depolarization is important to stimulate proliferating neurons to differente in the developing VZ (LoTurco et al., 1995). GABA also affects neural migration as a chemoattractant molecule in cortical organotypic cultures. Treatment with picrotoxin, an antagonist for both $GABA_A$ and $GABA_C$ receptors, prevents neural migration. In contrast, bicuculline, a $GABA_A$ specific antagonist, promotes

migration, resulting in a thicker cortical plate. The pharmacological investigation of GABA's role in neuronal migration using picrotoxin and bicuculline suggests that GABA might arrest neural migration specifically through a $GABA_A$ receptor mediated process during development. In addition, saclofen, a $GABA_B$ receptor specific antagonist, has only a mild effect on migration compared to picrotoxin. Thus, the pro-migratory effect by GABA seems to be mediated specifically through the $GABA_C$ receptor (Behar et al., 2000).

The trophic effects of GABA are not limited to proliferating neurons. In differentiated neurons, GABA also exerts an effect on neuronal morphology. For example, two week treatment of the $GABA_A$ specific agonist muscimol increases the size of GABAergic interneurons in hippocampal cultures dissociated at E17 (Marty et al., 1996). Also, treatment with bicuculline, a $GABA_A$ receptor antagonist, prevents the neurites outgrowth induced by muscimol, raising the possibility that $GABA_A$ receptor activity is necessary for neural outgrowth (Marty et al., 1996).

As revealed in the previous studies, GABA as a trophic effector could not be explained by its conventional role of an inhibitory neurotransmitter. It suggests that GABA responses must not be restricted to bring chloride influx, when GABA exerts trophic effects. Rather, GABA responses should connect GABA to second messenger systems to trigger cellular mechanisms involved in cell cycles, neurites outgrowth, and migration etc.

During the period in which GABA influences neural circuit development through its trophic effects on cell cycle, migration, and neurites outgrowth, GABA (as well as glycine) is excitatory, causing action potential firing or depolarizing membrane potential changes. During this developmental period, GABAergic response is depolarizing (and also excitatory) because intracellular chloride concentration ($[Cl^-]_i$) is maintained high, which results in the equilibrium potential for chloride ion (E_{Cl}) depolarizing considerably than the resting membrane potential (V_{rest}). Depolarization by GABA and glycine is linked to the activation of voltage-gated calcium channels, calcium influx, and increases in intracellular calcium concentration ($[Ca^{2+}]_i$) (Yuste and Katz, 1991; LoTurco et al., 1995). At this developmental stage, intracellular $[Ca^{2+}]_i$ fluxes modulate numerous calcium-dependent processes such as proliferation, differentiation, migration, dendrite formation, axon arborization, and refinement through plasticity (Represa and

Ben-Ari, 2005; Kriegstein and Owens, 2001; Kandler and Gillespie, 2005). Thus, the effects of GABA in shaping developing neural circuits, before its traditional role as an inhibitory neurotransmitter, might be caused by increment of $[Ca^{2+}]_i$ through voltage-gated calcium channels activated by GABAergic membrane depolarization. GABAergic depolarization also interplay with NMDA receptors by reducing voltage dependent Mg^{2+} block of NMDA receptors and potentiating $[Ca^{2+}]_i$ increase through NMDA receptor, which is important for the generation of Giant Depolarizing Potential (GDP) and associated with spontaneous and synchronous $[Ca^{2+}]_i$ increase in pyramidal neurons in hippocampus (Leinekugel et al., 1997).

Consistent with the above hypothesis, GABAergic effects on neural outgrowth seem to be mediated by voltage-gated calcium channels since neuronal outgrowth can be also blocked by nitrendipine, an L-type calcium channel blocker (Maric et al., 2001). Furthermore, furosemide, a known chloride co-transporter blocker, prevents neurites outgrowth as well, indicating that intracellular chloride concentration ($[Cl^-]_i$) might be involved in GABA's trophic effects (Maric et al., 2001). GABAergic effects on neuronal migration seem to involve calcium increment as well, since migrating neurons from the ventricular zone (VZ) express $GABA_A$ receptors, the activation of which is known to increase $[Ca^{2+}]_i$, and GABA-induced migration is blocked by the calcium chelating molecule, bis(2-aminophenoxy)ethane-N,N,N',N'-tetra-acetic acid (BAPTA) (Behar et al., 1996).

Despite a large body of evidence implicating the role of GABA in many important developmental processes, most likely through its capability to activate voltage gated calcium channels (Fiszman and Schousboe, 2004), a direct demonstration of the importance of GABA/glycine-mediated increases in $[Ca^{2+}]_i$ during specific developmental stages has not been made, let alone a detailed mechanism tested. This task has been historically challenging because of the lack of an available method with which to specifically modify GABA/glycinergic membrane polarizations and subsequent changes in $[Ca^{2+}]_i$.

1.2 POTASSIUM CHLORIDE CO-TRANSPORTER 2 (KCC2) REGULATES THE RESPONSE POLARITY OF GABA AND GLYCINE RESPONSE.

Whether their actions are excitatory or inhibitory, GABA and glycine both activate the same chloride permeable ionotropic receptors. How can the activation of these receptors cause an excitatory response during a transient developmental period, while activation of the same receptor by the same transmitter causes a hyperpolarizing response during later development?

The developmental regulation of intracellular chloride concentration ($[Cl^-]_i$) and the related equilibrium potential for chloride ion (E_{Cl}) is critical to determine the response polarity of GABA and glycine. $[Cl^-]_i$ is tightly regulated through the interplay of inward and outward chloride channels such as voltage dependent chloride channels (ClCs) and chloride co-transporters (CCCs). ClCs are important in stabilizing the membrane potential by bringing E_{Cl} near or below the resting membrane potential due to their large chloride conductance and lack of inactivation (Staley, 1994). Although it has been demonstrated that the increased ClC activity such as overexpression of ClC-2 can help bring E_{Cl} close to the resting membrane potential by quickly reacting to membrane voltage changes and preventing GABA-induced action potential firing (Staley et al., 1996), it is not sufficient to switch GABA responses to hyperpolarizing, because ClC activates at membrane potential negative to E_{Cl}, thus resulting Cl^- efflux, not influx (Staley, 1994). Because activation of ClC-2 requires membrane hyperpolarization than E_{Cl} (Staley et al., 1996), it is unlikely that activity of ClC would regulate the developmental polarity of GABA/glycinergic response.

On the other hand, CCCs use the ionic driving force created by the Na^+/K^+-ATPase and do not cause net ionic movement across the membrane; Because their activity is not regulated by resting membrane potential, function of CCC is well suited to keep chloride concentration away from the resting membrane potential (Payen et al., 2003). There are several molecules categorized as CCCs; Na^+–Cl^- co-transporters (NCCs), which use the Na+ concentration gradient to accumulate chloride, Na^+–K^+–$2Cl^-$ co-transporters (NKCCs), which utilize both the Na+ and K+ concentration gradient, also resulting in chloride accumulation, and the K^+–Cl^- co-

transporters (KCCs), which use the K^+ concentration gradient to pump chloride out across the membrane, thus lowering $[Cl^-]_i$. So far, one NCC, two KCCs and four KCCs have been discovered. Most of them are expressed in the central nervous system in neuronal and/or non-neuronal cells, except NCC and NKCC2, which are expressed in the kidney (Payne et al., 2003).

Among these transporters, KCC2 has gained intense interest from the neuroscience community due to its wide distribution within the central nervous system (Li et al., 2002; Vu et. al., 2000; DeFazio et al., 2000) and the fact that its gradual increase in expression level correlates with the GABA/glycinergic hyperpolarization switch (Clayton et al., 1998; Lu et al., 1999) as well as E_{Cl} (Payne 1997; DeFazio et al., 2000). In matured neurons where KCC2 expression is high, extracellular K^+ concentration regulates chloride concentration in both inward and outward direction, which is blocked by furosemide (DeFazio et al., 2000). Also, KCC2 is unique in that its expression is restricted to neuronal cells only, most likely because the promoter region of KCC2 contains a neuronal-restrictive silencing element (NRSE) that constitutes the binding site for a neuron-restrictive silencer factor (NRSF). NRSF proteins inhibit transcription of genes containing NRSE sites, resulting in neuron specific expression in the central nervous system (Karadsheh and Delpire, 2001).

The importance of KCC2 in the normal functioning of the nervous system has been shown in many diseases-related studies. In temporal lobe epilepsy patients, up-regulation of NKCC1 mRNA and down-regulation of KCC2 mRNA within the hippocampal subiculum are accompanied by GABAergic depolarization (Palma et al., 2006). Similarly, in the dentate gyrus of the hippocampus in traumatic brain injury, reduced KCC2 mRNA causes a depolarizing GABAergic reversal potential and reduces inhibitory efficiency (Bonislawski et al., 2007). After axotomy or nerve injury in rats, muscimol elicits an increase in intracellular calcium concentration in dorsal motor neurons of the vagus (DMV neurons), accompanied by a depolarizing equilibrium potential for GABA and down-regulation of KCC2 mRNA (Nabekura et al., 2002; Toyoda et al., 2003). Following peripheral nerve injury, neurons of lamina I of the superficial dorsal horn in the spinal cord shows a reduction in KCC2 activity and a corresponding disruption of anion homeostasis, resulting in up-regulation of the net excitability

of lamina I neurons due to the loss of inhibition (disinhibition), which is believed to be an important mechanism underlying chronic pain syndromes (Coull et al., 2003).

In addition to the correlations between KCC2 expression level (mRNA or protein) and GABAergic response polarity in disease- or injury-related conditions, direct evidence of the role of KCC2 in regulating GABA/glycine response polarity has been demonstrated using anti-sense silencing of KCC2 mRNA. With the transcription of KCC2 being knocked-down using anti-sense mRNA against KCC2, intracellular chloride concentration elevates, causing GABAergic membrane depolarization in three week old hippocampal neurons, where GABA is normally hyperpolarizing (Rivera et al., 1999). This pioneering research suggests a method by which the polarity of GABA/glycinergic responses could be modified in a manner opposite to normal development. Complete genomic knockout of KCC2 in mice (KCC2-KO mice) results in lethality at birth because of motor deficits, and abnormal network firing in the spinal cord and brainstem (Hubner et al., 2001). However, gramicidin perforated patch clamp recording from motor neurons in the spinal cord demonstrates that GABA is excitatory compared to the responses of wild type neurons from animals of the same age. As suggested by the KOs lethality at birth, KCC2 is critical for survival through its regulation of the GABA/glycinergic hyperpolarizing switch during development. When the expression of KCC2 is knocked down to only 5% of normal (KCC2-KD mice), GABA and glycine responses remain excitatory that is demonstrated in cortex and auditory brainstem, yet animals can survive up to P15~16 (Balakrishnan et al., 2003; Zhu et al., 2004). However, due to the disruption of the normal maturation of inhibition, animals exhibit severe seizures, probably resulting in death (Woo et al., 2002).

Although there have been many studies proving the important role of KCC2 in the normal functioning of neural circuits, little investigation reveals how neural circuits might be affected by the increased excitability caused by prolonging the GABA/glycinergic depolarizing period *in-vivo.* Also, even though there have been a few efforts made to reveal the importance of GABAergic depolarization during circuit development by abolishing the normal period of GABA/glycinerigc depolarization during early development (Chudotvorova et al., 2005; Ge et al., 2006; Akerman and Cline, 2006; Cancedda et al., 2007), still there is a considerable lack of

information about how circuits (such as inhibitory or excitatory) are affected in their wring under the absence of depolarizing response by GABA/glycine *in-vivo*. This deficiency might be attributable to the lack of a model system with which to elucidate the role of GABA/glycinergic response polarity changes in the brain. For example, in cortex or hippocampus, inhibitory circuits are extremely complicated due to the extreme diversity of inhibitory neurons, and the even more diverse forms of synaptic connections between inhibitory neurons and different types of postsynaptic neurons (Somogyi and Klausberger, 2005). In such a complex system, investigating the effects of reversing the normal response polarity of GABA/glycine on circuit development (maturation) can be complicating to prohibit proper interpretation of experimental result.

1.3 AUDITORY BRAINSTEM CIRCUIT DEVELOPMENT DURING DEVELOPMENT

In auditory system, sound information received in the cochlea is transmitted to the cochlear nucleus (CN), the first nuclei within the auditory brainstem. CN, in turn, sends excitatory synapses to the ipsilateral lateral superior olive (LSO) and the contralateral medial nucleus of trapezoid body (MNTB). The excitatory glutamatergic synapses in the MNTB from CN, which is called as the calyx of Held (details in Chapter III), is converted to inhibitory synapses, which in turn, transferred to the LSO neurons (Fig 1.1, Kandler and Friauf, 1995).

Thus, the lateral superior olive (LSO) receives inhibitory synaptic input from the contralateral medial nucleus of trapezoid body (MNTB) and excitatory synaptic input from the ipsilateral cochlear nucleus (CN) (Kandler an Friauf, 1995). By combining these two synaptic inputs from both ears, neurons in the LSO encode interaural intensity differences, an important cue for sound localization azimuthally. Inhibitory synaptic input from the MNTB is purely glycinergic in the adult, but has also been shown to contain a GABAergic component as well during early development in gerbil (Kotak et al., 1998), rat, and mice (Kullmann et al., 2002). Glycinergic MNTB synaptic inputs are topographically organized such that high frequency neurons in the MNTB make synaptic connections with high frequency neurons in the LSO, while

low frequency neurons in the MNTB project to low frequency neurons in the LSO (Sanes and Friauf, 2000).

Morphological and functional studies have revealed the MNTB-LSO pathway undergoes synaptic rearrangement during development. Axonal arbors from single MNTB neurons mature over a period from P12~13 to 3~4 weeks old, during which time the axonal arborization area along the tonotopic axis is significantly reduced in gerbil (Sanes and Siverls, 1991). Also in rat LSO, dendritic structures become less complex between P3 to P36; the number of dendritic end points decreases considerably, the number of appendages on dendrites (slender 2~5 μm short structures) also decreases, and the dendritic arbor area along the tonotopic axis becomes sharper when normalized to the size of LSO. The number of primary dendrites also decreases significantly, with mostly thin dendrites being eliminated by P10 (Rietzel and Friauf, 1998). These two previous studies suggest that auditory-driven activity plays an important role in the refinement of inhibitory synapses in the developing auditory system. Consistent with the importance of hearing activity, when this activity being removed by cochlear ablation, the spread of axonal boutons along the frequency axis of the LSO increases, with an accompanying increase in the number of branch points (Sanes and Takacs, 1993).

Even though morphological studies suggest that structural refinement occurs after auditory-driven activity starts, over a period from P12~P13 to P20~P30, it has also been shown that functional refinement of MNTB-LSO synapses occurs before hearing onset and morphological elimination. Using focal photolysis of caged glutamate, It has been demonstrated that the area of MNTB which synaptically activates a single LSO neuron decreases before hearing on-set, suggesting an elimination of presynaptic MNTB partners. During the same developmental period, the remaining synaptic inputs are strengthened, as revealed by an increase in the amplitude of synaptic response to minimal stimulation (Kim and Kandler, 2003). This research suggests that inhibitory MNTB synapses into the LSO area are refined through synapse weakening and strengthened in response to spontaneous activity before hearing on-set. However, LTP or LTD of MNTB-LSO synapses during the relevant time period, or any alternative mechanisms for the observed functional refinement, have yet to be demonstrated in neither mice nor rat.

There have been many investigations regarding inhibitory synaptic plasticity throughout the central nervous system, including neocortex, hippocampus, cerebellum, and the auditory system. Depending on developmental stage and brain area, high or low frequency stimulation could induce LTP or LTD (Review in Gaiarsa et al., 2002). High frequency stimulation in the presence of CNQX (AMPA receptor antagonist) and/or APV (NMDA receptor antagonist) elicits LTP in inhibitory synapses in pyramidal neurons in rat visual cortex at P20~P30 (Komatsu and Iwakiri, 1993), in rat hippocampal CA3 pyramidal neurons at P2~P4 (McLean et al., 1996), and in rat nucleus of the solitary tract at P17~36 (Glaum and Brooks, 1996). In rat deep cerebellar nuclei at P7~P9, high frequency stimulation of white matter elicits LTP of IPSCs in a NMDA receptor dependent manner (Ouardouz and Sastry, 2000). For the induction of LTP and/or LTD in inhibitory synapses, an increase in intracellular calcium concentration is important since calcium chelators such as EGTA or BAPTA occluds LTP and LTD. The calcium influx required for long term synaptic plasticity could come from an external source through NMDA receptors or voltage-dependent calcium channels, or an internal source such as Ins(1,4,5)P_3-Ca^{2+} stores. Among these conditions, the activation of voltage-gated calcium channels in the presence of APV and CNQX suggests that inhibitory synaptic input caused significant membrane depolarization to open voltage-gated calcium channels. However, direct demonstration of how, and to what degree, depolarizing GABA/glycinergic responses are necessary for inhibitory synaptic plasticity has not been made during a perinatal developmental period.

Also in the auditory MNTB-LSO synapses, the involvement of glycinergic transmission in inhibitory synaptic refinement has been suggested as well. When glycinergic responses is blocked by continuous strychnine, glycine receptor antagonist, application from a surgically implanted pellet, LSO dendrites examined at P21 exhibits larger arbors spread along a greater area of the frequency axis and a greater number of branching points (Sanes and Chokshi, 1992). Denervation of MNTB synaptic inputs by contralateral cochlear ablation has a similar effect (Sanes et al., 1992). Also, in organotypic cultures, addition of strychnine to the culture media also causes an increase in dendritic branching and total dendritic length (Sanes and Hafidi, 1996), similar to the observations made *in-vivo*, suggesting that glycinergic transmission is important for refinement in the LSO. As shown in other brain areas, the developmental switch in

the polarity of GABA/glycinergic responses has also been demonstrated in the auditory system of rat and mice. During the first postnatal week, MNTB stimulation causes action potentials and membrane depolarization in LSO neurons (Kandler and Friauf, 1995; Kullmann and Kandler, 2001), as well as an increase in intracellular calcium concentration through voltage gated calcium channels (Kullmann et al., 2002). During the second postnatal week, MNTB responses have switched to hyperpolarizing. Considering this developmental switches of MNTB-LSO synaptic responses and the equilibrium potential changes by contralateral cochlear ablation (Kotak and Sanes, 1996), the previous studies regarding the role of glycinergic response on the inhibitory MNTB to LSO maturation had not investigated adequately development of inhibitory synapses.

Considering the many difficulties in understanding mechanisms of inhibitory synaptic maturation and the lack of methods to actively regulate GABA/glycinergic responses, MNTB-LSO synapses in KCC2 activity modified environment (Rivera et al., 1999; Hubner et al., 2001; Woo et al., 2002) would provide a unique opportunity with which to elucidate how inhibitory neural circuits mature *in-vivo* in the absence of the GABA/glycinergic switch to hyperpolarization and their interplay with other synapses such as glutamatergic synaptic input from the CN, because 1) MNTB neurons are homogenous and project topographically to the LSO. Thus there is no need to consider the additional complexity of various interneuron and synaptic subtypes 2) KCC2 activity directly regulates E_{Cl} and thus its manipulation can be used to reverse the normal polarity of GABA/glycinergic responses during specific developmental stages.

In the following Chapters II and III, I investigate how MNTB-LSO synapses undergo synaptic maturation in the absence of the GABA/glycinergic switch to hyperpolarization using KCC2-KD mice. Since the LSO also receives topographic glutamatergic inputs from the CN, I further examine the interplay of GABA/glycinergic synapses with glutamatergic synapses under conditions of an imbalance in excitation-inhibition caused by the disturbed polarity of GABA/glycinergic responses.

Since knocking-out KCC2 in the adult results in GABAergic excitatory responses that mimicked those of an immature state, in Chapter IV, I address whether mature GABA /glycinergic hyperpolarizing responses could also be induced earlier than they would normally occur by overexpressing KCC2. This research allows us to address the role of the excitatory developmental GABA/glycinergic response by creating the environment which is lack of excitatory GABA/glycinergic response (or stronger GABA/glycinergic inhibition) under which neural circuit develops *in- vivo* (Appendix).

2.0 SYNAPTIC INPUT DEVELOPMENT INTO A LSO NEURON OF KCC2-KD MICE

2.1 INTRODUCTION

Excitatory neural circuits are refined through the elimination of exuberant synapses and the strengthening of remaining ones. During development, the refinement of neural circuits is critical in order for a system to mature into its adult-like form (Lichtman and Colman, 2000; Katz and Shatz, 1996; Aamodt and Constantine-Paton, 1999). Numerous studies have revealed rules and mechanisms for the synchronized strengthening and elimination of excitatory synapses, such as competition (Balice Gordon and Lichtman, 1994; Colman et al, 1997), AMPA receptor insertion (Takahashi et al., 2003), NMDA receptor-mediated increase of intracellular calcium concentration (Simon et al., 1992; Scheetz and Constantine-Paton, 1994), and the maturation of glutamatergic synapses by PSD-95 overexpression (El-Husseini et al., 2000; Ehrlich and Malinow, 2004). In many systems, refinement is influenced by spontaneous or experience-driven activity (Chen and Regehr, 2000; Goodman and Shatz, 1993; Stellwagen and Shatz, 2002). Recently, there have been efforts to address the importance of the maturation of inhibitory systems during development. However, the detailed mechanisms underlying these processes remain unknown.

The maturation of inhibitory responses is critical for a system to perform its physiological function. For example, GAD-65 (GABA synthesizing enzyme, glutamic acid decarboxylase isoform-65kDa) knock-out mice have reduced GABA release and impaired visual acuity (Hensch et al., 1998). Accelerated maturation of inhibition by BDNF overexpression is accompanied by premature termination of the critical period in the visual system (Hanover et al.,

1999; Huang et. al., 1999). Also, inhibitory response maturation during development is paralleled by the maturation of visual responses (Komatsu and Iwakiri, 1991). Recently, growing evidence has shown that, indeed, inhibitory synapses display activity-dependent synaptic changes, as shown by LTP/LTD in hippocampus (McLean et. al., 1996) and rat deep cerebellar nuclei (Morishita and Sastry, 1996; Ouardouz and Sastry, 2000) and LTP in rat neocortex (Komatsu and Iwakiri, 1991 and 1993), suggesting that inhibitory circuits might also be refined through synaptic elimination and strengthening (Gaiarsa et al., 2002).

A large number of investigations have tried to show that inhibitory synapses might be clustered and stabilized through post-synaptic density (PSD) molecules similar to those found in excitatory synapses, such as PSD-95 (El-Husseini et al., 2000; Craven and Bredt, 1998). Post synaptic $GABA_A$ receptors or glycine receptors are clustered through interactions with intracellular proteins such as GABARAP (GABA-associated proteins interacting with GABAA receptor $\gamma 2$ subunit and gephyrin), Plic1 (a ubiquitin-like protein binding to α and β subunits) (Bedford et al., 2001), and gephyrin, which has been demonstrated to play an important role in the clustering of $GABA_A$ (Essrich et al., 1998) as well as glycine receptors in anti-sense and gene knock-out studies (Kneussel et a., 1999; Kirsch et. al., 1993; Levi et al., 1999).Consistent with the hypothesis of LTP and LTD-like mechanisms of activity dependent synaptic plasticity of inhibitory synapses, gephyrin positive puncta move constantly into and away from synaptic sites (Maas et al., 2006) and glycine receptor activity is important for receptor clustering, since strychnine prevents receptor clustering in spinal cord (Kirsch and Betz, 1998; Levi et al., 1999) and causes retrograde gephyrin transport in cultured hippocampal neurons (Maas et al., 2006).

However, the mechanisms and extent of inhibitory synaptic refinement are not understood completely and remain controversial (Kneussel and Betz, 2000; Kneussell and Loebrich, 2007). Furthermore, whether stronger and weaker inhibitory fibers compete, and the possible mechanisms underlying the competition, have yet to be addressed at all.

Investigating the mechanisms of inhibitory system maturation requires experimental manipulation in a synapse-specific manner such as inhibitory projects to excitatory neurons or inhibitory projects to inhibitory neurons. However, the diversity of inhibitory systems (types of

inhibitory neurons, the expression pattern of calcium binding proteins, post synaptic target neurons and the subcellular location of synapses on postsynaptic neurons, etc.) has been an obstacle preventing researchers from exploring this issue in a synapse-specific manner and complicating the interpretation of experimental data (Markram et al., 2004; Somogyi and Klausberger, 2005).

It is also important to consider how excitatory and inhibitory synapses interact during development. Interactions between the strength of excitation and inhibition in response to altered neuronal activity have been described by homeostatic mechanisms that regulate neural excitability (Turrigiano and Nelson, 2004). Deprivation of sensory-driven activity causes an increase of excitatory synaptic responses, while concurrently reducing inhibition as shown in visual cortex (Desai et al., 2002; Morales et al., 2002). In the auditory inferior colliculus, cochlear ablation also caused increased EPSCs amplitude and reduced IPSC amplitude. (Vale and Sanes, 2002). Since, the balance between excitation and inhibition is critical for a system to function normally (Dani et al., 2005; Chih et. al., 2005), it is essential to investigate the modulation of inhibitory synapses along with excitatory synapses after disturbed activity in order to have a complete understanding of alterations in the normal circuit wiring caused by a change in activity. This is especially important during perinatal development when, in addition to any refinement of inhibitory synapses by changes in release of GABA or in GABA receptors, there is also an maturation of "inhibition," by changing E_{Cl} to switch synapses from depolarizing to hyperpolarizing (General Introduction I-2). Investigating inhibitory synapse refinement and maturation of "inhibition" requires a simpler model to achieve the challenging, but necessary, experimental conditions.

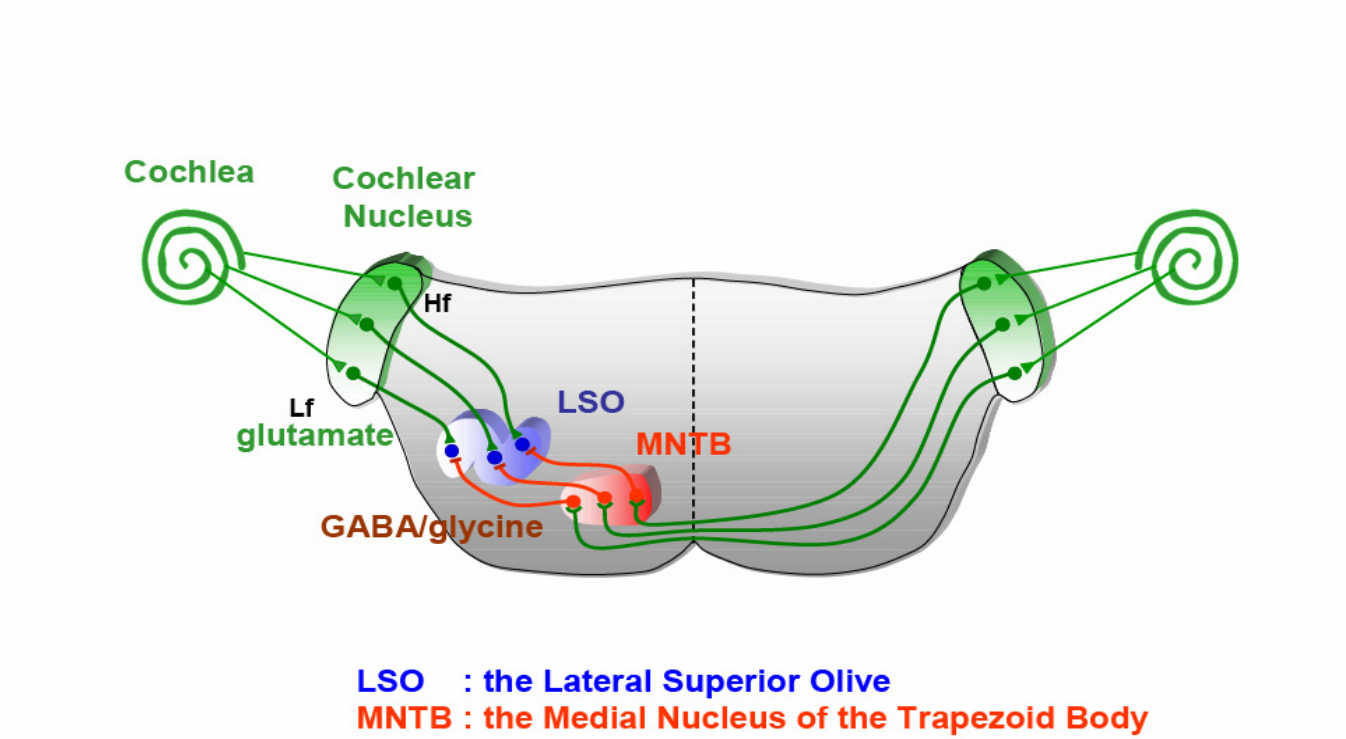

(Modified from Kandler and Gillespie, 2005)

Figure 1.1. Diagram of auditory brainstem circuit

Neurons within the Lateral Superior Olive (LSO) receive glutamatergic synaptic input from the ipsilateral cochlear nucleus (CN) and glycinergic synaptic input from the Medial Nucleus of the Trapezoid Body (MNTB) (Chapter II). The synaptic connections from MNTB to the LSO (as well as from the CN to the LSO) are topographically organized, thus neurons responding to the same sound frequency are connected between CN-LSO-MNTB pathways. During early development, MNTB releases GABA as well as glycine. In turn, MNTB neurons receive the largest and strongest glutamatergic synaptic input from the contralateral CN, called the "calyx of Held" (Chapter III). (Lf; low frequency, Hf; high frequency).

In the auditory brainstem nuclei, the lateral superior olive (LSO) combines inhibitory synaptic inputs from the contralateral medial nucleus of the trapezoid body (MNTB) and glutamatergic synaptic inputs from the ipsilateral cochlear nucleus (CN) (Kandler 2004, Sanes and Friauf, 2000; Figure 1.1). By integrating inhibition and excitation, the LSO plays a major role in sound localization (Boudreau and Tsuchitani, 1968; Tollin, 2003). Importantly, the MNTB is composed of a homogeneous population of inhibitory neurons, which release both GABA and glycine during early development, but glycine only in the adult (Kotak et al., 1998; Nabekura et al., 2004). In addition, MNTB projections to the LSO exhibit a topographic organization (reviewed in Sanes and Friauf, 2000; Kandler, 2004). In contrast to the overwhelming diversity found in the hippocampus and cortex, the simplicity of the auditory brainstem circuit provides an advantageous experimental system to study inhibitory circuit refinement, and the interaction between inhibition and excitation.

Previous studies from the MNTB-LSO system shows that synaptic changes occur in an activity dependent manner in the developing auditory system as well. When glycinergic transmission is reduced by contralateral cochlear ablation or strychnine treatment, the inhibitory synaptic response that LSO neurons receive is reduced, leading to reduced amplitude in inhibitory postsynaptic potentials (IPSP) in the LSO neurons (Kotak and Sanes, 1996). Activity dependent plasticity in the MNTB-LSO even occurs before hearing onset, as indicated by the presence of LTD induced by low frequency stimulation during the second postnatal week of gerbil (Kotak and Sanes, 2003; Chang et al., 2003). In rat, MNTB to LSO synapses are refined through synapse strengthening and functional elimination (Kim and Kandler, 2003) even before hearing. However, the direct demonstration of mechanisms responsible for MNTB-LSO synapse refinement has not been addressed.

During the period in which MNTB-LSO projections are refined (Kim and Kandler, 2003), MNTB synaptic responses switch from being excitatory (depolarizing) to being inhibitory (hyperpolarizing) because of a developmental decrease in $[Cl^-]_i$ relative to the resting membrane potential (V_{rest}), which shift an initially depolarizing GABA/glycinergic response to hyperpolarizing. During the first postnatal week, LSO neurons fire action potentials in response to MNTB activity (or applications of GABA and glycine) due to a depolarizing E_{Cl}. During the

second postnatal week, E_{Cl} is shifted to hyperpolarizing, causing an inhibitory response (Kandler and Friauf, 1995; Kullman and Kandler, 2001; Kullman et al., 2002). The correlation between a certain polarity with a certain respect of refinement leads to the hypothesis that the polarity switch of GABA/glycinergic responses is important for the refinement of MNTB-LSO synapses. Especially, data from a previous study suggests that stronger synaptic inputs from the MNTB to the LSO do not begin to appear until the second postnatal week in rat (Kim and Kandler, 2003), once the GABA/glycinergic synaptic responses in the LSO have switched to hyperpolarizing (Kandler and Friauf, 1995; Kullmann and Kandler, 2001). This correlation suggests that the hyperpolarizational switch of GABA/glycinergic responses is a critical mechanism for the strengthening of inhibitory synapses. This idea is supported by recent reports demonstrating that premature GABAergic hyperpolarization induces stronger inhibitory synapses by increasing $GABA_A$ receptor clusters and by increasing inhibitory responses measured electrophysiologically (Chudotvorova et. al, 2005; Akerman and Cline, 2006).

In LSO neurons, the transition from excitatory to inhibitory GABA/glycinergic responses during development results from a gradual reduction in the intracellular chloride concentration ($[Cl^-]_i$), which is regulated by outward chloride transporter, KCC2 during development (Balakrishnan et al., 2003). In particular, it has been demonstrated that in LSO neurons of mice, the developmental up-regulation of KCC2 activity causes a reduction in intracellular chloride concentration, resulting in GABA/glycinergic hyperpolarizing responses (Balakrishnan et al., 2003). When KCC2 expression is reduced by 95% (**KCC2-KD**) (Woo et al., 2002), the normal developmental decrease of $[Cl^-]_i$ is prevented, resulting in depolarizing GABA/glycinerigc response in both cortex and LSO until P12, when mice start hearing (Shnerson and Pujol, 1981; Kamiya et al., 2001; Ehret and Romand, 1992) and normally GABA and glycine responses are hyperpolarizing (Balakrishnan et al., 2003; Zhu et al., 2005).

To address whether the GABA/glycinergic switch to hyperpolarization is necessary for inhibitory synapse strengthening *in-vivo*, I used KCC2-KD mice in which GABA/glycinergic responses remain excitatory. Since the presynaptic MNTB area providing functional input to a single LSO neuron decreases primarily during the 1st postnatal week in rat (Kim and Kandler, 2003), I further examine elimination along with strengthening of MNTB-LSO synapses in

KCC2-KD mice. In order to address the above question, I use electrophysiological methods to measure the strength of synapses from the MNTB to the LSO activated by both minimal and maximal stimulation and compare these values between WT and KD mice. Since the LSO also receives glutamatergic synaptic input from the ipsilateral CN, I extend my research further by investigating how excitatory synaptic input from the CN might change in response to a prolonged period of depolarizing MNTB responses, especially with respect to the proposed maintenance of a homeostatic balance between opposing excitatory and inhibitory systems.

2.2 MATERIALS AND METHODS

2.2.1 Animals

Experimental procedures were performed in accordance with NIH guidelines and were approved by the IACUC at the University of Pittsburgh. KCC2-KD mice were a gift from Dr. Eric Delpire (Vanderbilt University). Wild type (WT) (C57BL/6J) and homozygote KCC2-KD mutant mice (KCC2-KD) were obtained from mating heterozygotes.

2.2.2 Slice preparation and genotyping

300 um thick coronal brain slices were made from P1 to P12 animals using a vibrating microtome as described previously (Kullmann and Kandler, 2001). Number of animals used for each experimental group was more than three except for Ca^{2+} imaging. For Ca^{2+} imaging, two animals were used. Brains were isolated by decapitation from the anaesthetized animals (isoflurane, Webster Veterinary, USA) and kept in ice cold ACSF (ACSF; composition in mM: NaCl 124, $NaHCO_3$ 26, glucose 10, KCl 5, KH_2PO_4 1.25, $MgSO_4$ 1.3, $CaCl_2$ 2, pH = 7.4, aerated with 95% O_2/5% CO_2) with Kynurenic Acid, ionotropic glutamate receptor antagonist, (1mM). Brain slices containing the LSO and MNTB were kept in an interface chamber and warmed to 32 ºC. In most cases, there was only one slice per animal. In the case when there were more than two slices prepared, the total synaptic strength was not measured since it is likely that if more than one slice was obtained from a single animal, each slice might not contain the total pathway from MNTB to LSO. The tails from each animal were kept and genotyped by PCR after electrophysiological recording. Accordingly, the researcher was blind in respect to animal genotype. Genotyping was done as described using sense primer; 5'-AGC GTG TGT CCG TGT GCG AGT G-3' and anti-sense primers for mutant; 5'-CCA GAG GCC ACT TGT GTA GCG C-3'and for wild; 5'-TTG TTG AGC ATG GTG GCT GCG C-3'. In older animals, blind

experiments were not possible due to the smaller body size and seizure behavior of KCC2-KD mice (Woo et al., 2002).

2.2.3 Electrophysiology

Synaptic responses were obtained with whole-cell voltage clamp recording from bipolar LSO neurons. Stimulation electrodes (patch pipettes) were filled with ACSF. Recording electrodes (2~3 MΩ) contained pipette solution 54 mM D-gluconic acid, 54 mM CsOH, 56 mM CsCl, 1 mM $MgCl_2$, 1 mM $CaCl_2$, 10 mM HEPES, 11 mM EGTA, 0.3 mM Na-GTP, 2 mM Mg-ATP, 5 mM QX314, 0.5% biocytin (pH 7.2, 280 mOsm/l). Current signals were filtered at 2 kHz and the access resistance was compensated by 80% with 10 μs lag with an Axopatch 1D amplifier. When access resistance measured more than 20 MΩ before compensation, the compensation could not be achieved by 80% and data were not acquired from those cells. GABA/glycinergic responses were isolated by adding Kynurenic acid (1mM) to the ACSF. To isolate glutamatergic responses, $GABA_A$ receptor antagonist, bicuculline (10μM) (Tocris) or SR95531 (10 μM) (Tocris), and glycine receptor antagonist, strychnine (1 μM) (Sigma) were added to the ACSF. The holding potentials were - 70 mV when recording GABA/Glycine-evoked currents, - 80 mV when recording AMPA currents, and + 60 mV when recording NMDA currents. APV (50 to 100 μM), NMDA receptor antagonist, was added to separate NMDA receptor-mediated currents from AMPA receptor-mediated currents. For the measurement of membrane property, Cs^+ was replaced with K^+. The membrane properties of LSO neurons in KCC2-KD mice were not different to WT at P10~P11 (Resting membrane potential (mV); - 57.6 ± 1.5 (n = 9) for WT, - 58 ±1.5 (n = 11) for KCC2-KD, Input resistance (MΩ); 290 ± 46 (n = 12) for WT, 258 ± 50 (n = 14) for KCC2-KD, membrane capacitance (pF); 37.3 ± 2.4 (n = 12) for WT, 39.3 ± 2.4 (n = 14) for KCC2-KD mice) ($p > 0.5$ for each measurements). Liquid junction potential was about 9 mV and corrected online. Electrical stimuli were delivered by Master 8 and Isoflex (AMPI, Israel). After recordings were finished, the location of the patched neuron in high frequency regions was determined by staining the biocytin filled cells with Diaminobenzidine (DAB) (Sigma) after fixation in 4% paraformaldehyde (PFA), and imaging with a CCD camera.

2.2.3.1 Minimal stimulation

To measure the synaptic responses that results from the activation of a single MNTB axon, minimal stimulation approaches were used. The stimulation electrode was positioned at the lateral end of MNTB and after a synaptic response was observed, the electrical stimulation intensity was lowered to a level that resulted in a failure rate higher than 50%. Electrical stimulation was repeated 50 to 200 times at 0.2 Hz. Success responses were determined after the peak values from every stimulus were plotted against the number of trials. The synaptic responses within a 1ms on-set latency window after stimulation were regarded as responses elicited by an individual presynaptic axon. Only responses with an on-set latency of < 5 ms were included. The mean peak amplitudes of the successful responses were regarded as the strength of the synaptic response from a single partner.

2.2.3.2 Maximal stimulation

To measure the synaptic responses elicited by the synchronous activation of all MNTB inputs into single LSO neurons, electrical stimulation was increased by 100 μA steps until the peak synaptic currents reached steady-state level or decreased slightly. In these experiments, I limited the maximum number of recordings per slice at five in order to reduce the effect of slicing variation. The average of three to four synaptic responses by maximal stimulation was taken as a maximal response into a LSO neuron.

2.2.3.3 Synaptic response to inputs from the cochlear nucleus (CN)

In order to measure the synaptic input from CN, the stimulation electrode was positioned into the ventral acoustic stria. In order to isolate glutamatergic input, Bicuculline (10 μM) and strychnine (1 μM) were added to the bath. In order to measure the synaptic strength of a single CN fiber, the same method was applied as was used to acquire the single fiber response from MNTB. Electrical stimulations were repeated from 20 to 150 times. Since in some cells stimulation at 0.2 Hz elicited a gradual reduction of the response amplitude, the stimulation frequency was lowered to 0.1 Hz. The peak of each response was plotted vs. trial number, from which the failure rate was determined. To measure synaptic strength of total CN fibers,

stimulation intensity was increase by 100 μA steps. Glycine (5 μM) was added in ACSF when NMDA receptor-mediated current was measured.

2.2.3.4 Data acquisition

Signals were filtered at 2 kHz (Bessel filter, Axoclamp-1D, Axon Instruments, Foster City, California) and digitized at 10 kHz. (Custom Labview acquisition program 5.0, National Instruments, Austin, Texas).

2.2.4 Rise time and decay time constant (τ) analysis

Rise and decay kinetics were analyzed with the program Mini analysis (6.0.3., Synaptosoft Inc., Decatur, GA) and Clampfit (9.2.0.09, CA). The rise time was measured for the time period from 10% to 90% of the peak amplitudes. Individual successful responses from minimal stimulation were analyzed and the averaged values from 4 to 40 responses per neuron were used as the rise time. For decay time constant (τ), decay components of every successful response per neuron were fitted. Fitting range was from 90% to 10% of the peak amplitude for both rise time and decay τ analysis. The decay time constants (τ) from a single exponential and a double exponential function were compared. If the R^2 (Goodness of Fit) value of a double exponential fit differed by 1% or more compared to the fit of a single exponential, then the decay τ from a double exponential fit was chosen. If not, decay τ from the single exponential fit was chosen. So, determination of the decay τ between a single exponential and a double exponential was objective. For the developmental ages analyzed, most MNTB-elicited responses were fit by a single exponential. Fitting errors, which might be caused by small response amplitude at P1-3 were minor since the averaged decay τ acquired by fitting the individual success responses and the decay τ acquired by fitting the averaged success responses were not different ($p > 0.5$). Therefore, decay τ was analyzed by fitting individual single fiber responses from 90 to 10 % range of the peak and the average value was acquired for P8-11.

2.2.5 Statistics

Distribution of data was tested with the Shapiro-Wilk test. The statistical difference between two groups was compared with an unpaired student t-test when normally distributed (parametric test) and with Kolmogorov-Smirnov tests and Mann-Whitney test (non-parametric test) otherwise.

2.2.6 Calcium imaging

Fura 2-AM labeling: The slices were labeled with the calcium indicator, fura-2AM, using a spin labeling procedure, since fura-2AM can not penetrate into LSO neurons older than P7 (Ene et al., 2007). 300 µm brain slices were prepared and placed on filter paper (12 µm pores; Corning Incorporated Life Sciences, Acton, MA) and transferred to the interface chamber for recovery. After 15 to 30 min, a slice was placed into a microcentrifuge tube (1.5 ml) containing a cut-off 10 kDa Microcon filter (Microcon YM-10 Centrifugal Filter Devices). Fura 2-AM (100 µM) was placed onto a slice within the microcentrifuge tube, which was then centrifuged at 430 g (IEC Clinical Centrifuge, International Equipment Company USA) for 15 to 20 min. After centrifugation, the slice was moved to the interface chamber again (at room temperature) where the slice was further incubated with 10 µM Fura 2-AM for more than 30 minutes.

Imaging acquisition: Ratiometric images (340 nm / 380 nm) were acquired using an inverted epifluorescence microscope (Nikon Eclipse TE200) equipped with 10X (NA: 0.5) and 20X (NA:0.75) air objectives using a computer-controlled monochromator (Polychrome II,TILL Photonics). Fluorescence images were acquired at 0.1 Hz with a CCD camera (IMAGO, T.I.L.L. Photonics, Martinsried, Germany) using 50 ms periods of excitation alternating between 340 nm and 380 nm (Polychrome II, T.I.L.L. Photonics). Background fluorescence was subtracted using Tillvision (TILL Photonics) as described (Ene et al., 2003). GABA, glycine and KCl were bath applied in aerated ACSF via the perfusion.

2.3 RESULTS

2.3.1 GABA and glycine are excitatory neurotransmitters and increase intracellular Ca^{2+} concentration $[Ca^{2+}]_i$ in LSO neurons of KCC2-KD mice at hearing onset.

I first investigated if GABA and glycine remain excitatory in LSO neurons of KCC2-KD mice at P11, which is just before hearing on-set (Shnerson and Pujol, 1981; Kamiya et al., 2001; Ehret and Romand, 1992). Since the switch from depolarization to hyperpolarization of GABA and glycine activity in the LSO occurs during the second postnatal week (Kullmann and Kandler, 2001) and is due to an increased function of potassium-chloride co-transporter-2 (KCC2) (Balakrishnan et al., 2003), in KCC2-KD mice, the shift of E_{Cl} to a hyperpolarizing potential is prevented in cortex (Woo et al., 2002; Zhu et al., 2005) and in the LSO neurons as well (Balakrishnan et al., 2003). Since depolarizing GABA/glycine responses can increase $[Ca^{2+}]_i$ through voltage-gated calcium channels (VGCC) in LSO neurons during the first postnatal week (Kullman and Kandler, 2001; Kullman et al., 2002), I first investigated whether prolonging the period of depolarizing GABA/glycine responses would have an effect on the $[Ca^{2+}]_i$ in LSO neurons at P11 in KCC2-KD mice using a calcium imaging method.

At P11 in WT mice, GABA did not increase $[Ca^{2+}]_i$ in the LSO neurons (0% of cells, n = 0/28), consistent with the fact that during the second postnatal week, GABA has already become hyperpolarizing (Kandler and Friauf, 1995; Kullmann and Kandler, 2001; Barlakrishnan et al., 2003). In contrast, in KCC2-KD mice of the same age, 80% of LSO neurons displayed an increase in $[Ca^{2+}]_i$ in response to GABA application (n=19/24), with only 20% (n=5/24) lacking an $[Ca^{2+}]_i$ increase (Fig 2.1.D).

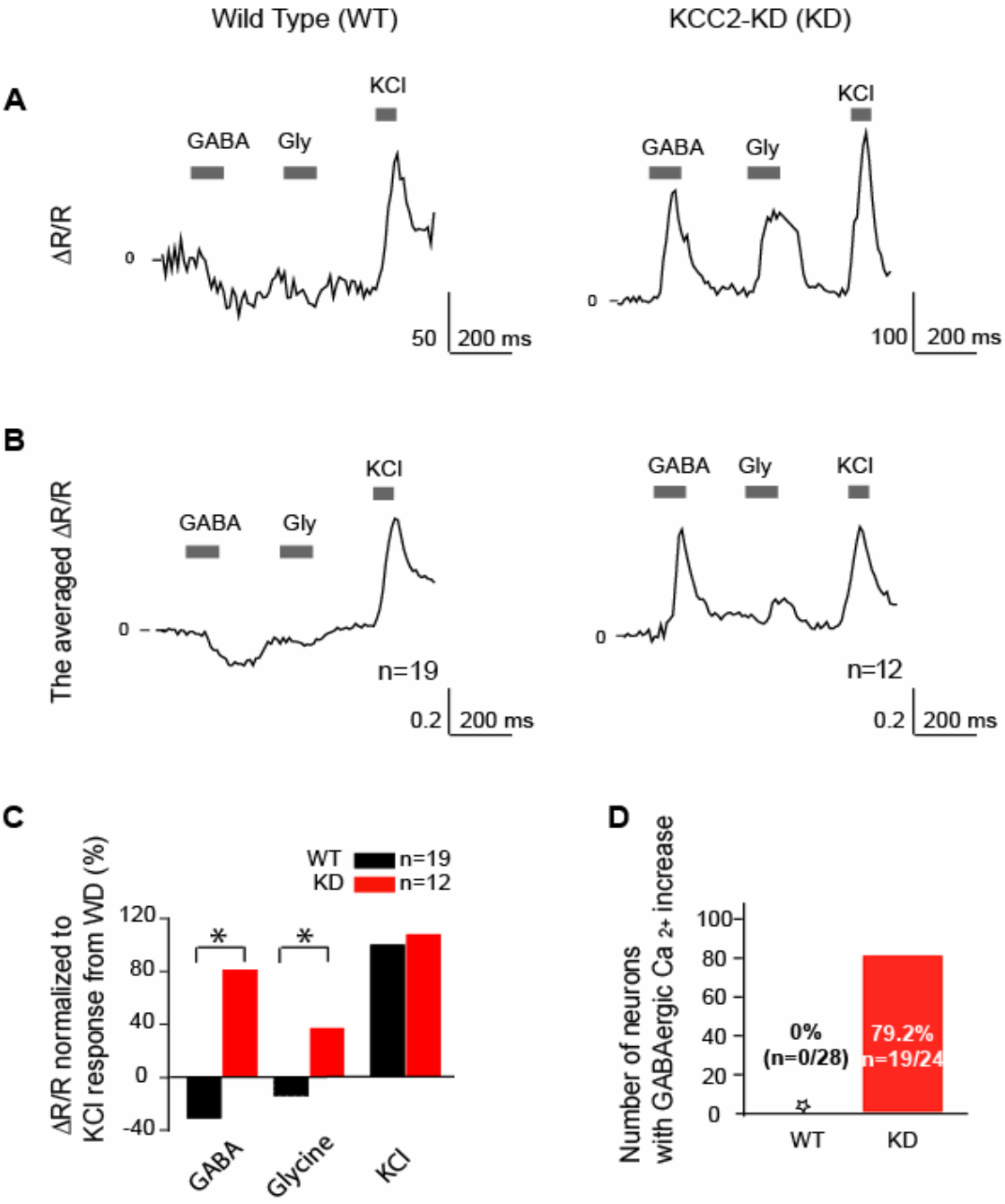
Wild Type (WT)
KCC2-KD (KD)
A
KCl
GABA
Gly
ΔR/R
0
50
200 ms
100
B
The averaged ΔR/R
n=19
n=12
0.2
C
WT
KD
n=19
n=12
ΔR/R normalized to KCl response from WD (%)
120
80
40
-40
*
GABA
Glycine
KCl
D
Number of neurons with GABAergic Ca 2+ increase
100
60
20
0%
(n=0/28)
79.2%
n=19/24

Figure 2.1.

Figure 2.1. GABA and glycine are excitatory and increase $[Ca^{2+}]_i$ in KCC2-KD mice at P11.

(A) Example traces of 340 / 380 fluorescence ratio (R) changes (Δ R/R) from a single LSO neuron from WT *(left)* and KCC2-KD *(right)*. GABA (2mM) and glycine (2 mM) were bath-applied for 100 seconds. KCl (60 mM) was applied for 60 seconds. **(B)** Averaged trace of Δ R/R from WT (n=19, *left*) and KCC2-KD (n=12, *right*). **(C)** The averaged ΔR/R in KCC2-KD mice was compared to the averaged Δ R/R normalized by KCl in WT mice. The same neurons as in **(B)** were used (n=19 for WT, n=12 for KCC2-KD). The peak ΔR/R by GABA, glycine, and KCl in WT and KCC2-KD mice were averaged and normalized to the value of KCl. In WT mice; decrease of $[Ca^{2+}]_i$ by GABA was 31 % and a decrease of $[Ca^{2+}]_i$ by glycine was 14 % (black bar, n=19). In KCC2-KD mice, increased $[Ca^{2+}]_i$ by GABA was 81 % and an increase $[Ca^{2+}]_i$ by glycine was 37% (red bar, n=12). **(D)** Number of neurons which increased $[Ca^{2+}]_i$ by GABA from WT and KCC2-KD ($p < 0.0001$, Fisher's exact test).

Since MNTB-LSO synapses release glycine in addition to GABA during the first and second postnatal weeks (Kotak et al., 1998; Nabekura et al., 2004), we investigated if an increase in $[Ca^{2+}]_i$ could be caused only by GABA, or by glycine as well. I first applied GABA and then glycine after wash out of GABA. In a WT LSO neuron, both GABA and glycine not only failed to induce an increase in $[Ca^{2+}]_i$, but caused a reduction in $[Ca^{2+}]_i$, as indicated by a 340/380 fluorescence ratio change (ΔR/R) (Fig 2.1. A, Left, WT). Averaged ΔR/R (normalized to the KCl response from each cell, n = 19) showed that in WT mice, the peak of GABA-induced ΔR/R was - 30.4%, while and the glycine-induced peak ΔR/R was - 11.9% compared to the KCl response as 100% (Fig 2.1. B, Left, WT), confirming that GABA and glycine both cause a reduction in $[Ca^{2+}]_i$ in WT LSO neurons. In contrast, in KCC2-KD LSO neurons, both GABA and glycine increased $[Ca^{2+}]_i$, as shown in a single cell example (Fig 2.1. A, Right). Collectively, averaged ΔR/R (normalized to KCl response from each cell, n = 12) after GABA application was 91.8 % and 31.5% after glycine (Fig 2.1.B, Right), demonstrating that GABA and glycine exert the same effect on $[Ca^{2+}]_i$ increment in KCC2-KD mice.

Since this analysis does not confirm that the change is not due to more general effects caused by the absence of KCC2 or by a depolarizing E_{Cl} value, I compared KCl-elicited $[Ca^{2+}]_i$ between WT and KCC2-KD mice by quantifying the difference in the $[Ca^{2+}]_i$ change induced by GABA and glycine between WT and KCC2-KD to the KCl-induced change in WT (Fig 2.1. C). ΔR/Rs were averaged without normalizing to the KCl value and the averaged peak ΔR/R was compared to the ΔR/R of the KCl response in WT as 100%. First, the averaged peak ΔR/R by KCl in WT and KCC2-KD mice did not differ (112.9 ± 20.4 for WT (n = 19), 104.6 ± 4.5 for KD (n = 12), 98% in KCC2-KD compared to WT, $p > 0.1$), suggesting that in KCC2-KD mice, LSO neurons maintain the full capacity to increase intracellular calcium concentration in response to a full membrane depolarization by KCl. In WT mice, GABA decreased ΔR/R by 30.7 % and glycine decreased it by 13.8 %. In KD mice, GABA increased ΔR/R by 81.0 % and glycine increased it by 36.7%. In addition, in KCC2-KD mice, GABAergic ΔR/R was of similar magnitude as the KCl-induced ΔR/R in WT mice (85.1 ± 17.7) ($p > 0.1$), implying that the GABA-mediated calcium response in KCC2-KD mice might be as robust as the increase in $[Ca^{2+}]_i$ mediated by a KCl-induced action potential.

In summary, my calcium imaging experiment confirmed that GABA and glycine, the two major inhibitory neurotransmitters within the LSO, maintain their excitatory actions in LSO neurons of KCC2-KD mice at hearing on-set.

2.3.2 MNTB-LSO minimal input strength

First, in order to test if the switch to hyperpolarizing GABA/glycine response is necessary for the strengthening of inhibitory synapses, I compared the synaptic strength by unitary MNTB fiber activation (considered as single fiber strength, MNTB-miniPSC) and maximal MNTB fiber activation (maximal input strength, MNTB-maxiPSC) between WT and KCC2-KD mice. I first applied minimal stimulation in order to measure unitary fiber strength in WT and KCC2-KD mice during development.

In WT mice, there was a 7-fold increase in MNTB-miniPSC during the first two postnatal weeks. At P1-3, the average MNTB-miniPSC was 31.9 ± 5.7 pA (n = 10). At P8-11, the average MNTB-miniPSC was 254.6 ± 71 pA (n = 45) (Fig 2.2. A, B, C, $p < 0.005$).

Similar to WT mice, in KCC2-KD mice there was about an 8-fold increase of MNTB-miniPSC. At P1-3, the average MNTB-miniPSC was 55.3 ± 10.9 pA (n = 14), and at P8-11, the average MNTB-miniPSC was 388.7 ± 111 pA (n = 37) ($p < 0.005$) (Fig 2.2. A, B, C). There was no significant difference in the MNTB-miniPSC between WT and KCC2-KD mice at P1-3 ($p > 0.5$) and P8-11 ($p > 0.5$) (Fig 2.2.C, D). This indicates that a hyperpolarizing GABA/glycinergic response is not necessary for the strengthening of unitary MNTB-LSO fibers.

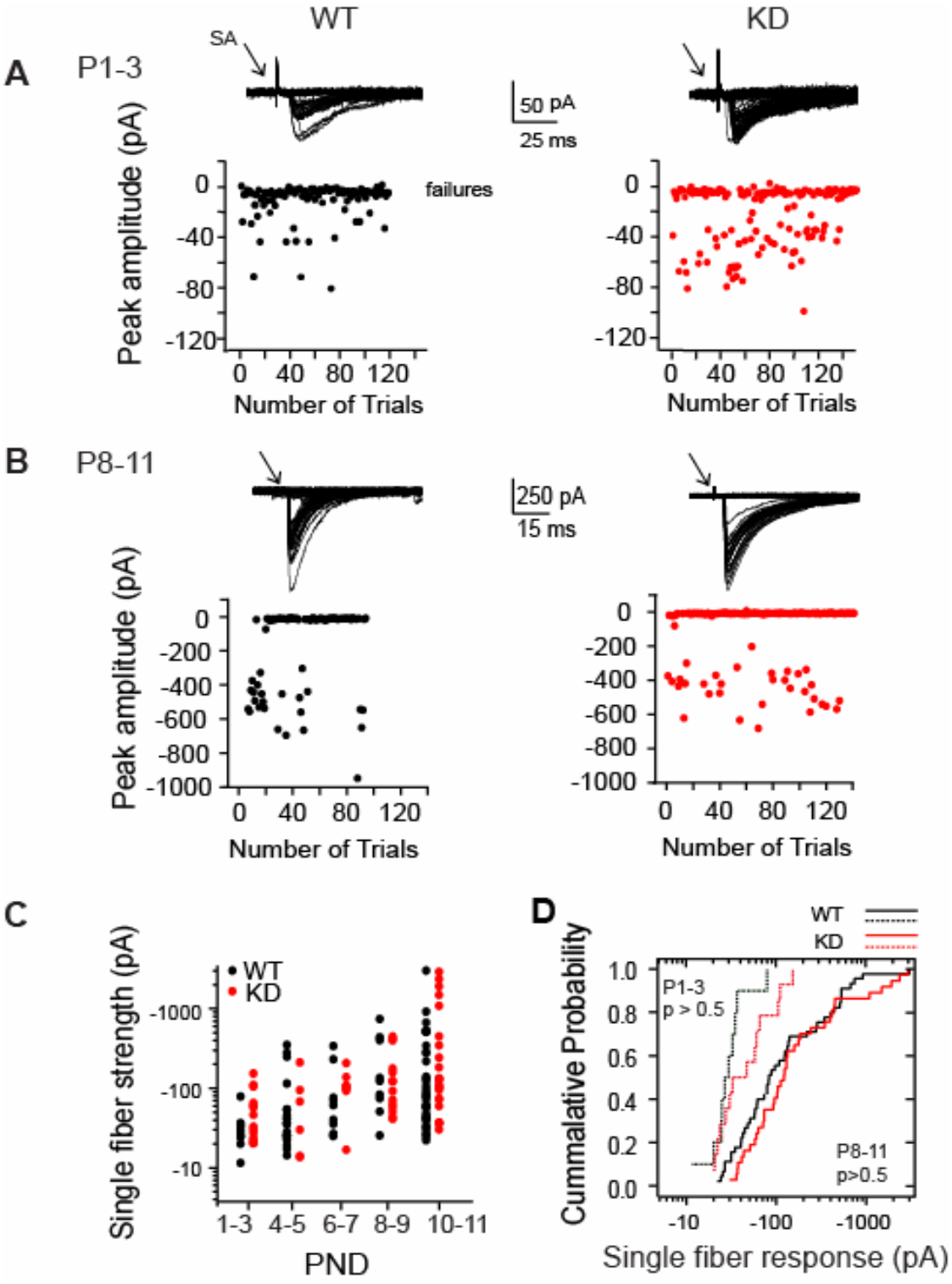
A
P1-3
WT
KD
SA
50 pA
25 ms
failures
Peak amplitude (pA)
0
-40
-80
-120
0 40 80 120
Number of Trials
B
P8-11
250 pA
15 ms
0
-200
-400
-600
-800
-1000
C
Single fiber strength (pA)
WT
KD
-1000
-100
-10
1-3 4-5 6-7 8-9 10-11
PND
D
Cummalative Probability
P1-3
p > 0.5
P8-11
p>0.5
1.0
0.8
0.6
0.4
0.2
0.0
-10 -100 -1000
Single fiber response (pA)

Figure 2.2.

Figure 2.2. Developmental increase of MNTB-miniPSC in WT and KCC2-KD.

(A) and **(B)** Examples of minimal stimulation responses in LSO neurons from WT (*left*) and KCC2-KD (*right*) animals at P1-3 **(A)** and P8-11 **(B)**. Traces are the superposition of > 50 individual responses. Peak response amplitudes are acquired by subtracting baseline (1~2 ms after stimulus artifacts) and are plotted against number of trials. **(C)** Semilogarithmic developmental time course of single MNTB fiber responses for WT (•) and KD (•) mice. (PND; postnatal day) **(D)** Cumulative probability histogram of MNTB-miniPSC for P1-3 (---, dashed line) and P8-11 (—, straight line) neurons from WT (—, black) and KCC2-KD (—, red) mice. Amplitudes at P8-11 were significantly larger than at P1-3 ($p < 0.005$, non-parametric test). Values from WT and KCC2-KD mice were not significantly different ($p > 0.5$, non-parametric test). Mean (± s.e.m.) for MNTB-miniPSC at P1-3; 31.9 ± 5.7 pA (n = 10) for WT and 55.3 ± 10.9 pA (n = 14) for KCC2-KD ($p > 0.5$, non-parametric test). P8-11; 254.6 ± 71 pA (n = 45) for WT and 388.7 ± 111 pA (n = 37) for KCC2-KD ($p > 0.5$, non-parametric test).

2.3.3 MNTB-LSO maximal input strength

In rat MNTB-LSO pathway development, the strength of maximal synaptic responses is increased as well, but to a lesser extent than the increase in MNTB-miniPSC following minimal stimulation. This results in a reduced convergence ratio during later developmental ages, implying that there is also elimination of presynaptic partners while remaining fiber strength is increasing (Kim and Kandler, 2003). Thus I investigated whether the absence of hyperpolarization would prevent synapse elimination. If this would be the case, I would expect that the strength of maximal stimulation responses (MNTB-maxiPSC) would be greater in KCC2-KD mice than WT, with the unitary MNTB fibers developing normally in KCC2-KD mice (Fig 2.2.). On the other hand, if there is normal elimination in the absence of GABA/glycinergic hyperpolarization, the strength of maximal MNTB stimulation in KCC2-KD mice should be similar to those found in WT at older ages.

Maximal stimulus intensity was used to activate all MNTB-axons that would innervate the recorded LSO neurons, which was determined as the plateau point of the stimulation-response plot (Fig 2.3). In WT mice aged P1-3, the average MNTB-maxiPSC was 0.7 ± 0.2 nA (n = 10) and at P8-11, the average MNTB-maxiPSC was 4.0 ± 0.7 nA (n = 34). Therefore, the maximal MNTB-LSO connection strength increased about 5-fold during the first two postnatal weeks ($p < 0.005$) (Fig 2.3. A, C). In KCC2-KD mice aged P1-3, the average MNTB-maxiPSC was 1.1 ± 0.4 nA (n = 8) and at P8-11, the average MNTB-maxiPSC was 3.3 ± 0.4 nA (n = 35), representing 3-fold increase ($p < 0.005$) (Fig 2.3. A, C). Both at P1-3 and P8-11, the MNTB-maxiPSC was not different between WT and KCC2-KD ($p > 0.5$, Fig 2.3. C, D). Taken together, the similarity in the strength of both unitary and maximal MNTB fiber responses in the MNTB-LSO pathway in WT and KCC2-KD mice suggests that the GABA/glycinergic hyperpolarizing switch is not necessary for the developmental strengthening. Importantly, the similarity in the strength of maximal responses between the two groups suggests that the MNTB-LSO pathway in KCC2-KD mice is also refined through a process of synapse elimination like that in WT.

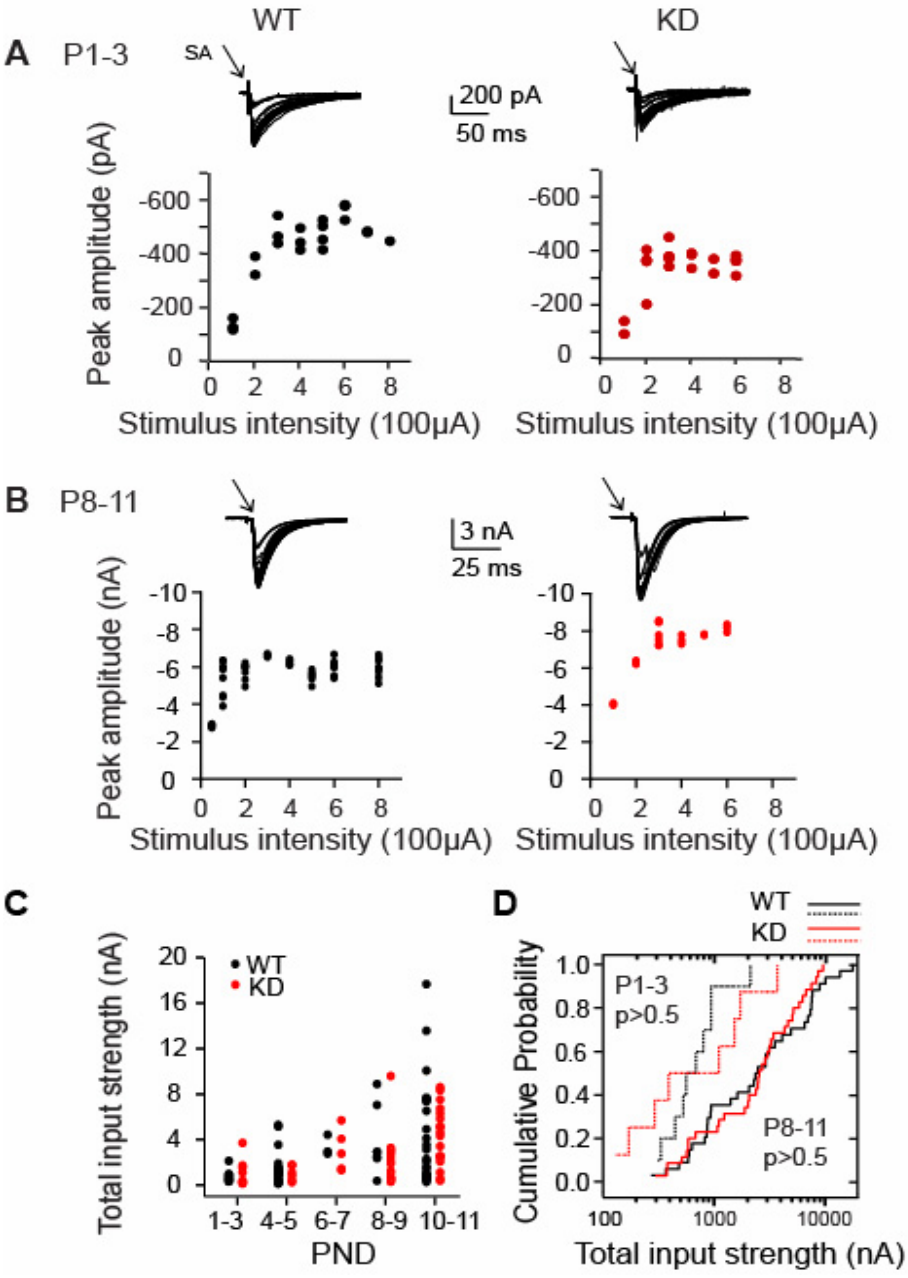
A
P1-3
WT
KD
SA
200 pA
50 ms
Peak amplitude (pA)
-600
-400
-200
0
0 2 4 6 8
Stimulus intensity (100µA)
B
P8-11
3 nA
25 ms
Peak amplitude (nA)
-10
-8
-6
-4
-2
0
C
Total input strength (nA)
20
16
12
8
4
0
WT
KD
1-3 4-5 6-7 8-9 10-11
PND
D
Cumulative Probability
1.0
0.8
0.6
0.4
0.2
0.0
P1-3
p>0.5
P8-11
p>0.5
100 1000 10000
Total input strength (nA)

Figure 2.3.

Figure 2.3. Developmental increase of MNTB-maxiPSC in WT and KCC2-KD.

(A) and **(B)** Examples of responses of LSO neurons WT (*left*) and KCC2-KD (*right*) at P1-3 (A) and P8-11 **(B)**. Current traces are superposition of individual responses elicited by increasing stimulus intensity by 100 μA. **(C)** Developmental time course of MNTB-maxiPSC during development for WT (•) and KCC2-KD (•) mice. **(D)** Cumulative probability histogram of MNTB-maxiPSC for P1-3 (---, dashed line) and P8-11(—, straight line) for WT (—, black) and KD (—, red) mice. The MNTB-maxiPSC became strengthened during development for WT and KCC2-KD mice. ($p < 0.005$, non-parametric test). Values from WT and KCC2-KD mice were not significantly different ($p > 0.5$, non-parametric test). Mean (± s.e.m.) for total fibers strength at P1-3; 0.7 ± 0.2 nA (n = 10) for WT and 1.1 ± 0.4 nA (n = 8) for KCC2-KD ($p > 0.5$, non-parametric test). P8-11; 4.0 ± 0.7 nA (n = 34) for WT and 3.3 ± 0.4 nA (n = 35) for KCC2-KD ($p > 0.5$, non-parametric test).

Indeed, the convergence ratio for WT decreased by 40%, from 24:1 to 15:1, in WT and by 60%, from 20:1 to 8:1, in KCC2-KD mice, suggesting that the absence of hyperpolarizing GABA/glycine responses does not prevent normal strengthening and elimination of inhibitory synapses.

2.3.4 Rise time of unitary MNTB fiber to a LSO neuron

In the hippocampus, inhibitory neurons synapse on CA1 pyramidal neurons on different subcellular locations with different amplitudes; the strongest inhibitory synaptic responses are located close to the soma while weaker inhibitory synaptic responses are located on more distal dendrites (Maccaferri et al., 2000). This indicates that there is a correlation between inhibitory synaptic strength and subcellular location. Since unitary fiber strength became stronger during MNTB-LSO development in WT (Fig 2.2), I investigated whether there would be a correlation between the strength of unitary MNTB fibers and their subcellular location. In order to investigate this possibility, I analyzed 10-90% rise time of MNTB-miniPSC, which could represent the relative distance of the synapse from the somatic recording site due to dendritic filtering effects (Spruston et al., 1993).

At P1-3 in WT, average 10-90% rise time for the MNTB-miniPSC was 2.1 ± 0.3 ms (n = 9, Fig 2.4. A and C). At this age, all MNTB-miniPSC were small, showing no correlation between unitary fiber strength and rise time (Fig 2.4. B upper panel, black circle). At P8-11, the average 10-90% rise time for the MNTB-miniPSC was 1.2 ± 0.1 ms (n = 44) (Fig 2.4. C), a significant decrease compared to P1-3 ($p < 0.05$, Fig 2.4. C and D).

Since unitary MNTB fibers have become strengthened by P8-11, I investigated if there is any correlation between synaptic input strength and rise time. As shown in figure 2.4. B, stronger fibers had faster rise times, while weaker fibers had slower rise times (Fig 2.4.B. below panel). The range of rise times for the weaker fibers was similar to those from single fiber strength at P1-3 (Figure 2.4. B). Together these data are consistent with the idea that stronger MNTB inputs are located closer to the soma of LSO neurons then weaker inputs.

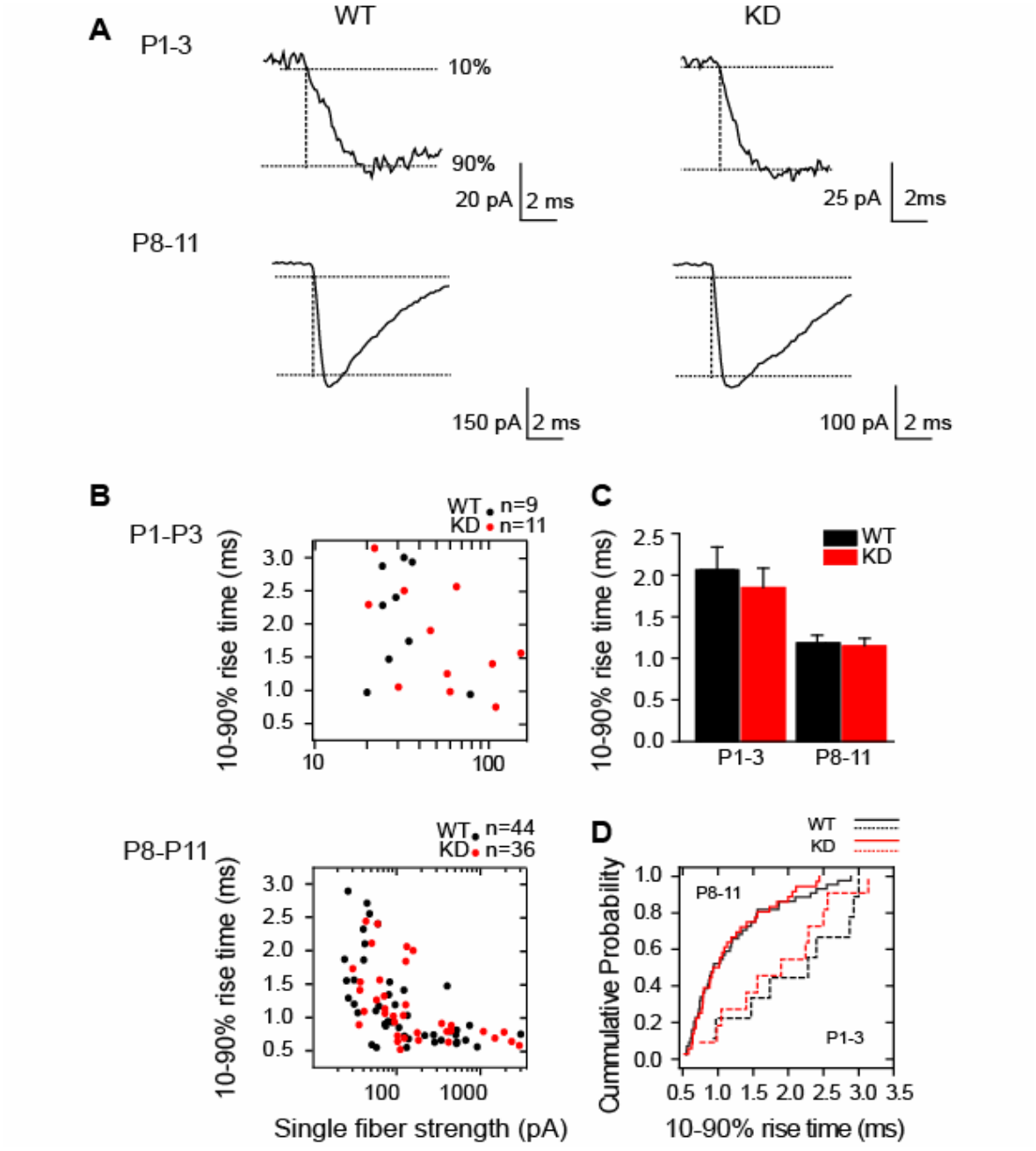
A
P1-3
WT
KD
10%
90%
20 pA
2 ms
25 pA
2ms
P8-11
150 pA
2 ms
100 pA
2 ms
B
P1-P3
WT n=9
KD n=11
10-90% rise time (ms)
3.0
2.5
2.0
1.5
1.0
0.5
10
100
P8-P11
WT n=44
KD n=36
100
1000
Single fiber strength (pA)
C
WT
KD
2.5
2.0
1.5
1.0
0.5
0.0
P1-3
P8-11
D
WT
KD
P8-11
P1-3
Cumulative Probability
1.0
0.8
0.6
0.4
0.2
0.0
0.5 1.0 1.5 2.0 2.5 3.0 3.5
10-90% rise time (ms)

Figure 2.4.

Figure 2.4. Developmental time course of 10-90% rise times of MNTB-miniPSC in WT and KCC2-KD mice.

(A) Example traces for 10-90% rise time analysis. The dotted line indicates 10% and 90% of peak amplitude. Rise time from example traces (ms); 2.7 for WT and 2.2 for KCC2-KD at P1-3, 0.6 for WT and 0.5 for KCC2-KD at P8-11. **(B)** Rise times vs. peak current plot for MNTB-miniPSC at P1-3 (*top*) and P8-11 (*bottom*). **(C)** Mean rise times. P1-P3 WT: 2.1 ± 0.3 ms (n = 9), P1-P3 KCC2-KD 1.9 ± 0.2 ms (n = 11); ($p > 0.5$, parametric test), P8-11 WT: 1.2 ± 0.1 ms (n = 44); P8-11 KCC2-KD 1.2 ± 0.1 ms (n = 36) ($p > 0.5$, non-parametric test). **(D)** Cumulative histogram for P1-3 (---, dashed line) and P8-11(—, straight line) for WT (—, black) and KCC2-KD (—, red). During development, there was significant increase of rise time by MNTB-miniPSC for WT and KCC2-KD ($p < 0.001$ for both cases, non-parametric test).

A previous immunocytochemical study demonstrated that inhibitory synapses into auditory neurons in the medial superior olive undergo soma-dendritic redistribution during development such that at older ages inhibitory synapses preferentially contact the soma of neurons (Kapfer et al., 2002). This redistribution was activity dependent since without normal hearing experience, gephyrin redistribution did not occur. Thus, I next investigated if MNTB-miniPSC and rise time would have a similar correlation in KCC2-KD mice as in WT, despite the fact that the polarity of MNTB inputs was reversed in KCC2-KD mice at P8-11.

At P1-3 in KCC2-KD, the average 10-90% rise time for MNTB-miniPSC was 1.9 ± 0.2 ms (n = 11) (Fig 2.4. A and C). Similar to WT, at this age there was no correlation between unitary fiber strength and rise time (Fig 2.4. B). At P8-11, the average 10-90% rise time for MNTB-miniPSC was 1.2 ± 0.1 ms (n=36) (Fig 2.4. C), similar to the age-matched WT group ($p > 0.5$) (Fig 2.4. D). Also, in KCC2-KD mice the rise time of MNTB-miniPSC became faster ($p < 0.005$, Fig 2.4. C and D), with stronger single MNTB responses having faster rise times and weaker single MNTB responses having slower rise times. The relationship between single fiber strength and rise time was almost identical to that of WT (Fig 2.4.B. Below panel), suggesting that in KCC2-KD mice, even if the polarity of strengthened single MNTB responses is opposite to WT, the soma-dendritic location of synaptic contacts might still be similar to WT.

2.3.5 Decay time constant (τ) of a MNTB-miniPSC to a LSO neuron

In neonatal rats, MNTB-LSO synapses releases both GABA and glycine, but at the end of the postnatal week, MNTB-LSO synapses only releases glycine (Kotak et al., 1998; Nebekura et al., 2004). GABA and glycine are even co-released from single vesicles (Nabekura et al., 2004). Although co-release of GABA and glycine seems to be a common phenomenon observed in developing inhibitory synapses (Gao et al., 2001; Kotak et al., 1998; Awatramani et al., 2005), the physiological implications of the switch in neurotransmitter phenotype are not understood.

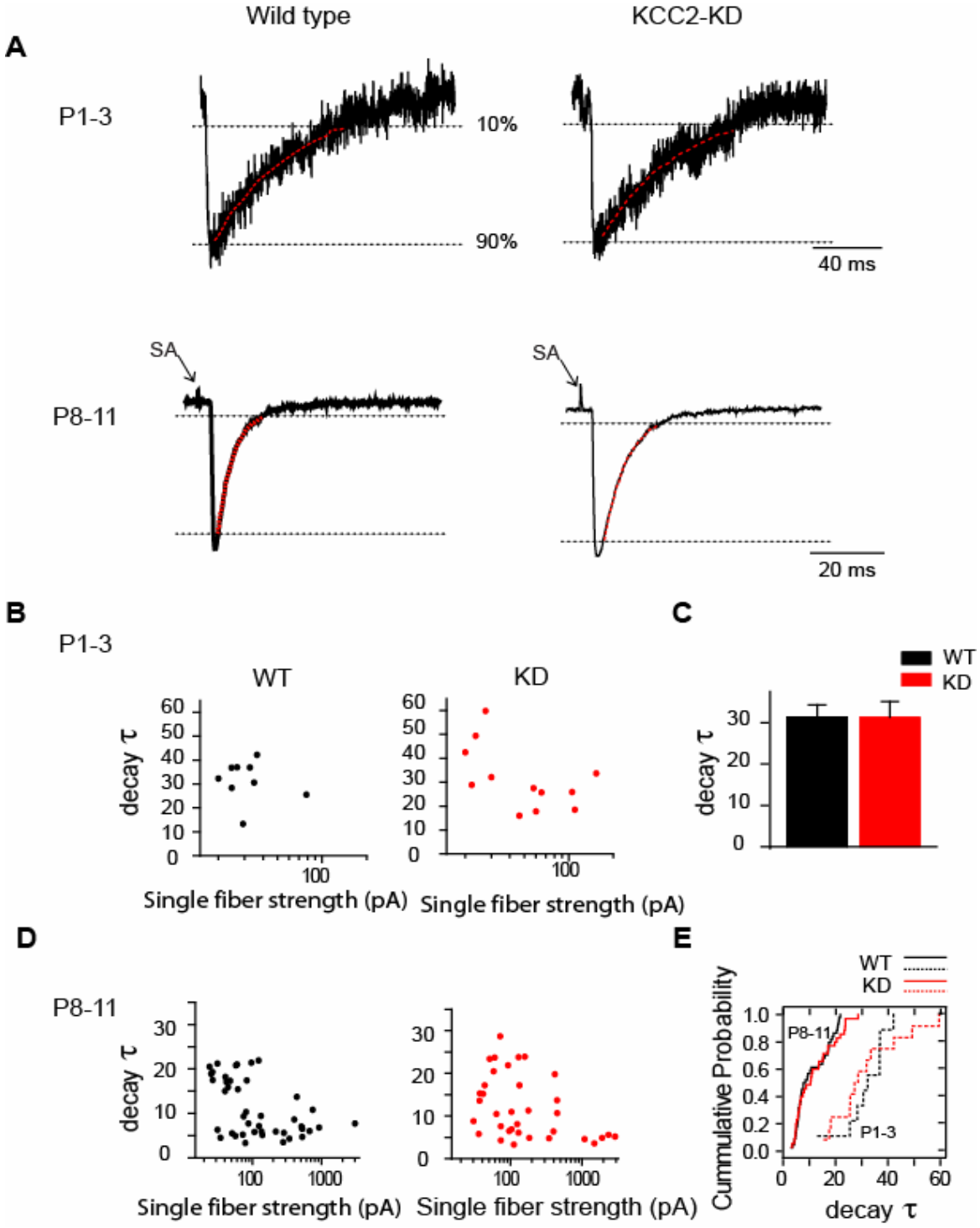
A
Wild type
KCC2-KD
P1-3
10%
90%
40 ms
SA
P8-11
20 ms
B
P1-3
WT
KD
decay τ
Single fiber strength (pA)
C
WT
KD
decay τ
D
P8-11
E
WT
KD
P8-11
P1-3
Cummulative Probability
decay τ

Figure 2.5.

Figure 2.5. Decay time constant (τ) of a MNTB-miniPSC response during development

(A) Example traces for τ analysis of MNTB-miniPSC. The dotted line indicates 10% and 90% of peak amplitude. Decay τ from example traces; 46.4 for WT and 54.9 for KCC2-KD at P1-3, 5.0 for WT and 6.9 for KCC2-KD at P8-11. **(B)** Decay τ of a MNTB-miniPSC are plotted to the corresponding amplitudes for P1-3 (• WT and • KD). **(C)** Mean ± s.e.m. of decay τ for WT and KCC2-KD at P1-3; WT: 31.4 ± 2.8 (n = 9), KCC2-KD: 31.3 ± 3.8 (n = 12) ($p > 0.5$, parametric test). **(D)** Decay τs of MNTB-miniPSCs are plotted to their corresponding amplitudes for P8-11 (• WT and • KCC2-KD). Two distinct populations in the decay τ distribution are discernible. Fast decay τ: WT - 6.7 ± 0.44 (n = 28), KCC2-KD - 7.3 ± 0.6 (n = 23) ($p > 0.5$ between WT and KCC2-KD, non-parametric test). Slow decay τ: WT - 18.7 ± 0.57 (n = 16), KCC2-KD - 20.9 ± 1.19 (n = 12) ($p > 0.05$ between WT and KCC2-KD, parametric test). **(E)** Cummulative probability for decay τ from MNTB-miniPSC for P1-3 (---, dashed line) and P8-11 (—, straight line) from WT (—, black) and KCC2-KD (—, red). During development, there was significant decrease in decay τs for both WT and KCC2-KD. ($p < 0.0001$ for P1-3 and P8-11, non-parametric test).

Because in rats, the switch from GABA to glycine in the MNTB-LSO pathway occurs at the end of first postnatal week, the time when GABA to glycine switch from depolarizing to hyperpolarizing, I investigated if the polarity switch would be important for the GABA to glycinergic switch. Because GABAergic and glycinergic responses could be discriminated by their decay kinetics with GABAergic currents having a longer decay time constant (τ) than glycinergic currents (Nebekura et al., 2004), I first analyzed the decay τ of unitary MNTB responses.

At P1-3, the mean decay τ of MNTB-miniPSC was 31.4 ± 2.8 ms (n = 9) in WT mice and it was 31.3 ± 3.8 ms (n = 12) in KCC2-KD mice (Fig. 2.5. A, C). There was no difference between the two groups ($p > 0.5$). At P8-11 in WT mice, the decay τs of MNTB-miniPSC clustered into two groups; a faster group with a mean of 6.7 ± 0.4 ms (n = 28) and a slower group of 18.7 ± 0.6 ms (n = 16) (Fig 2.5. A, D). The values of the faster group are similar to the values measured for pure glycinergic response in LSO neurons in rats (Nabekura et al., 2004). The developmental appearance of a group with shorter τ is consistent with a developmental switch from GABA to glycine in the MNTB-LSO pathway. From P1-3 to P8-11, overall decay τs of single fiber responses became faster ($p < 0.001$) (Fig 2.5. E).

At P8-11 in KCC2-KD mice, the decay τs of MNTB-miniPSC had two different clusters as well; a faster group of 7.3 ± 0.6 (n = 23) and a slower group of 20.9 ±1.2 (n = 12) (Fig 2.5. A lower panel and D), demonstrating that the decay τs of MNTB-miniPSC became faster in KCC2-KD mice as well ($p < 0.001$) (Fig 2.5. E). At P8-11, neither the faster nor slower group decay τs in KCC2-KD were different from WT ($p > 0.5$, Fig 2.5. D). The similar faster decay τs of MNTB-miniPSC in WT and KCC2-KD at P8-11 implies that the GABA to glycine switch in the MNTB-LSO pathway might not be affected by an elongated period of depolarizing responses in the LSO neurons by MNTB in KCC2-KD mice.

In order to further investigate whether the changes in decay τ of MNTB-miniPSC during development represents the switch from GABAergic to glycinergic transmission, I isolated glycinergic synaptic responses from MNTB-miniPSC at P8-11 animals using the $GABA_A$ specific antagonist, SR95531. In WT mice, unitary fiber MNTB-LSO transmission was mediated predominantly by glycine, since by SR95531 reduced MNTB-miniPSC by only 10%, with the residual currents being blocked by addition of strychnine (Fig 2.6. A). Consistent with the decay τ analysis of MNTB-miniPSC (Fig 2.5.), most MNTB-miniPSC in P8-11 WT mice were mediated by glycine (n = 8). Similarily, in P8-11 KD mice, the reduction of MNTB-miniPSC by SR95531 was also 10%, and was not different from WT mice (Fig 2.6. B). In KCC2-KD mice at P8-11, the mean glycine-mediated component of MNTB-miniPSC was 84.1 ± 11.2 % (n = 9), identical to the WT value of 90.0 ± 6.5 % (n = 8) (Fig 2.6. C), implying that even without the GABA/glycinergic hyperpolarizational switch, the transition from the use of GABA to glycine in MNTB-LSO synapses occurred normally.

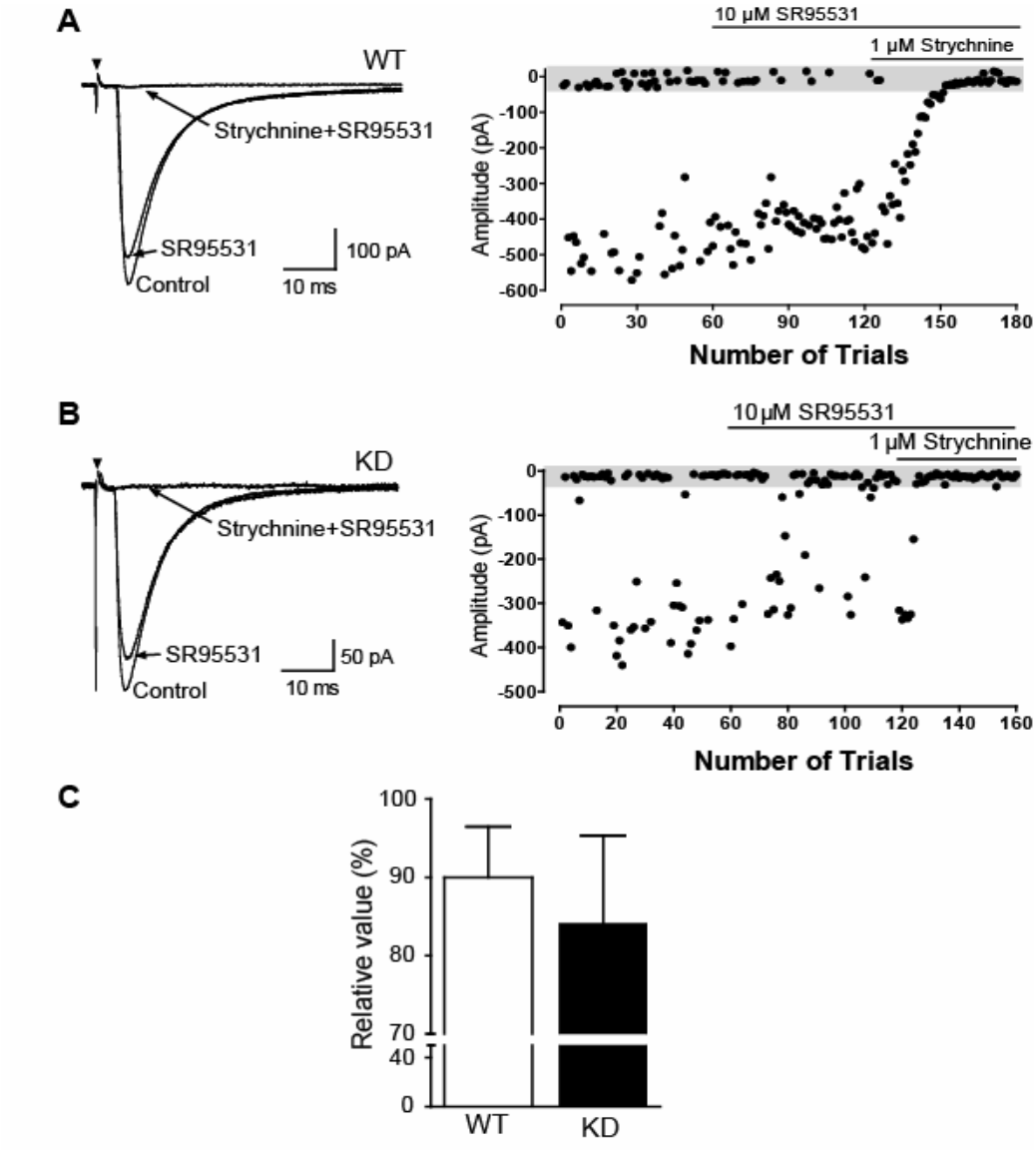

Figure 2.6. Developmental GABA to glycine neurotransmitter switch in MNTB-LSO synapses.

(A, B) Left panels, MNTB-miniPSC before and after application of the $GABA_A$ receptor antagonist SR95531 (10 µM) and the glycine receptor antagonist strychnine (1 µM). Arrow: stimulation artifact. SR95531 reduced response amplitude by 10% for both WT **(A)** and KD **(B)** mice. The remaining currents were abolished by additional application strychnine. Right panels: The peak MNTB-miniPSCs are plotted against trial number. Gray bar: failure responses. **(C)** Percentage of glycine component of MNTB-miniPSC for WT (90.0 ± 6.5 % (n = 8), white bar) and KCC2-KD (84.1 ± 11.2 % (n=9), black bar) ($p > 0.05$, student t-test). (Data provided by Dr. Jihyun Noh)

2.3.6 Balance between inhibition and excitation: Glutamatergic synaptic input to LSO neurons.

LSO neurons receive conventional excitatory inputs from the CN through glutamatergic synapses (CN-LSO pathway) (Kandler and Friauf, 1995; Kotak and Sanes, 1995). The CN-LSO pathway is functional as early as embryonic day 18, when synaptic responses can be elicited in LSO neurons (Kandler and Friauf, 1993 and 1995). Many previous studies have shown that neuronal systems maintain the level of excitability by counteracting increased or decreased neuronal activity (Turrigiano and Nelson, 2004). If similar regulatory mechanisms are in place in the LSO, then I would predict that glutamatergic synaptic input into the LSO neurons from the CN in KCC2-KD mice would be decreased in KCC2-KD mice at P9-12, when LSO neurons receive strengthened, but still depolarizing MNTB inputs (Fig 2.1., 2.2. and 2.3.).

First, I measured the synaptic strength of unitary CN fibers and the synaptic strength of maximal CN fibers at a holding potential of -80 mV. At this negative holding potential, the majority of glutamatergic currents were through AMPA receptors (CN-$_{AMPA}$ strength) (Ehrlich and Malinow, 2004). In WT mice, the average unitary CN-$_{AMPA}$ strength ($CN_{(AMPA)}$-miniPSC) was -89.2 ± 27.0 pA (n = 18, black bar) (Fig 2.7. A, C). In KCC2- KD mice, the average $CN_{(AMPA)}$-miniPSC was -81.9 ± 29.6 pA (n = 14, red bar) (Fig 2.7. A, C), statistically not different from WT animals ($p > 0.1$). In order to compare the maximal strength from the CN, the stimulus intensity was increased ($CN_{(AMPA)}$-maxiPSC) (Fig 2.7. B). In WT, the average $CN_{(AMPA)}$-maxiPSC was 247.4 ± 35 pA (n = 31), which also did not differ from the $CN_{(AMPA)}$-maxiPSC in KCC2-KD (205.6 ± 30 pA, n = 22, $p > 0.5$).

Glutamate activation of AMPA receptors results in depolarization of the membrane. AMPA-mediated membrane depolarization can remove the voltage-dependent Mg^{2+} block from NMDA receptors, which is important since NMDA-mediated synaptic responses are involved in synaptic plasticity, including LTP and LTD (Malenka and Nicoll, 1993), synapse elimination (Colonnese and Constantine-Paton, 2006; Colonnese et al., 2005), and neurogenesis in adult progenitors (Arvidsson et al., 2001; Luk et al., 2003). NMDA- receptors mediated synaptic

currents are developmentally down-regulated in cortex (Franks and Isaacson, 2005), as well as in the auditory system (Zhou and Parks, 1992). Since NMDA-mediated components are regulated in an activity dependent manner (Kotak and Sanes, 1996), I next investigated whether the NMDA receptor component of maximal stimulation by the CN pathway ($CN_{(NMDA)}$-maxiPSC) would be affected by the potentially increased activity within LSO neurons of KCC2-KD mice at P9-12.

In WT mice, $CN_{(NMDA)}$-maxiPSC (45~50 ms after stimulation, V hold at + 60 mV) was 52.2 ± 14.6 pA (n = 17), while $CN_{(NMDA)}$-maxiPSC in KCC2-KD mice was 46.4 ± 11.0 pA (n = 16), with no significant difference (Fig 2.8. A and B) ($p > 0.5$, non-parametric test). Also, the NMDA/AMPA ratio ($CN_{(AMPA)}$ measured at 5~8 ms after stimulation) was 0.83 ± 0.19 (n = 17) in WT and 0.81 ± 0.19 (n = 16) in KCC2-KD, suggesting that $CN_{(NMDA)}$-maxiPSC also did not differ between WT and KCC2-KD (Fig 2.8. A and C) ($p > 0.5$, student t-test).

In summary, the similar strength of the CN-LSO pathway in KCC2-KD mice ($CN_{(AMPA)}$-mini and maxiPSC, and $CN_{(NMDA)}$-maxiPSC) at P9-12 compared to WT mice implies that the persistent depolarizing action of GABA/glycinergic MNTB synaptic responses does not affect the strength of the glutamatergic CN synaptic pathway before hearing on-set in the developing MNTB-LSO pathway of mice.

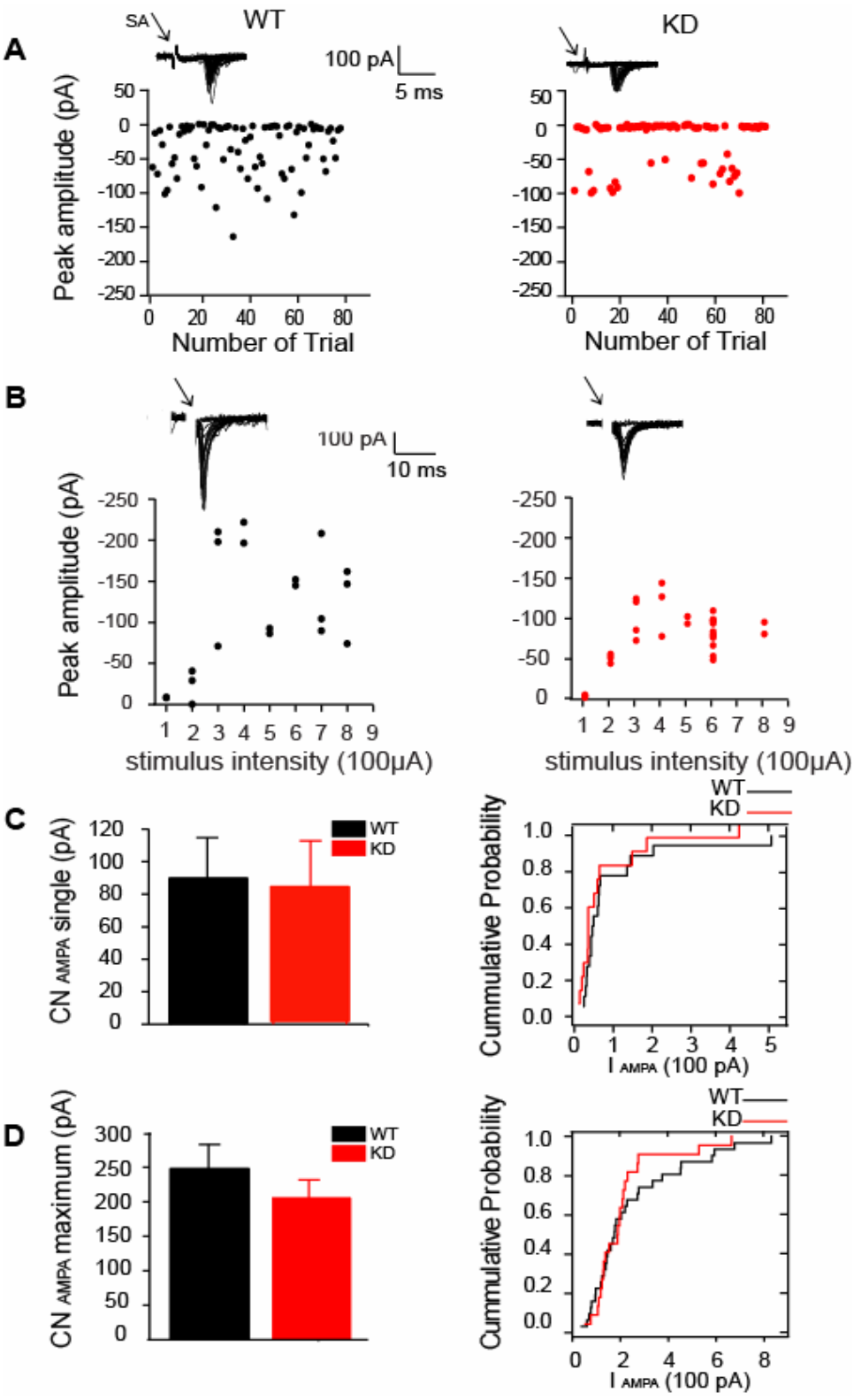
A
SA
WT
KD
100 pA
5 ms
Peak amplitude (pA)
Number of Trial
B
100 pA
10 ms
stimulus intensity (100μA)
C
CN AMPA single (pA)
WT
KD
Cummulative Probability
I AMPA (100 pA)
D
CN AMPA maximum (pA)

Figure 2.7.

Figure 2.7. AMPA receptor mediated responses in LSO neuron of KCC2-KD mice at P9-12.

(A) Examples for responses elicited by minimum stimulation of cochlear nucleus axons Vh; - 80 mV. *Top*; Superposition of > 50 individual current traces including failures. *Bottom*; Peak response amplitudes are acquired by subtracting baseline (1~2 ms after stimulus artifacts) and are plotted against number of trials.
(B) Examples for maximal stimulation responses (Vh; - 80 mV). *Top*; Superimposed traces of responses elicited by increasing stimulus intensity in 100 μA steps. *Bottom*; From the superimposed traces, the peak response amplitudes are acquired by subtracting baseline (1~2 ms after stimulus artifacts) and are plotted against corresponding stimulus intensity. Arrows point to stimulating artifacts. **(C)** Mean $CN_{(AMPA)}$-miniPSC for WT (-89.2 ± 27.0 (n = 18)) and KCC2-KD (-81.9 ± 29.6 (n = 14)). *Right panel*: Cumulative Probability for WT (—) and KCC2-KD (—). ($p > 0.1$, non-parametric test) **(D)** Mean $CN_{(AMPA)}$-maxiPSC for WT (-247 ± 35 (n = 31)) and KCC2-KD (-206 ± 30 (n = 22)). *Right panel*: Cumulative Probability for WT (—) and KCC2-KD (—) maximal response. ($p > 0.5$, non-parametric test)

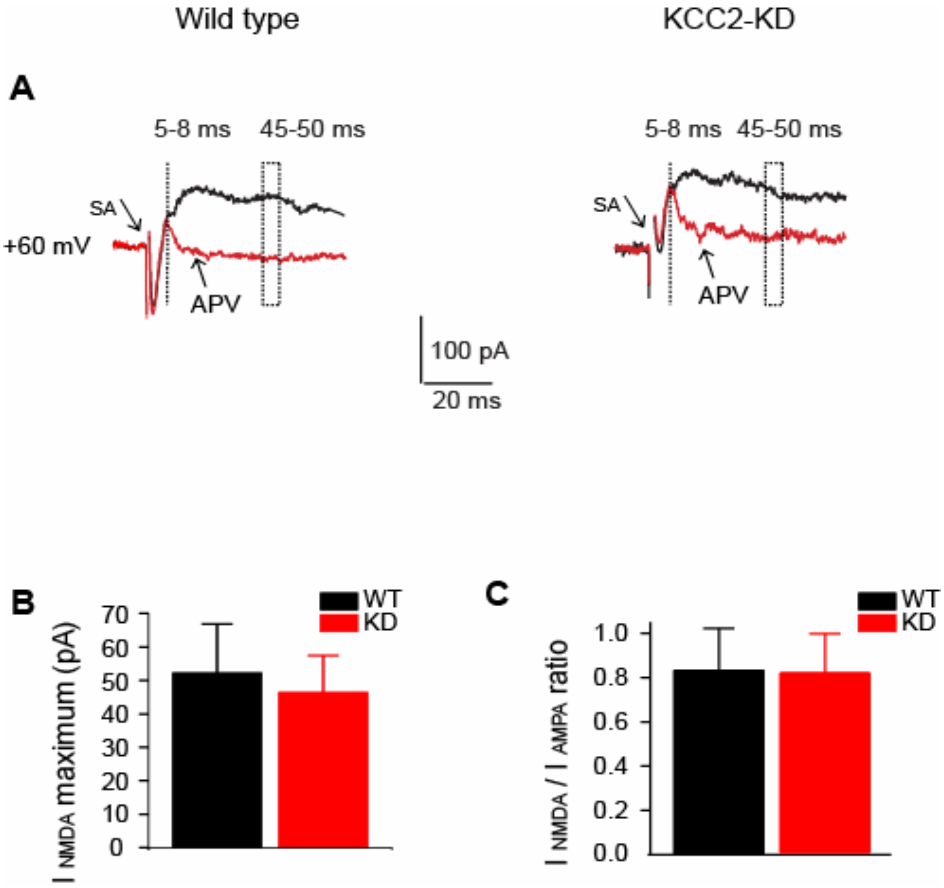

Figure 2.8. NMDA receptor mediated responses in WT and KCC2-KD mice at P9-12.

(A) Example traces for $CN_{(AMPA)}$-maxiPSC (red line) and $CN_{(NMDA)}$-maxiPSC (black line) currents at + 60 mV. $CN_{(NMDA)}$-maxiPSC can be isolated in the presence of APV (50 µM) (red line). The amplitudes of $CN_{(AMPA)}$-maxiPSC were measured from the average in the window 5-8 ms after stimulus. The amplitudes of $CN_{(NMDA)}$-maxiPSC were determined from the average in the window 45 -50 ms after stimulus. The total $CN_{(AMPA)}$-maxiPSC and $CN_{(NMDA)}$-maxiPSC from examples: WT; 50.4 pA for $CN_{(AMPA)}$ and 77.3 pA for $CN_{(NMDA)}$, KD; 100.7 pA for $CN_{(AMPA)}$ and 90.5 pA for $CN_{(NMDA)}$. APV (50 µM) was applied to isolated NMDA-mediated currents. **(B)** Mean (± s.e.m.) of $CN_{(NMDA)}$-maxiPSC for WT (black bar) and KCC2-KD (red bar). 52.2 ± 14.6 pA (n=17) for WT and 46.4 ± 11.0 pA (n=16) for KCC2-KD ($p>0.5$, non parametric test) **(C)** $CN_{(NMDA/AMPA)}$-maxiPSC for WT (black bar) and KCC2-KD (red bar). 0.83 ± 0.19 (n=17) for WT and 0.81 ± 0.19 (n=16) for KCC2-KD ($p>0.5$, student t-test).

2.4 DISCUSSION

In this Chapter, I investigated how synaptic inputs into LSO neurons develop *in-vivo* in the relative absence of KCC2, a key molecule responsible for switching GABA and glycine responses to hyperpolarizing (Delpire and Mount, 2002). I found that the development of the GABA/glycinergic MNTB-LSO pathway occurred normally, despite the fact that GABA/glycinergic synapses remained excitatory. In addition, in KCC2-KD mice synaptic transmission in the glutamatergic CN-LSO pathway also was normal, even though LSO neurons were experiencing abnormally high levels of depolarization due excitatory synaptic inputs from the MNTB.

2.4.1 Cellular mechanisms for inhibitory synapse strengthening

Until recently, the strength of inhibitory systems has been most commonly investigated by measuring the number of GABAergic neurons by detecting GABA (Hendry and Johns, 1986) or GABA synthesizing enzymes (GAD-65 and -67) (Swanwick et al., 2006), or in terms of synaptic conductances by measuring peak currents through post synaptic receptors (Marty et al., 2004; Marty et al., 2000; Swanwick et al., 2006; Kilman et al., 2002), quantal content (Frerking et al., 1995; Llano et al., 2000), and/or physiological response amplitudes based on the activities through pre- and postsynaptic contacts (Kilman et al., 2002; Hartman et al., 2006; Khazipov et al., 1995; Baldelli et al., 2002). Also, when the effect of BDNF, an important neurotrophin involving in inhibitory system, are investigated on the role in the maturation of inhibition during development (Huang et al., 1999), its effects in strengthening inhibition have been often described by comparing inhibitory postsynaptic currents (IPSC) amplitude or the degree of receptor clustering (Seil and Drake-Baumann, 1994, 2000; Marty et al., 2000; Brünig et al., 2001).

However, when the driving force of permeable ions is regulated independently of other components in GABAergic transmission, changes in synaptic markers – either immunohistochemical or physiological - can have opposite implications for the consequences in neural circuits. Synaptic strength of inhibitory system can be modulated by activity deprivation, sensory experience, and neurotrophins-involving signaling (Kilman et al., 2002; Jiao et al., 2006; Morales et al., 2002; Huang et al., 1999; Brunig et al., 2001). For example, reduced activity caused reduction in amplitude of miniature and evoked IPSCs both *in-vitro* and *in-vivo* (Kilman et al., 2002; Jiao et al., 2006; Morales et al., 2002). The reduced IPSCs by reduced activity would mean reduced inhibition in a neuronal network when GABA/glycinergic responses are hyperpolarizing. However, if GABA/glycinergic synapses are depolarizing, the same IPSCs reduction would mean that relative inhibition is increased, because the depolarizing strength, through GABA/glycinergic synapses rendered by depolarizing E_{Cl}, is reduced.

$[Cl^-]_i$, and thus $E_{Cl,}$ are developmentally regulated by the activity of inward and outward chloride transporters such as NKCC1 and KCC2 (Delpire and Mount, 2002). In particular, the expression level of KCC2, the outward chloride cotransporter, is not only increased gradually during development (Lu et al., 1999), but also regulated by neuronal activity, such as postsynaptic spiking activity alone (Fiumelli et al., 2005) or in conjunction with presynaptic activity (Woodin et al., 2003), epileptic activity (Rivera et al., 2004), activities of glutamatergic receptors (Kanold and Shatz, 2006), as well as by neurotrophins such as BDNF (Rivera et al., 2002; Wardle and Poo, 2003; Aguado et al, 2003, Rivera et al., 2004). Furthermore, BDNF's effect on KCC2 expression can have opposite effects, depending on the developmental stage. For example, embryonic BDNF overexpression increases KCC2 expression, resulting in an attenuation of GABAergic calcium responses (Aguado et al., 2003). In contrast, overexpression of BDNF in adult animals results in increased excitability of the neural circuit due to reduced KCC2 function and a reduction in GABAergic hyperpolarizations (Rivera et al., 2002, Wardle and Poo, 2003). These studies imply that E_{Cl} values can be modulated by neuronal activity.

Since activity (Kilman et al., 2002; Jiao et al., 2006; Morales et al., 2002) and neurotrophins such as BDNF (Huang et al., 1999; Brunig et al., 2001) can change synaptic conductance as well as the driving force of chloride ions through regulation of KCC2 (Fiumelli

and Woodin, 2007), it is necessary to consider its effects on the homeostasis of chloride ions when contemplating the strength of inhibition. Unfortunately, until recently, there has not been a clear demonstration that GABA/glycinergic synaptic strength and the maturation of E_{Cl} are regulated independently each other. In this regard, the normal strengthening of MNTB-LSO synapses in KCC2-KD mice provides a good first example, demonstrating that depolarizing GABA/glycinergic synaptic strength can be increased in the absence of the normal developmental maturation of E_{Cl} *in-vivo*. Also, it implies that the depolarizing GABA/glycinergic synaptic strength, when increased, does not necessarily mean "stronger inhibition" per se. This example emphasizes that chloride homeostasis must be considered along with the changes in synaptic strength in studies of inhibitory systems (Woodin et al., 2003; Fiumelli et al., 2005; Maffei et al., 2006; De Koninck, 2007).

Several lines of evidences support the hypothesis that the developmental switch from a depolarizing to hyperpolarizing action of GABA and glycine is an important cellular mechanism for the strengthening of inhibitory synapses. *In- vitro* and *in- vivo* studies demonstrats that when KCC2 is overexpressed in neurons (thus resulting in a premature hyperpolarizing GABA response (Lee et al., 2005-included in Chapter III), inhibitory synaptic strength become stronger (Chudotrodova et al., 2005; Akerman and Cline, 2006), as indicated by increased expression of $GABA_A$ receptors and an increase in IPSC amplitude and frequency as compared to control neurons. In line with these results, unpublished data from our laboratory indicate that single MNTB synapses become stronger during the second postnatal week (bigger than 1 nA), when MNTB-LSO responses are no longer depolarizing but have switched to hyperpolarizing. Therefore, I expected that strengthening of the MNTB-LSO pathway would be impaired in KCC2-KD mice due to the absence of GABA/glycinergic hyperpolarizing response. However, contrary to my expectation, the strengthening of MNTB-LSO synapses in KCC2-KD mice does not differ from WT mice, suggesting that regardless of GABA/glycinergic response polarity, GABA/glycinergic synapses from the MNTB indeed undergo the normal strengthening process. The consequences of the strengthened depolarizing MNTB synapse in KCC2-KD mice would not only fail to suppress excitatory synaptic response but also provide another major excitatory synaptic drive in addition to the conventional glutamatergic synaptic input from the CN (Fig 1.1).

Previous studies from the developing spinal cord demonstrates that activity through glycine receptors is a critical mechanism for inhibitory synapse strengthening by showing that glycine receptor clustering can be blocked by application the glycine receptor antagonist strychnine. Since glycine activity at this age is depolarizing and increases $[Ca^{2+}]_i$ through L-type calcium channels, glycine-mediated increases in $[Ca^{2+}]_i$ has been proposed as an important mechanism for inhibitory strengthening. Supporting this hypothesis, treatment with the L-type calcium channel antagonist nifedipine prevents glycine receptor clustering (Kirsch and Betz, 1998). However, several important issues have not been addressed, including whether the glycine receptor clustering would be accompanied by E_{Cl} maturation (to a hyperpolarizing direction) and whether an increase in $[Ca^{2+}]_i$ would be sufficient for the stabilization (maintenance) of clustered receptors or would require subsequenct E_{Cl} maturation. Indeed, in the previous study by Kirsch and Betz (1998), glycine receptor clustering was investigated in a relatively later stage (E14 dissociation + 6~10 days *in-vitro*), when glycinergic synaptic "inhibition" was already critical and regulated by increased KCC2 expression (Hubner et al., 2001; Stein et al., 2004). Accordingly, it is hypothesized that even if depolarizing glycinergic responses are necessary for the initiation of strengthening, subsequent switch to hyperpolarizing glycine response might be necessary for the maintenance of strengthened glycinergic responses. However, the results in this Chapter regarding the development of the MNTB to LSO pathway in KCC2-KD mice demonstrates that a hyperpolarizing E_{Cl} is not a necessary condition for the strengthening of GABA/glycinergic synapses, suggesting that an increase in $[Ca^{2+}]_i$ by depolarizing GABA/glycine might be sufficient for the strengthening (and maintenance) of MNTB synapses before hearing on-set.

Both the MNTB_miniPSC and MNTB_maxiPSC became strengthened normally in KCC2-KD mice during the developmental period before hearing on-set. In both WT and KCC2-KD mice, there was a decrease in the MNTB-LSO convergence ratio. This indicates that the number of presynaptic neurons making functional synaptic contacts onto a single LSO neuron decreases even if GABA/glycinergic responses do not switch to hyperpolarizing. With current electrophysiological methods, the convergence ratio-based degree of elimination is difficult to compare between WT and KCC2-KD mice especially because the convergence ratio is estimated

from MNTB-miniPSC and –maxiPSC, which were not differ at each developmental period between WT and KCC2-KD mice ($p > 0.5$ for each cases, Fig 2.2 and Fig 2.3). The similar strength of MNTB-miniPSC ad maxiPSC suggests that even if convergence ratio is not identical between WT and KCC2-KD mice during development, it does not reflect higher degree of elimination between two groups. Furthermore, the decreased convergence ratios do not provide information as to whether refinement occurs along the tonotopic axis, as shown by functional mapping within the MNTB (Kim and Kandler, 2003). It remains to be addressed that if the reduced convergence ratio in MNTB-LSO pathway would be parallel to the tonotopic map development in the MNTB in KCC2-KD mice during development.

2.4.2 Balance between inhibitory and excitatory inputs to LSO neurons in KCC2-KD mice

In past years, it has become apparent that many neural circuits regulate their excitability through homeostatic mechanisms. In the embryonic spinal cord of *Xenopus laevi*s, suppressed activity by overexpressing the inward rectifying K^+-channel (hKir2.1) increases the number of neurons expressing excitatory neurotransmitters, while decreases the number of neurons expressing inhibitory neurotransmitters. In contrast, enhanced activity by overexpressing the Na^+-channel (Na_v2a) leads to the reverse results (Borodinsky et al., 2004). For differentiated neurons, homeostatic mechanisms can work on the level of the number of postsynaptic receptors, the number of synaptic inputs, and the strength of those inputs. (Turrigiano and Nelson, 2004). Furthermore, homeostatic regulation of excitability seems to be widely observed throughout central nervous system *in- vitro* and *in- vivo* (Turrigiano and Nelson, 2004).

In light of these homeostatic mechanisms, the similarity of the strength of MNTB- and CN-LSO synapses in KCC2-KD mice around hearing on-set is surprising (Fig 2.7. and Fig 2.8.). One explanation for the absence of homeostatic mechanisms in the LSO could be that spontaneous activity before hearing on-set (Lippe, 1994) is too low to cause activity dependent synaptic modifications in the auditory system, in contrast to the visual system in which synaptic

refinement is significantly affected by spontaneous activity even before sensory-driven activity starts (Feller et al., 1997). However, previous studies demonstrats that auditory brainstem circuits do indeed undergo spontaneous activity-dependent modification. In congenital deafness (*dn/dn*) mice caused by chromosomal inversion on chromosome 19 (Vinas et a., 1998), cochlear hair cells degenerate shortly after birth (Pujol et al., 1983), and spontaneous activity originating from cochlea is absent (Durham et al., 1989). In *dn/dn* mice, the frequency of mIPSCs is increased, the amplitudes of mIPSCs are smaller in the MNTB (Leao et. al., 2004) at P12~P14, and evoked EPSCs were increased in the CN at around P13 (Oleskevich and Walmsley, 2002), implying that the level of spontaneous activity is indeed high enough to affect the development of auditory circuits *in- vivo*. Another example comes from studies in which inhibitory feedback innervations of inner hair cells is disrupted before hearing onset, a manipulation which most likely changes spontaneous cochlear-generated activity (Walsh et al., 1998). Before hearing on-set, the medial olivocochlear (MOC) fibers from superior olivary complex (SOC) form cholinergic synaptic connections to the inner hair cell (IHC) and modulate spontaneous activity (Glowatzki and Fuchs, 2000). Both MOC fiber transection and alpha9 knock-out mice, which have disrupted MOC input into hair cells due to the disruption of nicotinic acetylcholine receptor in hair cells (Elgoyhen et al., 1994; Vetter et al., 1999) shows impaired strengthening of MNTB-LSO synapses before hearing onset (Kim and Kandler, 2006), again indicating that spontaneous activity influences synaptic strength in auditory system before hearing onset. Thus, the current finding of normal strengthening of MNTB-LSO and CN-LSO synapses at hearing on-set in KCC2-KD mice could not be explained by an absence of spontaneous activity itself, emphasizing that in KCC2-KD mice, the breakdown in the balance of excitation-inhibition in LSO neurons during development is not attributable to the spontaneous activity changes possibly caused by the reduced KCC2 expression.

Currently, it is unknown whether LSO neurons simply do not exhibit homeostatic mechanisms or whether KCC2 expression is even linked to mechanisms responsible for establishing or maintaining a balance of inhibition and excitation. This is because 1) investigations regarding homeostatic mechanisms have not been conducted in LSO neurons yet and 2) while my investigation is conducted before hearing on-set (around P12), *in-vivo* investigations regarding homeostasis have been conducted after P12, when the nervous system is

no longer driven by spontaneous activity, is responsive to sensory-evoked stimuli (Desai et al, 2002; Maffei et al., 2004). In addition, 3) no investigation regarding homeostatic mechanisms has been demonstrated in the absence of the regulatory mechanisms for chloride homeostasis.

Nonetheless, my results demonstrating normal development of MNTB pathway and similar strength of CN inputs onto the LSO neurons in KCC2-KD mice represent the first example in which the balance of inhibition and excitation is broken specifically due to the impaired regulation of chloride homeostasis.

2.4.3 GABA to glycinergic neurotransmitter switch in KCC2-KD mice.

Similar to that found in developing spinal cord neurons (Gao et al., 2001), a change from GABA- to glycine- mediated synaptic responses has been observed in the developing MNTB-LSO pathway (Awatramani et al., 2005, Kotak et al., 1998). Since the period of transition in transmitter use in MNTB-LSO synapses corresponds to the time period when GABA/glycine responses become hyperpolarizing, the possibility has been suggested that the switch to hyperpolarization could be important for mediating the neurotransmitter switch (Nabekura et al., 2004). However, my results argue against this possibility. Result from decay τ analysis of MNTB-miniPSC and pharmacological isolation of glycine-mediated components at P8-11 in KCC2-KD mice demonstrates that the transition from GABA to glycine is a developmental process that is not affected by the polarity of the GABA/glycinergic responses (Fig 2.5. and Fig 2.6.). Also decay τ analysis of MNTB-miniPSC provides a good prediction of the response's glycine component, as demonstrated by pharmacological experiment (Fig 2.6.). Interestingly, I found that at P8-11 in WT, the amplitude of MNTB-miniPSC with a faster decay τ is considerably larger than the response amplitude of MNTB-miniPSC with a slower decay τ (Fig 2.5. D). At P8-11 in WT, the MNTB-miniPSC with the faster decay τ was 378.7 ± 108.3 pA ($n = 28$) and the MNTB-miniPSC with the slower decay τ was 52.0 ± 7.0 pA ($n = 16$) ($p < 0.01$). This analysis seems to suggest that strengthening of the MNTB-LSO pathway is mediated through a strengthening of glycinergic synapses or through an increase in the glycinergic component of

synapses. The latter scenario was recently observed for inhibitory synapse strengthening in MNTB neurons as well (Awatramani et al., 2005).

2.4.4 Kinetics of unitary fiber MNTB-LSO responses

While the MNTB-LSO pathway underwent refinement, the rise time of MNTB-miniPSC also showed developmental changes in mice. In WT, the rise time of MNTB-miniPSC at P8-11 was faster compared to those at P1-3 by 0.9 ms (more than 50%) on average. In addition, at P8-11, there was a correlation between synaptic strength and rise time; with stronger MNTB-miniPSCs correlating with faster rise times and slower MNTB-miniPSCs with slower rise times. Rise time can be determined by the coordinated release of neurotransmission (Magnusson et al., 2005), agonist concentration (Andrásfalvy Magee, 2001; Ali et al., 2000), and dendritic filtering effects caused by passive membrane properties (Spruston et al., 1993).

From my current study, the 10-90% rise time of MNTB-miniPSC is likely to represent the synaptic distance to the recording site. While agonist concentration can cause different rise times due to a coordination of postsynaptic receptor opening (Andrásfalvy and Magee, 2001; Ali et al., 2000) such a mechanism is unlikely to explain my data. This mechanism can not explain the relationship between unitary fiber strength and rise time in my study, because in WT at P8-11, rise times do not correlate with synaptic peak amplitudes, as would be expected if rise times were primarily determined by neurotransmitter concentration (Fig 2.4. B black dot). Secondly, with minimal stimulation I hardly observed an inflection in the rising slopes of synaptic responses, which would reflect individual vesicle release through uncoordinated synaptic transmission as demonstrated by Magnusson et al (2006). Thus, uncoordinated neurotransmission is not likely responsible for the rise time-peak amplitude relationship.

In the hippocampus, depending on the location of inhibitory synapses along soma-dendrites, the effects of the inhibitory synapses can differ. Perisomatic inhibition is efficient in preventing repetitive action potential firings, thus regulating the output of pyramidal neurons, while dendritic inhibition is efficient in suppressing calcium-dependent dendritic spikes (Miles et

al., 1996; Klausberger et al., 2003). In WT, stronger MNTB fibers, close to soma as implicated by faster rise time, will be effective to prevent repetitive firing following excitatory glutamatergic synaptic input from the CN, for example, by hearing activity. In KCC2-KD mice, MNTB-miniPSC and their rise time showed identical distribution as WT. i.e. stronger unitary inputs with faster rise time and weaker inputs are slower rise time. This suggests that whether MTNB synapses are matured as inhibitory synaptic inputs or not, the cellular contacts made by MNTB fibers seem to be determined mainly by strengthening of synapses.

Taken together, in KCC2-KD mice, the strengthened depolarizing MNTB synapse, with similar strength and kinetics, is expected to exert contrasting physiological effect into the LSO neurons than WT case. My study of the development of synaptic inputs from MNTB to the LSO indicates that inhibitory synapses undergo a robust process of maturation before hearing on-set, which occur independent of GABA/glycine response polarity. To my surprise, LSO neurons in KCC2-KD mice seem to fail to regulate its excitability through homeostatic mechanisms because of normal development of the depolarizing (and/or excitatory) MNTB and the conventional excitatory CN synaptic inputs, which is not different to WT.

3.0 KCC2 IS NECESSARY FOR THE FUNCTION OF THE CALYX OF HELD IN THE MEDIAL NUCLEUS OF TRAPEZOID BODY

3.1 INTRODUCTION

In LSO neurons, depolarizing GABA/glycine synapses undergo refinement through strengthening and elimination in KCC2-KD mice with no difference to WT. At later developmental ages at around hearing on-set, depolarizing MNTB-miniPSCs and MNTB-maxiPSCs shows normal developmental strengthening in the KCC2-KD mice, which does not attenuate conventional glutamatergic response from the CN (CN-mini and CN-max). This raises the question whether normal glutamatergic synaptic strength in the prolonged depolarizing GABA/glycinergic responses would be a general consequence or LSO neurons specific. Thus, I investigated glutamatergic synaptic response from the CN into another auditory brainstem nuclei, the Medial Nucleus of the Trapezoid Body (MNTB).

The principal neurons within the Medial Nucleus of the Trapezoid Body (MNTB) receive glutamatergic synaptic inputs from the contralateral cochlear nucleus (CN) (von Gersdorff and Borst, 2002). MNTB principal neurons then project to neurons in the ipsilateral lateral superior olive (LSO), thereby presenting the last inhibitory limb in the contralateral pathway to the LSO (Fig 1.1). The glutamatergic synaptic inputs from the CN to the MNTB are transferred by the calyx of Held, which is the largest and fastest synapse within the mammalian central nervous system (CNS). High fidelity coupled with unusually powerful synaptic strength enables the calyx of Held to accurately transmit fast sound information, up to 600 Hz in the adult (Wu and Kelly, 1993; Joshi et al., 2004; Taschenberger and von Gersdorff, 2000). Due to its large presynaptic structure, the calyx of Held has been widely used to study the pre- and post-synaptic mechanisms

that are responsible for the unique speed, strength, and fidelity of calyceal glutamatergic synaptic responses (von Gersdorff and Borst, 2002; Schneggenburger and Forsythe, 2006).

During development, synaptic contacts from the CN to the MNTB have been observed as early as P0, at which time the calyx takes the form of large and flat growth cones surrounding MNTB principal neurons. Even at this early stage, however, the contacts between pre- and post-synaptic partners are functional enough to elicit synaptic responses (Kandler and Friauf, 1993; Hoffpauir et al., 2006). In the first and second postnatal week, the calyx of Held undergoes drastic changes, both morphologically and functionally. Morphologically, the calyx begins to appear as a single process enveloping the MNTB cell surface. As development progresses, it becomes a more discontinuous structure with stalks and branches (Kandler and Friauf, 1993; Taschenberger et al., 2002). At the same time, quantal size increases, active zones become smaller, the surface area of the postsynaptic density (PSD) is reduced, and a larger pool of readily releasable vesicles is formed. Along with morphological maturation, important developmental refinement for high fidelity transmission is occurring. NMDA-mediated currents are decreased considerably (Futai et al., 2001; Taschenberger and von Gersdorff; 2000), presynaptic action potentials become briefer (Taschenberger and von Gersdorff, 2000), and there is also less AMPA receptor desensitization and changes in AMPA receptor subunit composition (Joshi et al., 2004; Wong et al., 2003; Renden et al., 2005). At P14 and before hearing onset, the calyx of Held has reached its adult-like structure and function, suggesting that its normal maturation can be completed without sensory driven activity.

A number of studies have focused on revealing the pre- and post-synaptic factors responsible for shaping the fast, high fidelity transmission of the calyx of Held during its maturation Nevertheless, surprisingly little is known about the role of neuronal activity in the development of the calyx of Held. In the MNTB, like in the LSO and many other brain areas, neurons also undergo a depolarizing to hyperpolarizing switch in the response to GABA/glycine (Awatramani et al., 2005). In this chapter, I investigated whether glutamatergic synaptic responses in the MNTB would be affected by the absence of the normal GABA/glycinergic switch to hyperpolarization. I applied electrophysiological method to compare the glutamatergic synaptic response from the MNTB neurons in WT and KCC2-KD mice at around hearing on-set.

3.2 MATERIAL AND METHODS

3.2.1 Animals, slice preparation, and genotyping

Experimental procedures are the same as described in Chapter I. 300 μm thick coronal brain slices were made from WT and KCC2-KD mice at P9~P12.

3.2.2 Electrophysiology

Electrophysiology experiments also follow the same procedures as described in Chapter I. Whole-cell voltage clamp recordings were made from principal neurons of the medial nucleus of the trapezoid body (MNTB). Glutamatergic responses were isolated with the $GABA_A$ receptor antagonist, SR95531 (10 μM) and the glycine receptor antagonist, strychnine (1 μM). Holding potentials were -70 mV. Signals were filtered at 10 kHz (Bessel filter, Axoclamp-1D, Axon Instruments, Foster City, California) and digitized at 10 kHz with a custom Labview acquisition program (5.0, National Instruments, Austin, Texas) and pClamp 10 (Axon Instruments). Kinetic analysis was performed using Mini analysis (6.0) and Clampfit (10.0). The fraction for decay time analysis was set as 0.001 in Mini analysis . SR95531 and strychnine were purchased from Sigma. Student's t-tests and Kolmogorov-Smirnov test were used for statistical analysis. The membrane properties of the MNTB neurons in KCC2-KD mice were not different to WT at P10~P11 (Resting membrane potential (mV); - 61.8 ± 0.5 for WT (n = 6), - 61.0 ±1.8 for KCC2-KD (n = 4), Input resistance (MΩ); 124 ± 13 (n = 6) for WT, 128 ± 3 (n = 4) for KCC2-KD, membrane capacitance (pF); 22.8 ± 1.3 (n = 6) for WT, 24.3 ± 1.7 (n = 4) for KCC2-KD mice) ($p > 0.5$ for each measurements). Number of animals used for each experimental group was more than three. For membrane properties, two animals were used.

3.3 RESULTS

3.3.1 Glutamatergic responses in the MNTB in WT mice

Similar to previous studies, I observed two types of glutamatergic responses in MNTB neurons from WT animals: calyceal and non-calyceal responses. Several criteria were used to distinguish calyceal and non-calyceal responses; amplitude, 10-90% rise time, on-set latency and decay time. As shown in Fig 3.1., the two types of synaptic responses could be clearly distinguished using those criteria. Calyceal responses were encountered in the majority of MNTB neurons (n = 20 / 29, 69%). Calyceal responses had a mean peak amplitude of 7.2 ± 0.5 nA, a 10-90% rise time of 0.26 ± 0.0 ms, an on-set latency of 1.2 ± 0.1 ms, time to peak of 1.7 ± 0.1 ms, and a decay time of 205 ± 21 ms. In contrast, mean non-calyceal responses were encountered more infrequently (n = 9 / 29, 31%). Non-calyceal responses had a peak amplitude of 0.7 ± 0.2 nA, a 10-90% rise time of 0.8 ± 0.2 ms, on-set latency of 3.4 ± 0.5, time to peak of 4.6 ± 0.6 ms, and a decay time of 19 ± 4 ms (Fig 3.1.) (Hamann et al., 2003). In addition, calyceal responses showed an all-or-none characteristic, since the response amplitudes elicited by minimal stimulation and maximal stimulation were not statistically different (~ 7 nA; Fig 3.1. A ~ C). In contrast, MNTB neurons with non-calyceal responses exhibited innervations by multiple fibers, since the peak amplitude increased in a step-wise manner in response to increased stimulation intensity, with more than two levels of response (Fig 3.1. D ~ E). In summary, large calyceal responses had faster 10-90% rise times, on-set latencies, and time-to-peak, and longer decay times. Smaller non-calyceal responses had longer 10-90% rise times, on-set latencies, and time to peak, and shorter decay times ($p < 0.001$ for each category).

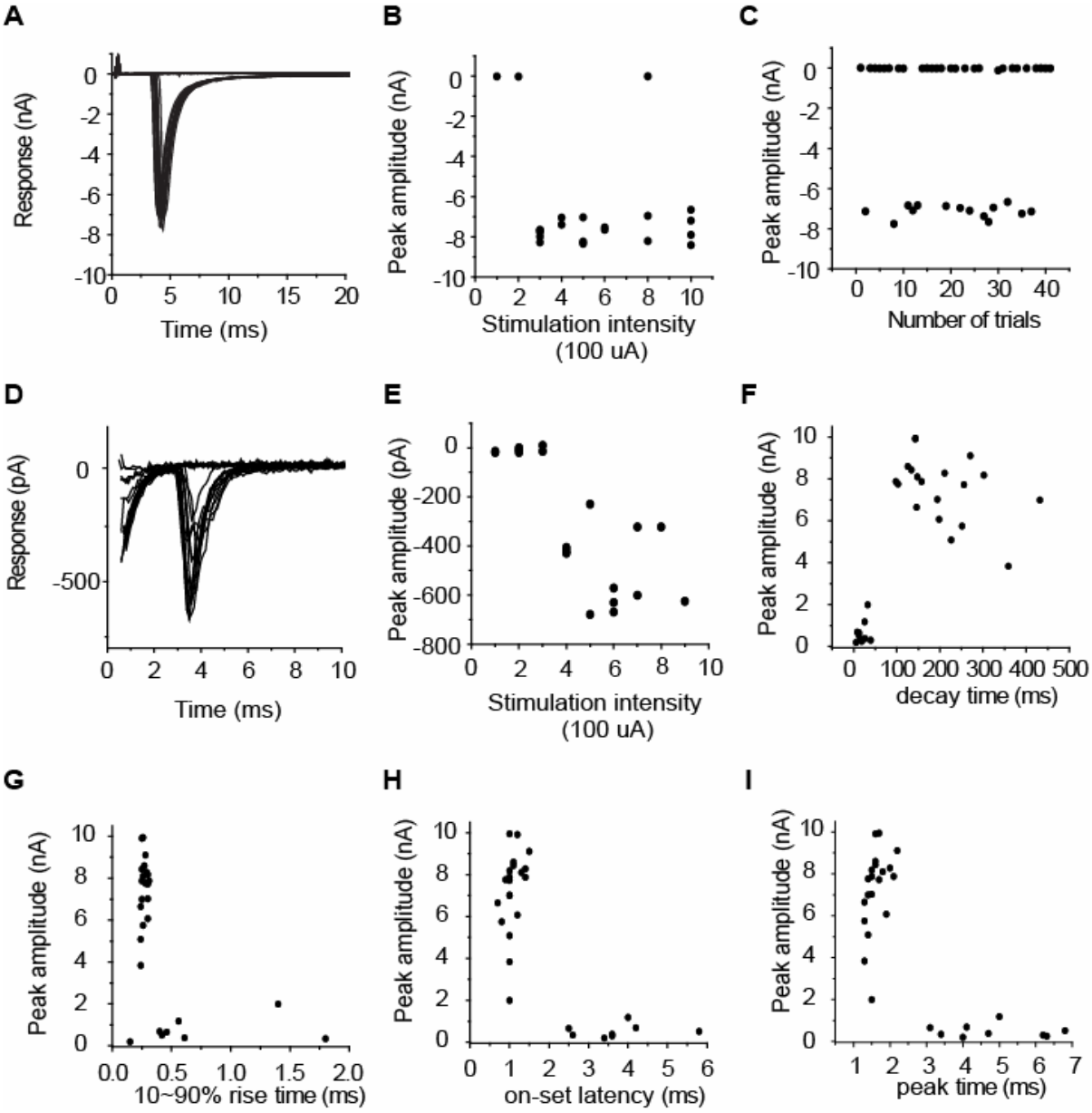
A
Response (nA)
Time (ms)
B
Peak amplitude (nA)
Stimulation intensity
(100 uA)
C
Peak amplitude (nA)
Number of trials
D
Response (pA)
Time (ms)
E
Peak amplitude (pA)
Stimulation intensity
(100 uA)
F
Peak amplitude (nA)
decay time (ms)
G
Peak amplitude (nA)
10~90% rise time (ms)
H
Peak amplitude (nA)
on-set latency (ms)
I
Peak amplitude (nA)
peak time (ms)

Figure 3.1.

Figure 3.1. Calyceal and non-calyceal responses in MNTB neurons of WT mice. **(A) - (C)** Examples of calyceal response from single MNTB neuron. **(A)** Calyceal responses were all-or-none as shown by superposing of individual failures and responses elicited by increasing stimulus intensities (100 μA -1000 μA). **(B)** Stimulus-response relationship. Maximal peak amplitude is 7.9 ± 0.1 nA. **(C)** The synaptic responses elicited by minimal stimulation. Average amplitude from success responses is 7.1 ± 0.1 nA, the failure rate is 66%. **(D) -(E)** Example of non-calyceal response **(D)** The synaptic responses elicited by increasing stimulus intensity are superimposed. **(E)** Stimulus-response relationship in response to increasing stimulus intensity. The peak amplitudes to the increasing stimulus intensity are plotted. (Maximal response amplitude was 0.7 ± 0.0 nA). **(F) - (I)** The kinetics of maximal responses are plotted against amplitude. **(F)** decay time, **(G)** 10-90% rise time **(H)** on-set latency **(I)** time to peak (n = 29).

3.3.2 Glutamatergic responses in the MNTB in KCC2-KD mice.

Next, I investigated whether the absence of the normal switch to GABA/glycinergic hyperpolarization would have any effect on glutamatergic responses in MNTB neurons. Calyceal and non-calyceal responses were also observed in KCC2-KD mice, although the distinction between calyceal and non-calyceal responses was not as clear as in WT. Nevertheless, there still appeared to be a difference in 10-90% rise time, on-set latency, time to peak, decay time, and amplitude between calyceal and non-calyceal responses. Examples of calyceal and non-calyceal responses are presented in Fig 3.2. ((A)~(B) for calyceal response, (C)~(D) for non-calyceal response). MNTB neurons with non-calyceal responses showed responses indicative of innervations by multiple fibers (Fig 3.2. (C)~(D)), similar to those seen in WT.

As a first step to investigate the effect of the absence of hyperpolarizing GABA/glycine responses on the calyx of Held function during development, I compared the peak amplitude of maximal glutamatergic responses in WT and KD. As shown by cumulative probability histogram, peak amplitudes of glutamatergic responses in MNTB neurons in KCC2-KD mice were considerably smaller than in WT ($p < 0.001$, KS test) (Fig 3.2. E) (mean ± s.e.m.; 5.2 ± 0.6 nA for WT ($n = 29$), 2.5 ± 0.5 nA for KD ($n = 29$)).

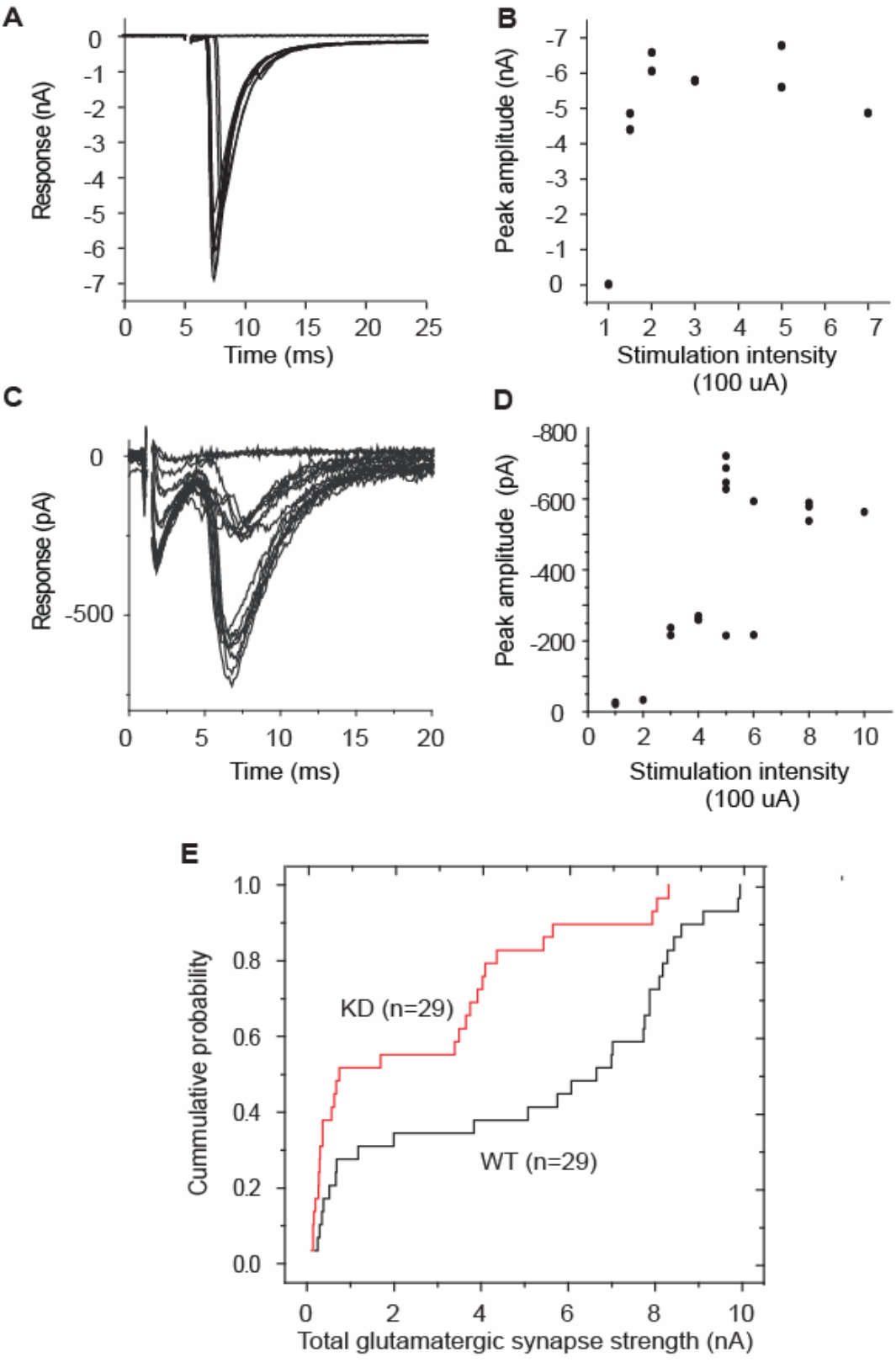
A
Response (nA)
0
-1
-2
-3
-4
-5
-6
-7
0
5
10
15
20
25
Time (ms)
B
Peak amplitude (nA)
-7
-6
-5
-4
-3
-2
-1
0
1
2
3
4
5
6
7
Stimulation intensity
(100 uA)
C
Response (pA)
0
-500
0
5
10
15
20
Time (ms)
D
Peak amplitude (pA)
-800
-600
-400
-200
0
0
2
4
6
8
10
Stimulation intensity
(100 uA)
E
Cummulative probability
1.0
0.8
0.6
0.4
0.2
0.0
KD (n=29)
WT (n=29)
0
2
4
6
8
10
Total glutamatergic synapse strength (nA)

Figure 3.2.

Figure 3.2. Glutamatergic responses were significantly smaller in KCC2-KD.

(A) - (B) Example of calyceal responses. **(A)** The synaptic responses elicited by increasing stimulus intensity are superimposed. **(B)** Stimulus-response relationship in response to increasing stimulus intensities. The peak responses to the increasing stimulus intensity are plotted. (maximal response: 6.1 ± 0.2 nA). **(C) ~ (D)** Example of non-calyceal responses. **(C)** The synaptic responses elicited by increasing stimulus intensity are superimposed. **(D)** Stimulus-response relationship in response to increasing stimulus intensity. The peak responses to the increasing stimulus intensity are plotted (maximal response amplitude: 0.7 ± 0.0 nA). **(E)** Cumulative probability for the total glutamatergic synaptic strength for WT and KCC2-KD mice. Black line for WT (n = 29) and red line for KCC2-KD (n=29). Average amplitude (mean ± s.e.m.); 5.2 ± 0.7 nA for WT, 2.5 ± 0.5 nA ($p < 0.001$, K-S test).

3.3.3 Reduced amplitudes of calyceal responses in KCC2-KD mice

The reduced strength of glutamatergic synapses in KCC2-KD mice could be due to either: 1) fewer neurons that receive calyceal synaptic inputs, suggested by the large difference in peak amplitude between calyceal and non-calyceal responses, or 2) reduction in the overall synaptic strength. In order to differentiate between these two possibilities, I first identified calyceal and non-calyceal responses in KCC2-KD mice. Since the kinetic analysis of responses in WT was well suited to distinguish between calyceal and non-calyceal responses (Fig 3.1.), I analyzed the response kinetics of peak amplitudes in KCC2-KD mice.

The kinetic analysis in KD mice resulted in similar distinguishing characteristics of calyceal and non-calyceal response (Fig 3.3.). The 10-90% rise time of faster responses was 0.3 ± 0.0 ms (n = 12), while the rise times in slower responses was 0.9 ± 0.2 ms (n = 11) ($p < 0.05$). The on-set latency of faster responses was 1.1 ± 0.1 ms (n = 18), while the slower one was 3.5 ± 0.2 ms (n = 10) ($p < 0.001$). The time to peak of faster responses was 1.8 ± 0.1 (n = 17), while the slower responses had time to peak of 5.0 ± 0.3, n=12 ($p < 0.001$). The decay time of slower responses was 243 ± 32 ms (n = 17), while the faster one was 28 ± 4 ms (n = 12). Of the four kinetic analysis categories, the time to peak most accurately reflected whether the response was calyceal or non-calyceal irrespective of the amplitude of the response (Fig 3.1. I and Fig 3.3. D). Accordingly, I categorized calyceal and non-calyceal responses based on the time to peak. The average amplitude for responses showing a faster time to peak (1.8 ± 0.1) was 4.1 ± 0.6 nA (n = 17) and the average amplitude for responses with a slower time to peak (5.0 ± 0.3) was 0.3 ± 0.0 nA (n = 12) (Fig 3.3. E and F). This suggests that the averaged peak amplitude of the calyx of Held in KCC2-KD mice is 4.1 ± 0.4 nA (n = 17). In KCC2-KD mice, 59% of MNTB neurons exhibited calyceal responses, suggesting that the number of neurons with calyceal response was not different from WT ($p > 0.05$). The average response amplitude of non-calyceal responses was not different between WT and KD mice either (0.5 ± 0.1 nA for WT (n = 9), 0.3 ± 0.1 nA for KD (n = 12), $p > 0.1$) (Fig 3.3. F).

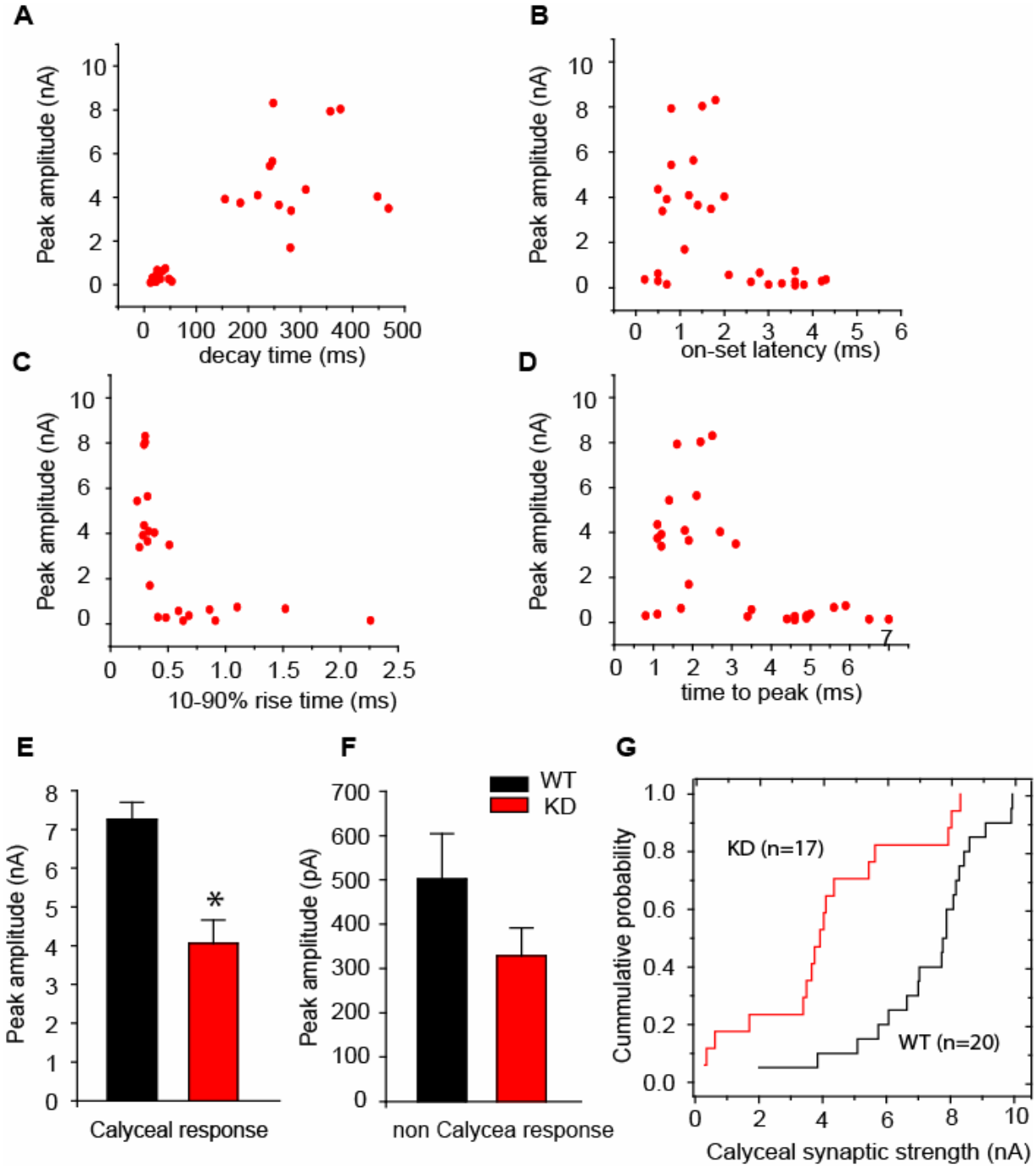
A
Peak amplitude (nA)
decay time (ms)
B
Peak amplitude (nA)
on-set latency (ms)
C
Peak amplitude (nA)
10-90% rise time (ms)
D
Peak amplitude (nA)
time to peak (ms)
E
Peak amplitude (nA)
Calyceal response
F
WT
KD
Peak amplitude (pA)
non Calycea response
G
Cummulative probability
KD (n=17)
WT (n=20)
Calyceal synaptic strength (nA)

Figure 3.3.

Figure 3.3. Calyceal responses were considerably smaller in KCC2-KD mice.

(A) - (D) The kinetics of maximal responses are plotted against amplitude. **(A)** decay time, **(B)** on-set latency **(C)** 10-90% rise time **(D)** time to peak (n = 29). **(E).** Mean peak amplitudes for calyceal responses 7.3 ± 0.4 nA (n = 20) for WT, 4.1 ± 0.6 nA (n = 17) for KD. The mean amplitude of calyceal responses was considerably smaller in KCC2-KD mice (*: $p < 0.001$, Student t-test). **(F)** Mean peak amplitude for non-calyceal response: 0.5 ± 0.1 nA (n = 9) for WT, 0.3 ± 0.1 nA (n = 12) for KD ($p > 0.1$). **(G)** Cumulative probability histogram for the strength of glutamatergic responses. Black line for WT, red line for KD ($p < 0.001$, KS test).

However, the peak amplitude of calyceal responses in KCC2-KD mice was significantly smaller than WT (Fig 3.3. E and G) (7.3 ± 0.4 nA (n = 20) for WT, 4.1 ± 0.6 nA (n = 17) for KD, $p < 0.001$), suggesting that in KCC2-KD mice, calyceal synaptic responses are significantly reduced.

3.3.4 Activity dependent depression of calyceal responses in KCC2-KD mice

Interestingly, among calyceal responses in KCC2-KD mice, 30% of the calyceal responses had a peak amplitude that decreased gradually upon repeated stimulation (n = 5 / 17) until it finally disappeared (Fig 3.4.). Although it initially appeared that these neurons received multiple calyceal inputs as shown in Fig 3.4. A, the multiple amplitude steps can be attributed to a single calyx of Held because: 1) the decreased amplitude was induced by the same stimulation intensity (Fig 3.4. C), and 2) there was no relationship between stimulus intensity and response amplitude; i.e. the increased stimulation intensity did not increase the response amplitude, nor did it recover the missing response (Fig 3.4. B). Surprisingly, the gradual reduction of amplitude was seen when stimuli were delivered at 0.1 Hz, a very low stimulation frequency for this ultra-fast and reliable synapse. In WT mice, this stimulation frequency never produced depression of calyceal responses consistent with previous studies (Futai et al., 2001; Taschenberger et al., 2002; Wong et al., 2003).

In addition to the gradual reduction (disappearance) upon repeated, low-frequency stimulation, the remaining calyceal responses in KCC2-KD mice which did not show gradual reduction showed increased synaptic depression with high frequency stimulation. In order to investigate synaptic depression in KCC2-KD mice further, I first applied a 0.1 Hz stimulus to measure the amplitude of calyceal responses, which was followed by 15 trains of 100Hz stimulation (Fig 3.5. A and B). The amount of depression at the 14~15th response was compared to the peak amplitude of the response to the 1st stimulus. The synaptic depression caused by the 15 trains was considerably smaller in KCC2-KD mice than in WT mice. In fact, increased synaptic depression in KCC2-KD mice also present with 0.1 Hz stimulation ($p < 0.05$) (Fig 3.5. (C), open square for WT, open circle for KD). With 100 Hz stimulation, the difference in synaptic depression between WT and KCC2-KD mice became even larger.

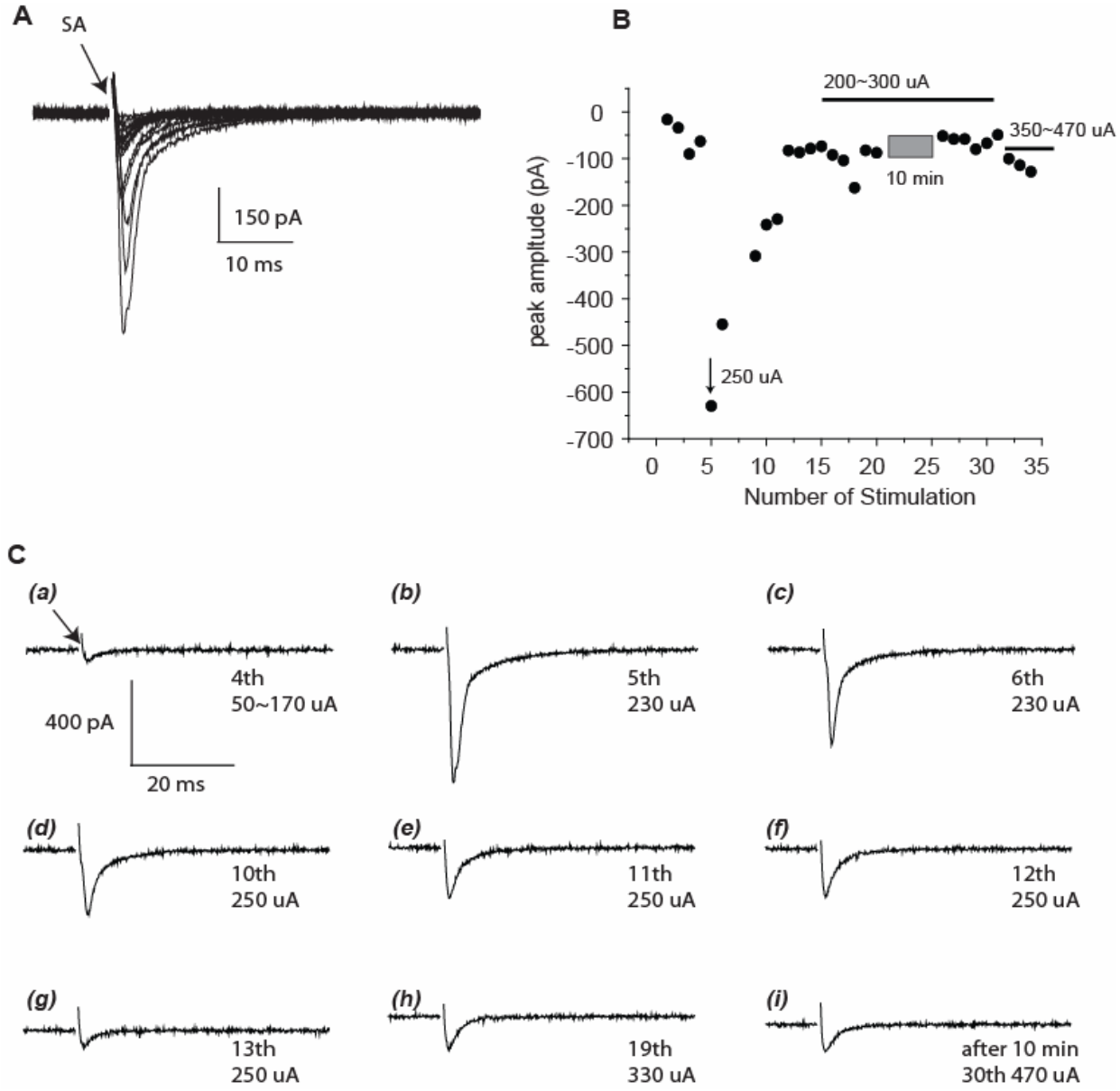
A
SA
150 pA
10 ms
B
200~300 uA
350~470 uA
10 min
250 uA
peak amplitude (pA)
0
-100
-200
-300
-400
-500
-600
-700
0
5
10
15
20
25
30
35
Number of Stimulation
C
(a)
4th
50~170 uA
400 pA
20 ms
(b)
5th
230 uA
(c)
6th
230 uA
(d)
10th
250 uA
(e)
11th
250 uA
(f)
12th
250 uA
(g)
13th
250 uA
(h)
19th
330 uA
(i)
after 10 min
30th 470 uA

Figure 3.4.

Figure 3.4. Activity dependent decrease of calyceal responses in KCC2-KD mice.
(A) Individual calyceal responses elicited by identical stimulus intensity are superimposed. (SA; stimulus artifact) **(B)** Peak amplitudes are plotted against number of stimulation. Stimulus intensity for each response is indicated above bars. Stimulation frequency was 0.1 Hz. Gray bar: no stimulation was applied for 10 min. **(C)** Response examples from responses shown in **(B)**. ***(a)*** No-response trace (4^{th} data point in (B)) ***(b)*** First response elicited with 230 uA (5^{th} data point) ***(c)*** Second response elicited with 230 uA (6^{th} data point) ***(d) - (f)*** Sixth to eighth response elicited with 250 uA (10^{th} ~12^{th} data point) ***(g)*** no response was elicited with 250 uA (13^{th} data point) (h) no response was elicited with 330 uA (19^{th} data point) ***(i)*** no response was elicited with 470 uA after 10 minutes without stimulation. (Arrow: stimulus artifact).

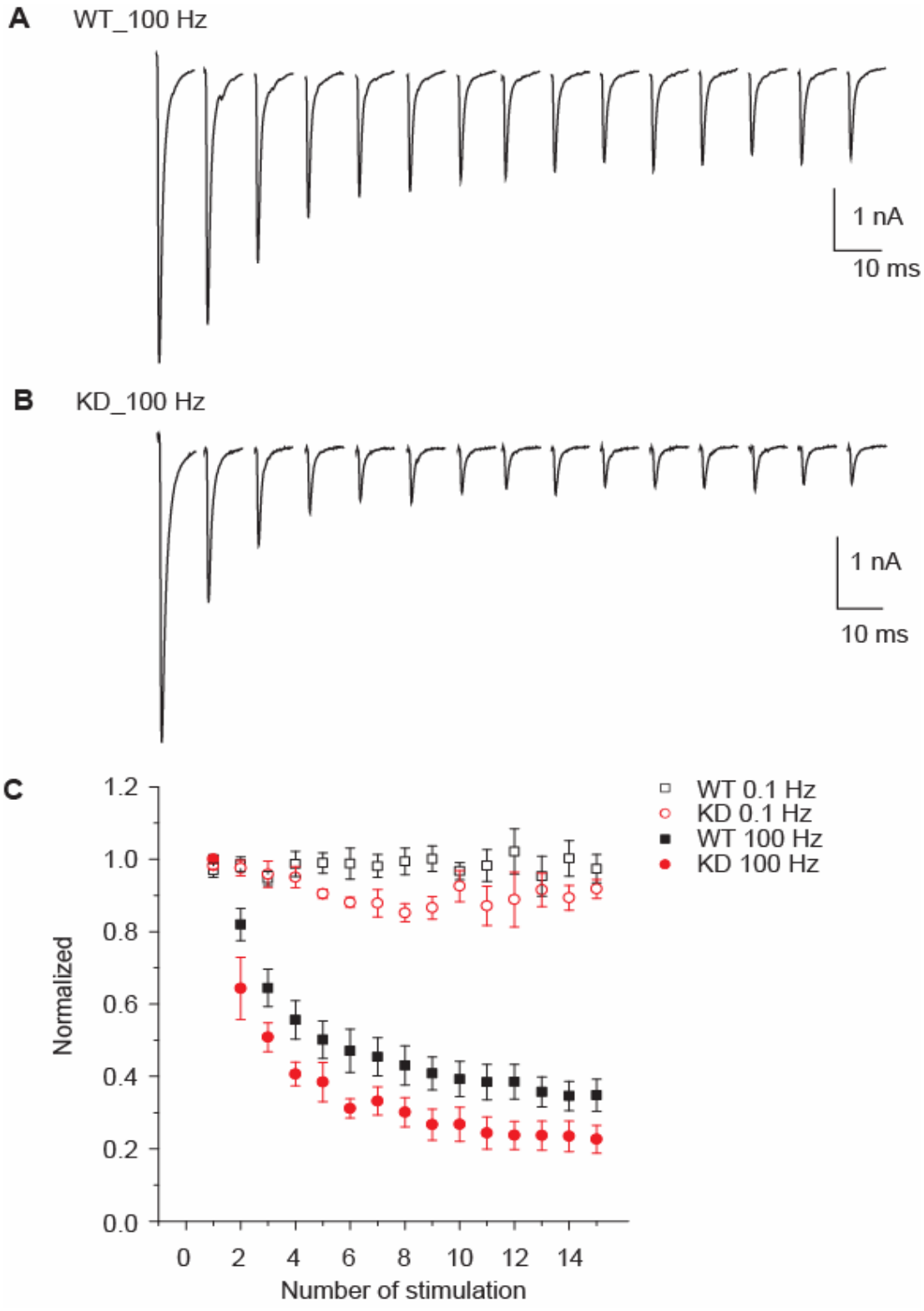
A
WT_100 Hz
1 nA
10 ms
B
KD_100 Hz
1 nA
10 ms
C
WT 0.1 Hz
KD 0.1 Hz
WT 100 Hz
KD 100 Hz
Normalized
1.2
1.0
0.8
0.6
0.4
0.2
0.0
0
2
4
6
8
10
12
14
Number of stimulation

Figure 3.5.

Figure 3.5. Short-term synaptic depression induced by high frequency stimulation was larger in KCC2-KD mice.

(A) - (B) Trains of 15 responses elicited by high frequency stimulation (100 Hz). **(A)** for WT, **(B)** for KCC2-KD **(C)** Synaptic depression by high frequency stimulation was larger in KCC2-KD mice. Responses amplitudes were normalized to the peak amplitude of the 1st stimulation (□; WT 0.1 Hz, ○; KD 0.1 Hz, ■; WT 100 Hz, ●; KD 100 Hz). ($p < 0.05$ for 0.1 Hz at 14~15 th stimulation (n=9 for WT, n=10 for KD), $p < 0.001$ for 100 Hz at 14 ~15 th stimulation (n=12 for WT, n=14 for KD)).

With 100 Hz, synaptic depression for WT was 65.2 ± 0.0 % (n = 6). For KD, synaptic depression was by 77.4 ± 0.0 % (n = 7) ($p < 0.001$, Fig 3.5. C, closed square for WT, closed circle for KD), suggesting that without GABA/glycinergic hyperpolarization, calyceal responses undergo more synaptic depression after repetitive stimulation.

The reduced amplitude of calyceal responses in KCC2-KD mice (either gradual reduction by low frequency stimulation or synaptic depression by repetitive high frequency stimulation) suggests that the developmental switch of hyperpolarizational GABA/glycinergic response is necessary for the maintenance or maturation of glutamatergic synaptic strength in the calyx of Held within the MTNB.

3.4 DISCUSSION

In contrast to the lack of a change in the strength of glutamatergic synapses in the LSO, the strength of glutamatergic synapses in the MNTB was considerably decreased, due primarily to the decreased amplitude of the calyx of Held response in the KCC2-KD mice around hearing on-set. The calyx of Held response in KCC2-KD mice showed an activity-dependent reduction in amplitude after low frequency stimulation (0.1 Hz), along with increased synaptic depression following high frequency stimulation (100 Hz). These data suggest that the developmental switch to GABA/glycinergic hyperpolarization (hyperpolarizing E_{Cl}) is necessary for the maintenance and/or maturation of the normal function of the calyx of Held in the MNTB.

Compared to our extensive knowledge of the pre- and post-synaptic mechanisms underlying functional maturation of the calyx of Held (von Gersdorff and Borst, 2002), remarkably little is known about mechanisms responsible for maintaining or developing the strength of the calyx of Held. In contrast to the many other components of the auditory brainstem, the calyx of Held does not seem to undergo significant developmental strengthening during neonatal development, since its strength has already almost reached its mature level by P4~5 (Taschenberger ad von Gersdorff, 2000; Hoffpauir et al., 2006; for contrary results, refer to Futai et al, 2001). In addition, changing normal neuronal activity does not cause a reduction or delayed maturation in the strengthening of the calyx of Held synapses (Oleskevich et al., 2004; Erazo-Fischer et al., 2007). Thus, the reduced amplitude of the calyx of Held response in KCC2-KD mice provides a unique condition in which mechanisms for the maintenance (or development) of the calyx of Held can be investigated. Although exact mechanisms for synaptic depression in KCC2-KD mice are not known, several possible mechanisms might contribute to synaptic depression at the calyx of Held. I would like to discuss some possible mechanisms that

might explain the abnormal function of the calyx observed in KCC2-KD mice in relation to the disturbed chloride homeostasis.

First, the greater synaptic depression in KCC2-KD mice could be explained through presynaptic mechanisms, involving complex interactions of presynaptic receptors such as metabotropic glutamate receptors (Group III mGluR) (Barnes-Davies and Forsythe, 1995; Renden et al., 2005) or $GABA_B$ receptors (Takahashi et al., 1998; Isaacson, 1998; Turecek and Trussell, 2001). However, the role of mGluRs in synaptic depression is somewhat controversial since an mGluR specific antagonist did not have an effect on the synaptic depression in the calyx of Held (von Gersdorff et al., 1997; Billups et al., 2005). Any potential effect of mGluRs also seems to be different depending on developmental stages, since a greater effect was seen at P10~12 than the little effect observed around P18 (Renden et al., 2005). Still, the developmental reduction of effect of mGluRs on synaptic transmission does not correspond to the ages when my current study is conducted.

GABAergic activation of another metabotropic receptor, the $GABA_B$ receptor, reduces the calyx of Held EPSC considerably (Takahashi et al., 1998; Isaacson, 1998; Turecek and Trussell, 2001). In the calyx of Held nerve terminal, the chloride concentration is maintained high so that E_{Cl} is depolarizing (Price and Trussell, 2006). However, even when E_{Cl} is depolarized, presynaptic GABA and glycine can exert opposing effects on glutamatergic synaptic responses by differently affecting the release of glutamate. For example, when it activates presynaptic $GABA_B$ receptors, of which activation reduces calcium influx (Takahashi et al., 1998; Isaacson, 1998). Thus, GABA reduces the amplitude of calyceal EPSCs by more than 50%. In contrast, glycine increases EPSC amplitude by opening the glycine-gated chloride channel (Turecek and Trussell, 2001; Forsythe and Clements 1990; Scanziani et al., 1992), thus increasing calcium influx through voltage-gated calcium channels due to the depolarizing E_{Cl}. Thus, prevailing activity by GABA, if it is present, through $GABA_B$ in KCC2-KD mice could reduce glutamate release considerably as demonstrated in Fig 3.3. However, no evidence has clearly demonstrated that differential chloride homeostasis might affect $GABA_B$ ($GABA_B$ 1 and 2) expression level, which can support the assumption that $GABA_B$ activity might be higher in KCC2-KD mice at around hearing on-set. Although developmental down regulation of the

$GABA_B$ 1 subunit has been observed starting from P15 within rat hippocampus, the expression of $GABA_B$ 2 does not change during development (Fritschy et al., 1999; López-Bendito et al., 2004). In addition, agonist binding affinity is increased by 10 fold during the same period when $GABA_B$1 expression level is decreasing, probably due to the developmental regulation of intracellular binding proteins. Thus, the complexity of the functional development of $GABA_B$ signaling systems makes it difficult to predict the functional relevance of decreased immunoreactivity in terms of decreased $GABA_B$ function (Malitschek et al., 1998). Also, in conditions where E_{Cl} is depolarizing in the adult brain, such as seizure or epilepsy, the changes in $GABA_B$ expression level vary greatly, with no demonstration of consistency. For example, $GABA_B$ receptor immunoreactivity increased after kindling seizure in rat (Kokaia and Kokaia, 2001). On the other hand, kindling induced seizure caused a rapid loss of $GABA_B$ receptor staining in CA1, accompanied by long-term upregulation in dentate gyrus granule cells in rat (Straessle et al., 2003). Also, there was no change in $GABA_B$ expression in the hippocampus of gerbils after seizure (Park et al., 2004). Based on these highly variable observations, it is not likely that chloride homeostasis has an effect on the functional expression of $GABA_B$ receptors.

Also, in the calyx of Held, there are no known axo-axonic synapses which can elicit GABA and/or glycinergic effects on glutamatergic responses mimicking synaptic activity *in-vivo*. Thus if $GABA_B$ activation is responsible for my experimental condition, reduced glutamatergic responses in KCC2-KD mice through $GABA_B$ should be due to spillover from GABA/glycinergic synapses (Isaacson et al., 1993), and be identifiable as a di-synaptic event in my recordings. However, the on-set latency of calyceal responses in KCC2-KD mice are not different from WT, implying that synaptic responses measured after axonal pathway stimulation woule be through mono-synaptic responses in both WT and KCC2-KD mice. Thus, the reduced calyceal response in KCC2-KD mice is not likely due to $GABA_B$ activation on the nerve terminal (Fig 3.3.). In addition, GABA spillover could not be observed *in- vivo* (R. Turecek, unpublished observations, Awatramani et al., 2005), suggesting that any presynaptic effect involving $GABA_B$ is not likely to explain the reduced glutamatergic synaptic strength seen in KCC2-KD mice.

A reduced number of vesicles or quantity of neurotransmitter within a single vesicle might also explain the reduced amplitude of calyx of Held responses in KCC2-KD mice, since

intracellular chloride can have an effect on glutamate loading and endocytosis of synaptic vesicles. Previously it has been shown that $[Cl^-]_i$ greater than 20 mM in the nerve terminal can inhibit glutamate loading into synaptic vesicles (Tabb et al., 1992; Varoqui et al., 2002) and causes slow endocytosis (Hull and von Gersdorff, 2004). However, a contrasting result seems to be suggested by Price and Trussell (2006), where they demonstrates that varying the intracellular chloride concentrations in the calyx of Held using whole cell patch clamp of the nerve terminal (clamped at 5-100 mM) do not affect miniature EPSC amplitude in MNTB neurons (Price and Trussell, 2006), suggesting that chloride concentration might not have an effect on glutamate loading. However, chloride concentration is difficult to clamp using whole-cell mode as demonstrated by DeFazio et al (2000), who have demonstrated that there is a 40% disparity between the intracellular chloride concentration of the pipette solution and the chloride concentration estimated from E_{Cl} measured by whole-cell patch clamp mode in the presence of chloride regulatory machinery. Also, previous studies that loaded chloride using an intracellular pipette *in-vitro* are not likely to reflect the true effect of chloride concentration *in-vivo*, especially the long-term accumulating effect taking place during development in KCC2-KD mice. Considering this controversial effect of chloride on presynaptic mechanisms of modulating synaptic strength, it is necessary to further investigate the presynaptic effects of KCC2-KD, possibly through the use of the electron microscopy (EM) to determine if the number of vesicles is changed, or by measuring quantal content through mEPSCs (Taschenberger et al., 2002).

Postsynaptically several developmental changes contribute to the strong, yet high fidelity synaptic transmission in the calyx of Held synapse, most of which are complete by hearing on-set. First, the NMDA component is decreased by 50 % between first and second postnatal week in rats. Since the NMDA mediated component decays with a longer time constant, it contributes considerably to the failed synaptic responses following high frequency stimulation. Thus, the reduced NMDA mediated synaptic transmission in mature synapses is beneficial to prevent failure following high frequency auditory stimulation (Futai et al., 2001; Taschenberger and von Gersdorff 2000). If develo1pmental down-regulation of NMDA receptors is impaired in KCC2-KD mice, the NMDA receptor-mediated component would remain high, providing a possible explanation for the increased failure rate following 100 Hz stimulation (example trace not shown) and greater synaptic depression observed in KCC2-KD mice (Fig 3.5).

Concurrent with the reduction in NMDA receptor-mediated current, AMPA receptors also undergo a series of developmental changes. AMPA receptors are heteromeric receptors composed of GluR subunits 1~4. The presence or absence of GluR2 determines the receptors permeability to Ca^{2+}, since GluR2 prevents Ca^{2+} permeability (Hollmann et al., 1991). In MNTB, it was shown that AMPA receptors do not contain GluR2 throughout development, suggesting they are Ca^{2+} permeable throughout the entire developmental period (Joshi et al., 2004). However, during development, AMPA receptors in MNTB shift from containing mainly GluR1 to primarily GluR3/4 subunits. The developmental increase of GluR4-containing AMPA receptors in MNTB neurons could explain the faster decay time of mature calyx of Held responses, as shown in both the rat and chick auditory systems (Geiger et al., 1995; Ravindranathan et al., 2000; Joshi et al., 2004).

Furthermore, GluR4 subunits in the mature calyx of Held are the "flop" variant (Koike-Tani et al., 2005; Joshi et al., 2004), which conveys resistance to receptor desensitization (Trussell et al., 1993; Otis et al., 1996; Taschenberger et al., 2002; Wong et al., 2003). However, in younger ages, the degree of AMPA receptor desensitization is higher due to a high level of AMPA receptors containing the "flip" splice variant. AMPA receptors in MNTB neurons undergo the transition from GluR4_flip to GluR4_flop primarily during the first two postnatal weeks when GABA/glycinergic responses switch from depolarizing to hyperpolarizing (Awatramani et al., 2005), suggesting that there might be a correlation between chloride homeostasis and AMPA receptor subunit changes, especially for the GluR4 splice variants. The immature form of AMPA receptors also display slower recovery from AMPA receptor desensitization (~ 9 sec at P7/8 and ~3 sec at P11/12) (Joshi and Wang, 2002), which might also contribute to the greater synaptic depression in KCC2-KD mice. (Barnes-Davies and Forsythe, 1995; Taschenberger et al., 2002). The likely high amount of GluR4 "flip" splice variant-containing AMPARs in KCC2-KD mice could contribute to the greater synaptic depression following high frequency stimulation, as well as the increased failure rate following repetitive stimuli (Taschenberger et al., 2002).

.

Can increased AMPA receptor desensitization (or slower recovery from desensitization) explain the activity dependent reduction of calyceal responses shown in Fig 3.4.? In KCC2-KD mice, 30% of calyceal responses showed a disappearance of the calyceal response following repetitive activation. However, in order to elicit this unexpected gradual reduction and disappearance, high frequency stimulation was not necessary, indicating that glutamate binding to the postsynaptic receptor itself might be sufficient to induce reduction of the synaptic response. In addition, the missing responses did not recover even after several minutes without synaptic activation, suggesting that the available number of AMPA receptors might be considerably reduced, and even eventually absent from the membrane surface altogether. Because the recovery time of AMPA receptor desensitization and endocytosis is shorter than the time course I observed (Fig 3.4), it might not adequately explain the gradual, activity-dependent reduction of the calyx of Held response.

Regulation of AMPA receptor mobility by activity has been long been known to play a key role in excitatory synaptic plasticity. Treatment with AMPA receptor antagonists causes an increase in AMPA receptors on the membrane surface (Liao et al., 1999; O'Brien et al., 1998). Rapid delivery of AMPA receptors into synaptic sites following an LTP-eliciting protocol also takes place in an NMDA receptor-activity dependent manner (Shi et al., 1999; Hayashi et al., 2000), important for both an increased number of functional synapses and synapse stabilization. $GABA_A$ receptor blockade by an antagonist also reduces AMPA receptor insertion in cultured neurons (Lissin et al., 1998). Consistent with the effects of treatment with the $GABA_A$ receptor antagonist, a prolonged increase in activity in cultured neurons causes a decrease of miniature AMPA amplitude (Turrigiano et al., 1998). AMPA receptor mobilization is rapid; AMPA receptor loss from synaptic sites could be detected as soon as 5 minutes after agonist treatment. For the AMPA receptor motility, AMPA receptor activity in particular is required since depolarization by high potassium in the bath fails to change AMPA receptor mobility (Lissin et al., 1999).

AMPA receptor loss from synaptic sites following activation resembles what was observed in KCC2-KD mice, suggesting that AMPA receptors might be internalized and undergo the degradative endocytosis pathway, as suggested by Ehlers (2000). Through this pathway,

AMPA receptors would be targeted to late endosomes or lysosomes, finally being degraded and reducing the number of AMPA receptors expressed at the surface (Ehlers, 2000). After AMPA receptors are activated, they can either undergo recycling into the synaptic site or degradation in a NMDA receptor dependent manner. NMDA receptor activity is necessary for the AMPA receptor reinsertion since AMPA receptor activity without NMDA activity prevents AMPA receptors from being inserted into the surface for 60 min. Therefore, in the absence of NMDA receptor activation, a considerable number of AMPA receptors would undergo degradation, which could explain the reduced amplitude of the calyx of Held response in KCC2-KD mice (Fig 3.3). In summary, additional studies investigating both NMDA receptor-mediated and AMPA receptor modifications in KCC2-KD mice are necessary to more fully elucidate the mechanisms underlying the impaired function of the calyx of Held.

Previously, a reduction in the calyx of Held response had not been demonstrated in any activity modified environment. For example, *dn/dn* mice, which exhibit hereditary deafness due to the disruption of hair cell function (Pujol et al., 1983; Marcotti et al., 2006), do not display a significant difference in the strength of the calyx of Held, even though there was an increase in the strength of the endbulb synapse in the anteroventral cochlear nucleus (AVCN) (Youssoufian et al. 2005; Oleskevich et al., 2004). In addition, in Cav1.3 knock-out mice, which lack spontaneous nerve activity due to an inability of the inner hair cells (IHCs) to fire calcium-action potentials (Platzer et al., 2000), the amplitude of AMPA-mediated synaptic responses are larger at P14~P17 (Erazo-Fischer et al., 2007).

Considering the lack of previous studies investigating the mechanisms of the maintenance of the calyx of Held, the reduced calyceal synaptic strength in KCC2-KD mice seems to be the first system in which the mechanisms responsible for the strengthening (or maintenance) of the calyx of Held can be addressed. In conclusion, my study illustrates the importance of the developmental switch of GABA/glycinergic responses from depolarizing to hyperpolarizing in maintaining the strength of the calyx of Held synapses within the MNTB.

4.0 KCC2 EXPRESSION IN IMMATURE RAT CORTICAL NEURONS IS SUFFICIENT TO SWITCH THE POLARITY OF GABA RESPONSES

4.1 INTRODUCTION

In Chapter II~III, I investigated how a neural circuit develops when GABA/glycine response remain depolarizing. However, little is known about how neural circuit develops in the absence of developmental depolarizing (excitatory) GABA/glycinergic response. This is mainly due to the lack of tools to prematurely switch the polarity of GABA/glycine response to hyperpolarizing. Thus, in this Chapter, I describe my attempts to develop an experimental method to render GABA/glycinergic hyperpolarizing. The results from this Chapter have been published (Lee et al., 2005).

GABA and glycine, the major inhibitory neurotransmitters in the central nervous system, activate ligand-gated anion channels that are primarily permeable to chloride. In mature neurons, opening of a $GABA_A$ receptors or glycine receptors leads to membrane hyperpolarization (Bormann et al., 1987). In the immature brain, however, GABA and glycine, via activation of $GABA_A$ and glycine receptors, produce membrane depolarizations and, in many cases, are considered to be transiently excitatory (Ben Ari, 2002; Kandler et al., 2002). The developmental conversion from excitatory to inhibitory is caused by a decrease in the intracellular Cl concentration ($[Cl]_i$; Owens et al., 1996; Ehrlich et al., 1999; Rivera et al., 1999). In immature neurons, the electrochemical equilibrium potential for chloride (E_{Cl}) lies above the resting membrane potential (V_{rest}) and, as a result, activation of $GABA_A$ or glycine receptors results in a net efflux of Cl and membrane depolarization. During maturation, regulation of Cl shifts E_{Cl} values negative to V_{rest} and activation of $GABA_A$ or glycine receptors produces Cl influx and membrane hyperpolarization.

The neuron-specific potassium chloride cotransporter KCC2 (Payne et al., 1996; Payne, 1997) plays an important role in generating and maintaining an E_{Cl} below V_{rest}. This is supported by a number of studies that have demonstrated a correlation between the GABA reversal potential (E_{GABA}) and the expression level (Clayton et al., 1998; Lu et al., 1999; Rivera et al., 1999; Coull et al., 2003; Galanopoulou et al., 2003; Shibata et al., 2004; Stein et al., 2004), membrane location (Balakrishnan et al., 2003), phosphorylation (Kelsch et al., 2001; Vale et al., 2003), and/or activity of KCC2 (Woodin et al., 2003). Loss-of-function studies using antisense KCC2 RNA (Rivera et al., 1999), targeted gene knockout (Hubner et al., 2001), or gene knockdown (Woo et al., 2002; Zhu et al., 2005) have shown that KCC2 is necessary for creating and maintaining a low $[Cl]_i$. However, it has yet to be established whether KCC2 is also sufficient, in and of itself, for decreasing E_{Cl}. Here, I have addressed this issue by prematurely over-expressing human KCC2, hKCC2 (Song et al., 2002) in tissue culture of embryonic cortical neurons which, lack or have a very low level of KCC2. Parts of the data presented here have been published previously in abstract form (Lee et al., 2003).

4.2 MATERIALS AND METHODS

4.2.1 Subcloning of hKCC2

hKCC2 was subcloned into pMES vector, which contains a cytomegalovirus enhancer, a β-actin promoter (Swartz et al., 2001) and an internal ribosome entry site (IRES), followed by an enhanced green fluorescence protein (EGFP) sequence (Fig. 4.1.).

4.2.2 Transfection of COS7 cells and cortical neurons

COS7 cells were maintained in 5% CO_2 at 37 °C in Dulbecco's modified Eagle's-H21 medium with 10% Cosmic calf serum containing penicillin and streptomycin. For transfection, cells were electroporated (0.4 kV; 1070 microfarads) with 10 µg of DNA per 15-cm plate. Cortical primary cultures were prepared from embryonic day 17 rat fetuses as previously described (Hartnett et al., 1997). Rat fetuses were obtained from timed-pregnant Sprague-Dawley rats, killed by CO_2 inhalation following procedures in accordance with USA National Institute of Health, guidelines and approved by the Institutional Animal Care and Use Committee at the University of Pittsburgh. After three days in culture, cells were transfected with 1.5 µg of plasmid DNA per well using LipofectAMINE 2000 (Life Technologies, Inc., Grand Island, NY, USA) as previously described (Pal et al., 2003).

4.2.3 Immunoblotting

Two days following transfection, COS7 cells were fractionized by sonification and the non-nuclear fraction was centrifuged (35 000 r.p.m., SW 55 Ti rotor, Beckman for 35 min, 4 °C). The membrane pellet was re-suspended in SDS sample buffer (New England Biolabs, Beverly, MA, USA), and 50 µg of protein was separated by electrophoresis through 8.5% SDS-

polyacrylamide gel. Proteins were transferred to nitrocellulose membrane. KCC2 protein was visualized by enhanced chemiluminescence (Pierce, Rockford, IL, USA) using affinity purified polyclonal anti-rat KCC2 [1 : 2000, 2 h at room temperature (RT)] (Upstate, NY, USA; Williams et al., 1999) and horseradish peroxidase-conjugated rabbit secondary antibody (1 : 4000, 2 h at RT) (Amersham, Arlington Heights, IL, USA).

4.2.4 Immunocytochemistry

Cells were fixed (4% paraformaldehyde in 0.1 m PBS, pH 7.2, RT for 40 min) and permeabilized for 3 h in blocking solution containing 0.02% saponin, 2% bovine serum albumin, and 1% fish skin gelatin in PBS buffer. Cells were incubated with KCC2 antibody (1 : 200; 3 h at RT; Williams et al., 1999), rinsed with PBS, incubated with Cy3–labeled secondary antibodies (1 : 1000 for 2 h at RT; Jackson Immuno Laboratory, ME, USA), rinsed again and coversliped with Slowfade (Molecular Probes, Eugene, OR, USA). Analysis was performed on an epifluorescent microscope (Axiophot, Zeiss, Germany) using 40× objective (Neofluar, NA 0.75) or on a laser scanning confocal microscope (Olympus Fluoview, USA) at 60× (PlanApo, NA 1.4).

4.2.5 Gramicidin-perforated patch clamp recordings

Cell plates were moved into a recoding chamber mounted to an inverted epifluorescent microscope (Zeiss IM 35) and superfused with a solution containing (in mm): NaCl 140, KCl 5, $MgCl_2 \cdot 7H_2O$ 1, d-glucose 24, $CaCl_2$ 2, HEPES 10, pH adjusted to 7.2 with NaOH. Patch pipettes (3–5 MΩ) contained (in mm): K_2SO_4 77, KCl 5, $CaCl_2$ 0.5, EGTA 5, HEPES 10, pH adjusted to 7.3 with KOH (Kyrozis & Reichling, 1995). Gramicidin (10 mg/mL in DMSO) was prepared fresh every 2 h and added to the pipette solution resulting in a final concentration of 100 ng/ml. Series resistance was approximately 40–50 MΩ and was not compensated. Off-line correction of series resistance did not change the estimated value of E_{GABA} ($P > 0.6$ for both KCC2-transfected and control neurons). In voltage clamp experiments, voltage gated calcium channels and fast sodium channels were blocked with lanthanum (30 μm) and TTX (1 μm; Owens et al., 1996).

Liquid junction potential with a 2 m KCl agar bridge as the reference electrode was less than 2 mV. As the same extracellular solution was used for recordings from transfected and non-transfected cells, membrane potential values were left uncorrected for the small liquid junction potential.

GABA was applied to the soma of neurons using a multibarrel fast perfusion system (Warner Instruments, Hamden, CT, USA). All recordings were performed at 23–26 °C. Data were filtered at 0.5–1 kHz and digitized at 1–2 kHz using Axopatch 1C Amplifier, Digidata 1200 Interface, and Clampex 8.0 (Axon Instruments, Union City, CA, USA).

4.2.6 Calcium imaging

Cells were incubated for 0.5–2 h in Fura-2-containing (10 μm, TEF labs, Austin, TX, USA) artificial cerebrospinal fluid (ACSF) composition in mm: NaCl 124, $NaHCO_3$ 26, $MgSO_4 \cdot 7H_2O$ 1.3, KCl 5.0, KH_2PO_4 1.25, dextrose 10, $CaCl_2$ 2.0, kynurenic acid 1.0; pH 7.4 when gassed with 5% CO_2 95% O_2 37 °C). Cover slips were placed in a submerged-type recording chamber mounted on an inverted epifluorescence microscope (Nikon Eclipse TE200) equipped with 10× (NA 0.5) and 20× air objectives (NA 0.75) and were superfused with oxygenated ACSF without kynurenic acid. All drugs were applied through a superfusion system. Before recording calcium responses, EGFP expression was identified with 480 nm excitation light. Ratiometric imaging (340 nm/380 nm) was performed as described elsewhere (Kullmann et al., 2002) using a computer-controlled monochromator (Polychrome II, TILL Photonics, Martinsried, Germany) and a CCD camera (IMAGO, TILL Photonics). 340/380 nm image pairs were acquired at 0.1 Hz using TILLvisION v 4.0. Digital images were low pass filtered with a Gaussian 3 × 3 kernel and background fluorescence was subtracted as described previously (Ene et al., 2003). GABA was applied through a superfusion system. Only cells that responded to 60 mm KCl were analyzed. 340/380 nm fluorescent ratios (R) were measured from the cell body.

Data were analyzed and plotted using OriginPro 7.0 SR4 [v7.0552 (B552)] (OriginLab Corporation, MA, USA). For the calcium imaging experiment, data analysis was performed while the experimenter was blinded with regards to the transfection history of cells.

4.2.7 Statistical analysis

Statistical significance was tested using Fisher's exact test and Student's *t*-test. Throughout the text, values are expressed as arithmetic mean ± standard error of mean (SEM).

4.3 RESULTS

4.3.1 Expression of hKCC2

COS7 cells were transfected with hKCC2 cDNA or control EGFP vectors (Fig. 4.1.A). In Western blots prepared from crude membrane fractions of hKCC2 transfected cells, anti-rat KCC2 recognized a protein with a molecular weight of ≈150 kDa (Fig. 4.1. B), similar to the molecular weight of KCC2 extracted from mouse and rat brain (Lu et al., 1999; Williams et al., 1999; Stein et al., 2004). No corresponding signal or other non-specific bands were present in Western blots prepared from cells that had been transfected with the control EGFP vector.

I next transfected embryonic primary cortical neurons (E17 + 3 DIV) in which the expression of endogenous KCC2 is very low (Fig. 4.1. D; Lu et al., 1999; Rivera et al., 1999; Balakrishnan et al., 2003; Stein et al., 2004; Zhu et al., 2005). Two days after transfection, hKCC2-transfected, but not pMES-transfected, neurons showed strong immunoreactivity for KCC2 in cell bodies and neurites (Fig. 4.1.F). Similar to endogenous KCC2 expression in mature neurons (Williams et al., 1999; Balakrishnan et al., 2003; Zhu et al., 2005), KCC2 immunoreactivity was highest close to the plasma membrane (Fig. 4.1.H). In contrast to KCC2, bicistronically expressed EGFP was homogenously distributed throughout the cell body and processes (Fig. 4.1.G). In the absence of primary antibody, no signal was detected (data not show).

4.3.2 Effect of KCC2 expression on E_{GABA}

To test whether the premature expression of hKCC2 resulted in a functional chloride outward transporter, I examined the membrane potential response to GABA using the

gramicidin-perforate patch clamp method, which leaves the intracellular chloride concentration intact (Kyrozis & Reichling, 1995). In voltage clamp recordings and while voltage-gated sodium and calcium currents were blocked by lanthanum (30 µm) and TTX (1 µm; Owens et al., 1996), short pulses of GABA (0.5 mm, 200 ms) elicited inward currents in control neurons (holding potential −60 mV, Fig.4. 2. A), but outward currents in KCC2-transfected neurons (Fig.4. 2. B). In control cells, E_{GABA} was −53.5 ± 1.1 mV (non-transfected −53.7 ± 2.2 mV, n = 4; pMES-transfected −53.3 ± 0.7 mV, n = 4, P > 0.1, unpaired Student's t-test). This value is very similar to E_{GABA} measured in acute cortical slices at the corresponding age (corrected for differences in extracellular [Cl^-]; Owens et al., 1996). In contrast, in hKCC2 expressing neurons, E_{GABA} was −67.3 ± 2.2 mV (n = 5; Fig. 4. 2. C), significantly more negative than E_{GABA} in control neurons (P < 0.001, unpaired Student's t-test).

In current clamp recordings, without the presence of lanthanum and TTX, GABA induced depolarizing responses with action potential firing in control neurons while generating hyperpolarizations in KCC2-transfected neurons (Fig.4. 2. D–F). In control neurons, E_{GABA} was −48.3 ± 4.1 mV (n = 8) and in hKCC2 transfected neurons E_{GABA} was significantly more negative at −76.5 ± 3.1 mV (n = 5; P < 0.005). The resting membrane potential (V_{rest}) was not significantly different between both groups (control −67.6 ± 4.5 mV, n = 8; hKCC2-transfected neurons −62.8 ± 3.7 mV, n = 5; P > 0.1), resulting in negative shift of the electrochemical potential (E_{GABA} − resting membrane potentials) from +19.3 ± 4.9 mV in control neurons to −12.2 ± 4.3 mV in KCC2 transfected neurons.

The larger negative shift of E_{GABA} in current clamp (−28.2 mV) compared to voltage clamp (13.8 mV) most likely reflects the contribution of voltage-gated sodium and calcium conductances in current clamp recordings.

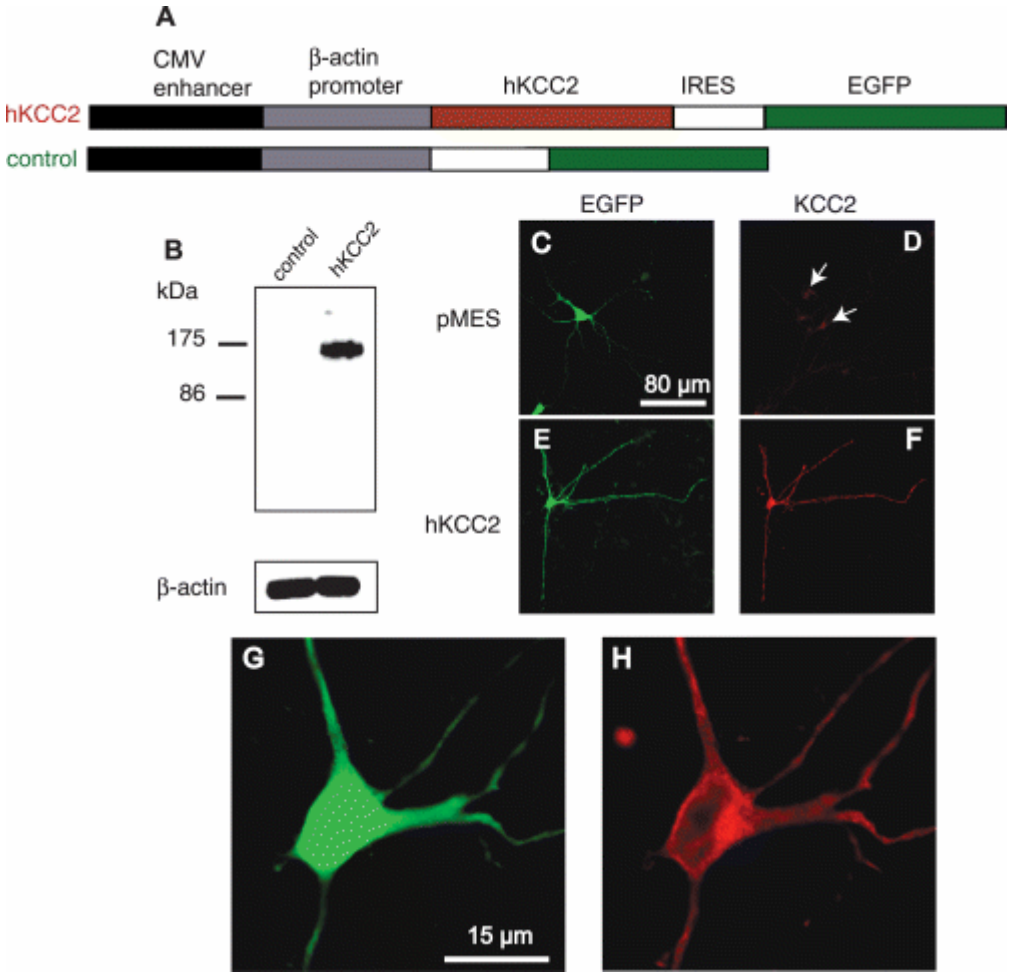

Figure 4.1. Heterologous expression of hKCC2.

(A) pMES vector (control) and hKCC2 expression vector used in this study. **(B)** Western blotting reveals a protein of approximately 150 kDa molecular weight in hKCC2 transfected COS7 cells but not in vector-transfected cells. β-actin (42 kDa) was detected using a different blot from the same membrane preparation. **(C)** Embryonic cortical neurons transfected with control vector (pMES) showed high EGFP-expression (green) but only very low levels of KCC2 expression (red) that were detectable only when drastically increasing the gain of the photomultiplier tube **(D)**. **(E and F)** KCC2-immunoreactivity was high in KCC2 transfected cells. **(G and H)** Higher magnification shows that KCC2 appeared to be concentrated in or near the cell membrane **(H)**.

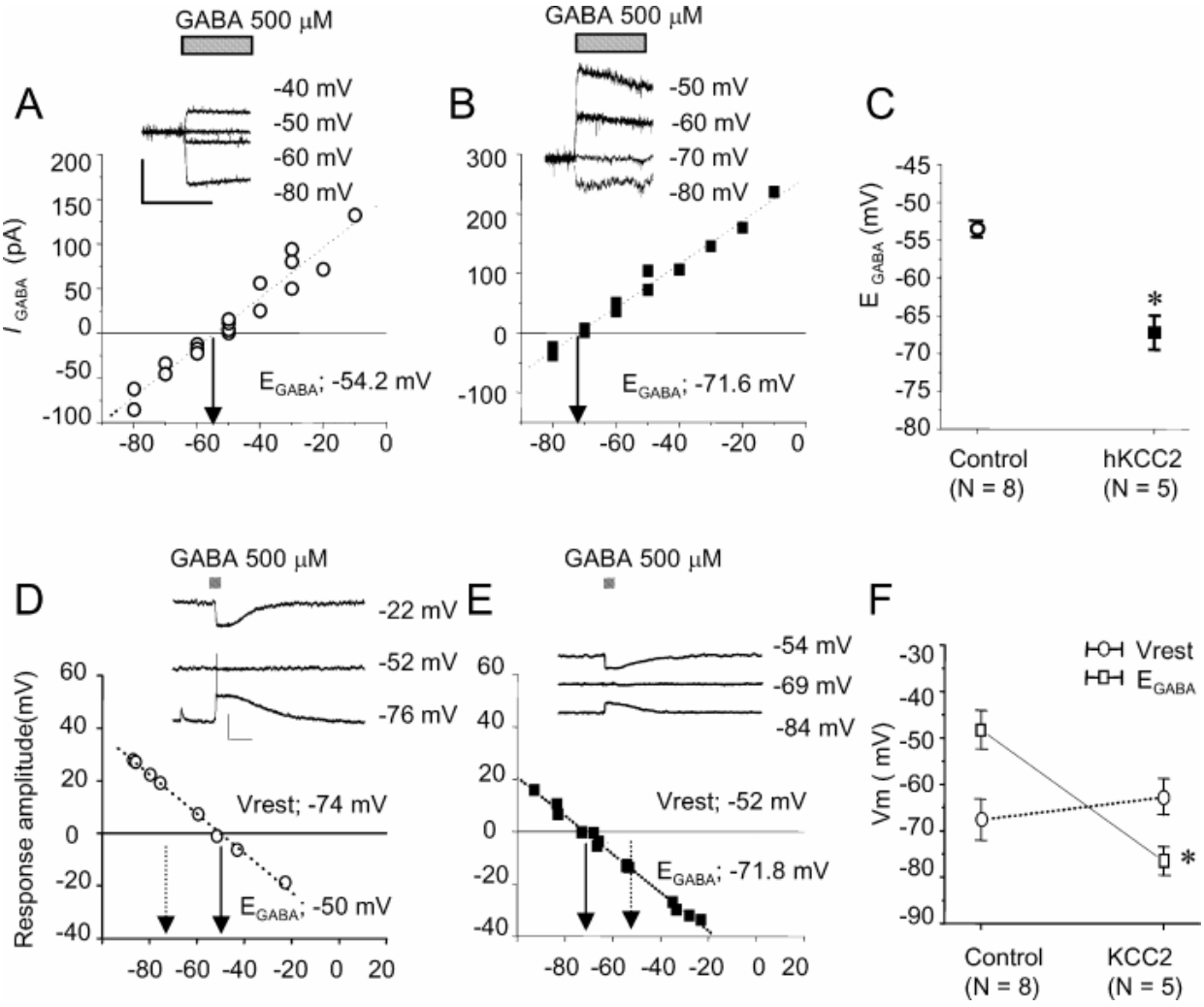

Figure 4.2. Overexpression of hKCC2 produces a negative shift in E_{GABA} in immature cortical neurons.

Gramicidin-perforated patch clamp recordings from cortical neurons in voltage clamp **(A–C)** and current clamp **(D–F)**. Voltage–current relationship of membrane potential and GABA-elicited (0.5 mm, 200 ms) currents in a control neuron **(A)** and a KCC2-transfected neuron **(B)**. **(C)** Summary data. **(D)** GABA-elicited membrane potential responses in a control neuron **(D)** and a hKCC2-transfected neuron. **(F)** Summary data. **P* < 0.001, Student's *t*-test. Scale bars, 200 ms, 50 pA (A and B); 1 s, 20 mV (D and E).

4.3.3 Effect of KCC2 expression on GABAergic calcium responses

In immature cortical neurons, depolarizing GABA increases the intracellular calcium concentration ($[Ca^{2+}]_i$) by activating voltage-gated calcium channels (Connor et al., 1987; Yuste & Katz, 1991; Owens et al., 1996) or by removing the magnesium block from NMDA receptors (Ben Ari et al., 1997). I therefore tested whether, and to what extent, the hKCC2 induced negative shift of E_{GABA} and was correlated with a loss of the capacity of GABA to elevate intracellular Ca^{2+} levels. GABA (1 mm) elicited a transient increase in $[Ca^{2+}]_i$ in 88% of control cells (716/807 cells; non-transfected cells 671/756, control vector-transfected cells 45/51; Fig.4. 3. D) but in only 44% of hKCC2-transfected cells (23/52 cells; $P < 0.01$, Fisher's exact test). In hKCC2 expressing neurons that showed a GABAergic calcium response, peak amplitudes were significantly smaller than in control neurons (38% reduction, $P < 0.05$, unpaired Student's t-test, Fig. 4.3. E). Response amplitudes to KCl-induced depolarization were not affected by KCC2 expression. Peak amplitudes ($\Delta R/R$) in control neurons were 1.36 ± 0.03 ($n = 45$), in non-GABA responding KCC2-transfected cells 1.41 ± 0.05 ($n = 29$), and 1.46 ± 0.05 in GABA responding KCC2 transfected cells ($n = 23$; $P > 0.05$, two-tailed Student's t-test).

The $GABA_A$ receptor agonist muscimol (30 μM) elicited calcium-responses in the same fraction of cells as did GABA (500 μM) (muscimol 90% ($n = 112/124$), GABA 87% ($n = 108/124$), $P > 0.1$). The amplitude of 30 μM muscimol-elicited responses was slightly larger than those elicited by 500 μM GABA (muscimol 117% of GABA). This might reflect GABA uptake by glial cells or might reflect smaller membrane depolarizations by the additional activation of $GABA_B$ receptors. In the presence of bicuculline (100 μM) the percentage of cells responding to GABA was decreased by 90% ($n = 90$ cells) and the percentage of cells responding to muscimol was decreased by 71% ($n = 56$). The amplitudes of responses in the remaining cells were reduced by 86.2% ($n = 16$). Bicuculline did not reduce KCl-elicited responses (change 96.4%, $n = 32$, $P = 0.2$).

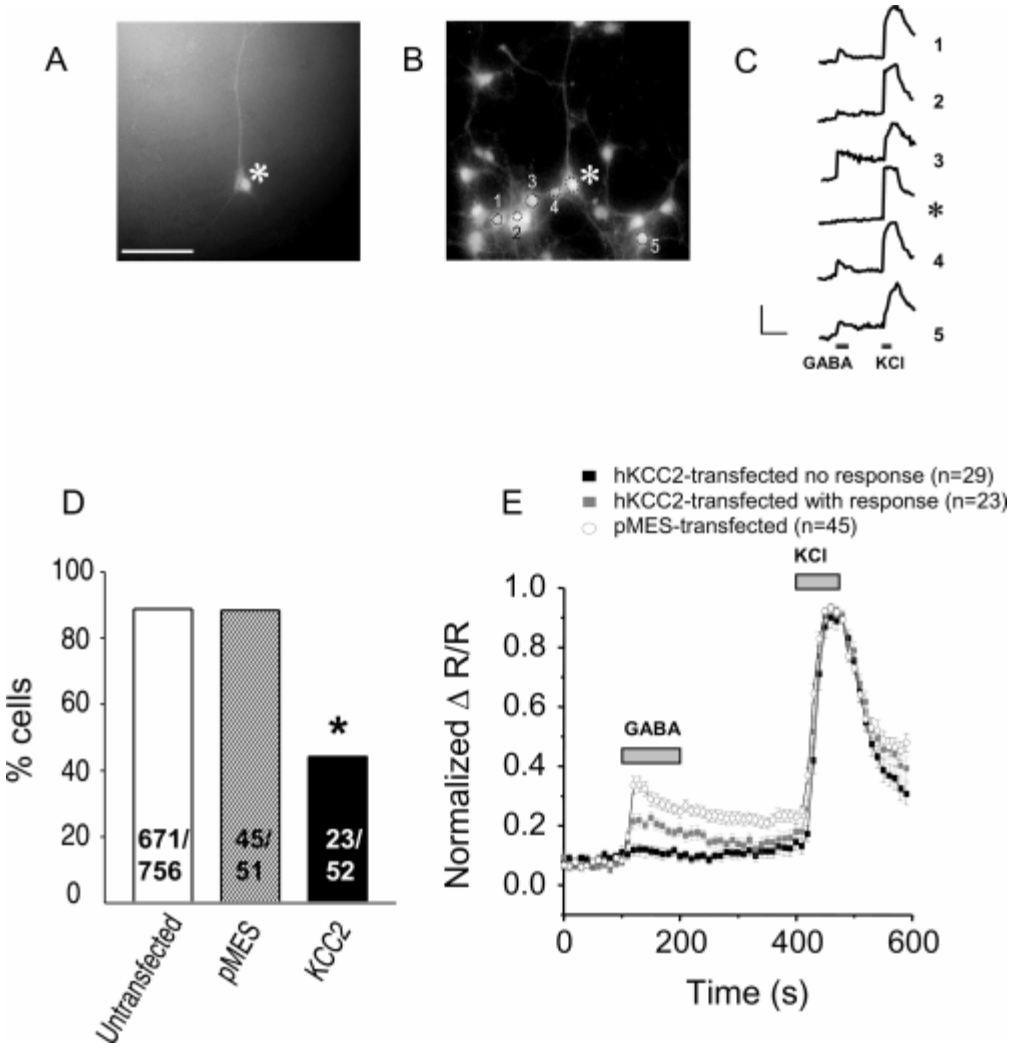

Figure 4.3. KCC2 expression decreases GABA-elicited calcium responses.

(A) Photomicrograph of EGFP fluorescence (488 nm excitation) of an hKCC2-transfected neuron. **(B)** Same field showing Fura-2 labeling (380 nm excitation). **(C)** Calcium responses to GABA (1 mm) and KCl (60 mm) of cells numbered in **(B)**. The hKCC2 transfected cell (asterisk) did respond to KCl but not to GABA (arrow). Calibration: 0.4 ΔR/R, 100 s. **(D)** Percentage of KCl responding cells that also responded to GABA (*P < 0.01, Fisher's exact test). **(E)** Calcium responses (ΔR/R normalized to KCl response) of hKCC2-transfected, GABA responding and GABA non-responding cells. Scale bar, 100 μm (A and B).

4.4 DISCUSSION

The results presented here demonstrate that exogenous expression of hKCC2 in embryonic cortical neurons induces a negative shift of E_{GABA}, and as a consequence, abolishes or significantly decreases GABA-elicited calcium responses. These results provide the first evidence that KCC2 is not only necessary, but also sufficient to induce the end of the depolarizing and excitatory period of GABA during cortical development.

In KCC2 overexpressing neurons, E_{GABA} was 13 mV more negative than in age-matched control neurons. As GABAergic currents in early neonatal cortical neurons are carried primarily by $GABA_A$ receptors and chloride flux (Luhmann & Prince, 1991; Owens et al., 1996) a shift of E_{GABA} from −54 mV to −67 mV corresponds to an estimated decrease in $[Cl]_i$ from ≈18 mm to ≈11 mm, calculated with the Nernst equation. Interestingly, the 7 mm decrease in $[Cl]_i$ observed here *in-vitro* closely matches the 6–8 mm decrease that occurs during the first two postnatal weeks in rat cortex development *in- vivo* (P0–P4 18–20 mm, P16 11.7 mm; Owens et al., 1996). This result was somewhat unexpected as it is unlikely that hKCC2 transfected cultured neurons, in which hKCC2 transcription is driven by the *beta*-actin promoter, express similar levels of KCC2 protein as cortical neurons *in-vivo*, in which KCC2 expression is under normal endogenous control. It is possible, however, that both *in- vitro* and *in- vivo*, KCC2 activity was high enough to establish a thermodynamic equilibrium at the given extra- and intracellular K^+ and Cl concentrations, or that both *in- vitro* and *in- vivo*, KCC2 activity is similarly regulated by $[Cl]_i$ (Breitwieser et al., 1990; Schomberg et al., 2003). In addition, it is possible that phosphorylation of KCC2 (LoTurco et al., 1995; Kelsch et al., 2001; Vale et al., 2003; Stein et al., 2004) or availability of membrane anchoring proteins could act as functional limiting factors, regardless of the expression levels of the transporter.

My studies could not exclude the possibility that increased hKCC2 activity induces the down-regulation of the activity in chloride inward transporters, such as the sodium potassium chloride cotransporter (NKCC) that is present in immature cortical neurons (Sun & Murali, 1999). This possibility, however, seems unlikely because, in developing auditory neurons, up-

regulation of KCC2 activity and the negative shift of E_{Cl} is paralleled by an up-regulation of NKCC expression. This indicates that up-regulation of KCC2 is not negatively coupled to NKCC expression and that KCC2-mediated outward Cl transport can overcome NKCC-mediated inward Cl transport (Balakrishnan et al., 2003). On the other hand, NKCC activity is up-regulated by an increase in $[Ca^{2+}]_i$ (Sun & Murali, 1998; Schomberg et al., 2001), a situation which is less likely to occur in hKCC2-transfected neurons (Fig. 4.3.). Clearly, additional studies are necessary to investigate in detail the possible direct and indirect interactions between KCC2 and other chloride transporters.

Because premature expression of KCC2 protein resulted in a functional chloride transporter, the mechanisms for membrane trafficking and post-translational modifications that are required for KCC2 activation (Payne, 1997; Strange et al., 2000; Kelsch et al., 2001; Balakrishnan et al., 2003; Stein et al., 2004) already have to be present before developing cortical neurons endogenously up-regulate KCC2 expression. This conclusion is supported by a recent *in- vivo* study, which demonstrated phosphorylation of KCC2 in cortex even before the steep increase in KCC2 expression levels, suggesting that the developmental negative shift in E_{GABA} is primarily caused by transcriptional up-regulation of KCC2 expression (Stein et al., 2004). As such, the developmental regulation of KCC2 activity in cortical neurons seems to differ from other brain areas in which the developmental increase in KCC2 activity is regulated primarily by post-translational mechanisms (Kelsch et al., 2001; Vale et al., 2003), and/or subcellular translocation (Balakrishnan et al., 2003). Nonetheless, my results clearly indicate that KCC2 function is the determining factor in converting a GABAergic response from excitatory to inhibitory during brain development.

5.0 GENERAL DISCUSSION

In my dissertation, I investigated the functional significance of the developmental switch of GABA/glycine from being excitatory to inhibitory, using an auditory brainstem circuit as a model system. The major conclusions I have drawn from my investigations are: 1) The developmental switch from GABA/glycinergic excitation to inhibition is not necessary for the developmental strengthening of inhibitory connections (Chapter 2), 2) The balance between inhibition and excitation is impaired if GABA and glycine remain excitatory (Chapter 2), and 3) The developmental switch of hyperpolarizing GABA/glycine responses is necessary to maintain the normal strength of the calyx of Held synapse in MNTB neurons (Chapter 3).

In addition, I demonstrated that KCC2 overexpression was sufficient to terminate the GABAergic excitatory period earlier than in normal development (Chapter 4). Based on this result I generated KCC2OVER mice in which KCC2 could be overexpressed in a temporally regulated, neuronal-specific manner (Appendix).

5.1 DEPOLARIZING GABA/GLYCINERGIC SYNAPSE STRENGTHENING IN LSO NEURONS IN KCC2-KD MICE

GABA/glycinergic MNTB-LSO synapses showed normal development in KCC2-KD mice as demonstrated in Chapter II. This suggests that developmental synaptic strengthening and E_{Cl} maturation are not causally related.

Many studies have investigated how GABA/glycinergic synapses are affected by activity changes, but how neural circuit might change when depolarizing GABA/glycinergic responses are maintained has not been investigated. During development *in-vivo*, the strength of GABAergic synapses in layer II/III pyramidal neurons in visual cortex increase and, when reared in a dark environment, developmental strengthening of GABAergic IPSCs is prevented (Morales et al., 2002). Also *in-vitro*, reducing neuronal activity by blocking action potentials with TTX decreases the amplitude of miniature IPSCs, indicating that neuronal activity is important for the regulation of GABA function mediated through $GABA_A$ receptor (Kilman et al., 2002). In an organotypic culture system from new born mice, when all activity is abolished by TTX and increased Mg^{2+} treatment, inhibitory synapses undergo drastic changes including reduced somatic inhibition and increased dendritic inhibition (Seil and Drake-Baumann, 1994). Activity-dependent changes in inhibitory synaptic strength suggest that inhibitory systems are plastic, undergoing modifications in strength following disturbed neuronal activity. However, these previous studies have not addressed whether GABAergic synapses undergo strength changes either in conjunction with a changing E_{Cl} or concurrent with a constant E_{Cl} value. For example, in the embryonic spinal cord, reduced spontaneous activity causes an increase in mIPSC amplitude during the developmental period of GABAergic depolarization (Gonzalez-Islas and Wenner, 2006). However, it is not clear whether the increased mIPSC amplitude is a GABAergic synapse strengthening through depolarizing GABA activity or hyperpolarizing GABA activity, since activity changes can also affect E_{Cl} value through regulation of KCC2 activity (Fiumelli and Woodin, 2007). Therefore, my investigation of how the GABA/glycinergic MNTB pathway into LSO neurons develops in KCC2-KD mice is a unique example of how GABA/glycinergic synapses become wired up under the influence of prolonged GABA/glycinergic depolarization.

Suggestive but similar examples to my result of how inhibitory circuits might change under continued depolarizing GABA/glycinergic responses can be found in disease-related conditions such as epilepsy. In the epileptic neural circuit, changes in functional expression levels of NKCC1 and KCC2 occur in hippocampal sclerosis (HS) and focal cortical dysplasia (FCD) patients (Sen et al., 2007) as well as temporal lobe epilepsy patients (Palma et al., 2006). The increased NKCC1 expression and/or decreased KCC2 expression during epileptic neuronal activity disturbs chloride homeostasis and results in GABAergic depolarization even in the

mature brain (Woo et al., 2002; Palma et al., 2006). In an animal model of inherited spontaneous epileptic seizure, mIPSC frequency and amplitude in the substantia nigra pars reticulata (SNr) are not changed (Kumar et al., 2006). Also, identical IPSCs have been observed in epileptic hippocampal slices isolated from epilepsy patients (Isokawa, 1996). The unaltered strength of IPSCs in epileptic patients, along with the normal strengthening of the MNTB-LSO pathway in KCC2-KD mice, suggests that GABA/glycinergic synapses maintain their normal strength even if there is increased excitability in the neuronal network due to depolarizing GABA/glycinergic synaptic responses.

Accordingly, it would also be interesting to investigate further how inhibitory synapses in other brain regions such as the hippocampus might be affected in KCC2-KD mice, which could provide valuable information on how neural circuits undergo changes under conditions of epileptic neuronal activity.

5.2 REDUCED STRENGTH IN THE CALYX OF HELD SYNAPSE; COULD IT BE AN EXPLANATION FOR THE NORMAL STRENGTH OF THE MNTB-LSO PATHWAY IN KCC2-KD MICE?

The absence of GABA/glycine hyperpolarizing responses resulted in reduced amplitudes of calyceal EPSCs in MNTB neurons (Chapter III). This could mean that LSO neurons receive less activity from the MNTB in KCC2-KD mice because MNTB neurons receive weaker glutamatergic drive from the contralateral CN. The weaker glutamatergic drive onto MNTB neurons would result in reduced MNTB activity into LSO neurons (Fig 1.1), which, again, would suggest that the normal strengthening of the MNTB-LSO pathway in KCC2-KD mice might be due to the reduction of activity. This, however, is not supported by cochlear ablation experiments.

When the contralateral cochlea is ablated during development before hearing onset, excitatory drive into MNTB neurons is reduced, resulting in less MNTB input into LSO neurons. Supporting this idea, the effect of cochlear ablation can be mimicked by treatment with strychnine, an antagonist of glycinergic transmission, a major neurotransmitter in the MNTB-LSO pathway. When there is a reduction in MNTB activity either by cochlear ablation or strychnine treatment, dendritic arborizations of LSO neurons and MNTB axonal spreading within the LSO are greater (Sanes et al., 1992; Sanes and Siverls, 1991). Also, cochlear ablation causes a reduction in the number of LSO neurons showing IPSPs elicited by activation of the MNTB pathway, as well as reduced LSO IPSP amplitude (Kotak and Sanes, 1996), suggesting that the reduction of inhibitory synaptic strength in the MNTB-LSO pathway results from reduced activity in the MNTB. These previous studies of cochlear ablation and/or strychnine treatment demonstrats that, when activity in the MNTB is reduced, the MNTB-LSO pathway undergoes changes different from those that occurs during normal development. However, MNTB-LSO synapses in KCC2-KD mice were not different compared to WT (Fig 2.2~ Fig 2.6), implying that activity in the MNTB might not be reduced even if calyceal EPSCs in MNTB neurons is reduced in KCC2-KD mice. Therefore, the smaller amplitude of calyceal EPSCs of MNTB neurons could not explain the normal development of the MNTB-LSO pathways observed in KCC2-KD mice.

Nonetheless, unfortunately, I am not able to address whether or not the MNTB-LSO pathway would still develop normally under the prolonged depolarizing GABA/glycinergic responses in the LSO neurons even when calyceal EPSC in the MNTB is similar to WT. Addressing this question would require a conditional genetic mouse model in which the function of KCC2 is absent specifically in LSO neurons, which is currently unavailable.

Whether glutamatergic synapses are normal or reduced in strength as demonstrated in an auditory brainstem circuit in KCC2-KD mice, neural circuits fail to function normally in the absence of GABA/glycinergic hyperpolarization. 1) In the case of LSO neurons, maintaining normal glutamatergic synaptic strength results in a breakdown of the homeostatic regulation of excitability because normal strengthening takes place in depolarizing GABA/glycinergic synaptic inputs 2) In the case of MNTB neurons, the reduced calyceal glutamatergic synapse are

abnormal in that they fail to maintain their normal strength as well as fidelity following synaptic activities. Therefore, my dissertation studies provide detailed information on how neural circuits fail to adapt to activity changes in the absence of hyperpolarizing GABA/glycinergic responses.

5.3 CAN A CHANGE IN SPONTANEOUS ACTIVITY EXPLAIN THE OBSERVED REDUCTION IN THE STRENGTH OF THE CALYX OF HELD SYNAPSE IN KCC2-KD MICE?

Spontaneous activity exerts a considerable impact on synaptic strength even early in development. As shown in embryonic spinal cord, reducing spontaneous activity for 2 days *in-vivo* resulted in increased miniature EPSC amplitude and frequency, which was also accompanied by an increase in the amplitude of miniature IPSCs (Gonzalez-Islas and Wenner, 2006). In the visual system, chronic activation of NMDA receptor in the superior colliculus (SC) before sensory-driven activity starts (at P8) caused a decrease in mEPSC frequency when examined at hearing onset (Shi et al., 2001). In KCC2-KD mice, one could argue that the reduced calyceal synapses into MNTB neurons are due to a different spontaneous activity level or pattern caused by reduced KCC2 activity. However, the reduced calyceal EPSC in MNTB neurons in KCC2-KD mice is not likely due to a change in spontaneous activity. The calyceal synapse originates from the CN, which also sends glutamatergic synapses into another nucleus, the LSO, in the auditory brainstem (Fig 1.1.). The glutamatergic CN-LSO synaptic strength, however, was not different between WT and KCC2-KD mice (Fig 2.7 ~ Fig 2.8), implying that the activity of the CN itself might be very similar between WT and KCC2-KD mice. It is very unlikely that a change in the spontaneous activity of the CN would result in differences in glutamatergic synaptic strength in one nucleus (such as in the MNTB) and no change in another (such as in the LSO). Therefore, the normal strengths of glutamatergic synapses in LSO neurons, supports the hypothesis that the decreased calyceal EPSC in the MNTB in KCC2-KD mice is not due to a change in spontaneous activity itself. As discussed in Chapter 3, possible mechanisms for the reduced strength of the calyx of Held in KCC2-KD mice involve presynaptic vesicle number, quantal content, postsynaptic receptor recycling, and the subunit or splice variant of

postsynaptic receptors between WT and KCC2-KD mice. Addressing the mechanisms involved in the reduction of the calyx of Held synaptic strength will help us to understand the importance of the developmental switch of GABA/glycinergic responses to hyperpolarization.

5.4 INHIBITORY SYNAPTIC INPUT INTO MNTB NEURONS IN KCC2-KD MICE

In addition to the calyceal synaptic inputs, MNTB neurons also receive inhibitory synaptic inputs. The inhibitory synaptic responses also display developmental strengthening as well as a switch in response polarity from depolarizing to hyperpolarizing as demonstrated in other systems (Awatramani et al., 2004; Price and Trussell, 2006). It has been shown that inhibitory synapses in the auditory system undergo activity-dependent modifications. In congenitally deaf *dn/dn* mice, mIPSC frequency in MNTB neurons is greater by 50% and the amplitude is reduced, with a slower decay time course (Leao et al., 2004). When the cochlea is ablated bilaterally, IPSCs into the Inferior Colliculus (IC) are reduced (Vale and Sanes, 2002). It has also been shown *in-vitro* that inhibitory synaptic activity controls inhibitory synapse formation for both glycinergic (Kirsch and Betz, 1998) and GABAergic (Ganguly et al., 2003) synapses. On the other hand, in the absence of E_{Cl} maturation in the hyperpolarizing direction, inhibitory synaptic strength developed normally in the MNTB-LSO pathway (Chapter 2). In the embryonic spinal cord where GABA is depolarizing, mIPSC amplitude is increased when the spontaneous activity level is reduced (Gonzalez-Islas and Wenner, 2006). Thus, it would be interesting to investigate how GABA/glycinergic synapses mature in the MNTB in KCC2-KD mice. Would GABA/glycinergic synapses be increased to compensate for the reduced glutamatergic synaptic response because GABA/glycinergic responses are depolarizing? Or would the inhibitory synaptic responses be decreased as was found in the calyceal glutamatergic synaptic responses, because both glutamatergic and GABA/glycinergic pathways share the same downstream homeostatic mechanisms? Or, would inhibitory synapses not be affected, as shown in the inhibitory synapses in the LSO in KCC2-KD mice (Chapter 2), supporting the idea that in

the absence of KCC2, there is no cross talk between glutamatergic synapses and GABA/glycinergic synapses?

5.5 HETEROLOGOUS OVEREXPRESSION OF KCC2

My demonstration that heterologous KCC2 overexpression can terminate excitatory GABA/glycinergic responses earlier than in normal development (Chapter 4) is important because the result suggests that we can use KCC2 overexpression as a tool to study the role of excitatory GABAergic responses in neural circuit development. Moreover, the premature hyperpolarizing shift of E_{Cl} was able to abolish GABAergic calcium responses (Figure 4.3), which implies that it is also possible to address the role of GABAergic calcium responses during development through the regulation of KCC2 function. We anticipate that GABAergic calcium responses are important for neuronal maturation during perinatal development, but how and why it would be important has not been tested because there has been no method available which modulates GABA-elicited calcium responses specifically. Therefore, overexpressing KCC2 and terminating GABAergic calcium responses in immature neurons can provide a valuable tool for future research to address the role of GABA-elicited calcium increment.

There is still a lack of understanding of how KCC2 activity is regulated. In many systems, the regulation of KCC2 function occurs on a transcriptional level. In this case, KCC2 mRNA parallels the E_{Cl} value, and the level of KCC2 mRNA is a determinant for the polarity of GABA/glycine responses. The results in Chapter 4, where it was demonstrated that KCC2 overexpression resulted in the hyperpolarizing shift of E_{Cl} in immature cortical neurons, imply that the regulation of functional KCC2 does not require additional post-translational modification after transcription.

However it should be noted that functional expression of KCC2 can also be regulated by posttranslational mechanisms such as phosphorylation. When KCC2 was heterologously

expressed in HEK293 cells, a dominant-negative form of brain-type creatine kinase (CKB) shifted E_{Cl} in a depolarizing direction, suggesting that the phosphorylation of KCC2 is an important regulatory mechanism for KCC2 function (Inoue et al., 2006). Consistent with this, in auditory brainstem nuclei such as the MNTB and LSO, the level of KCC2 protein expression is high even when GABA/glycine responses are depolarizing. The lack of correlation between KCC2 expression level and the polarity of GABA/glycinergic responses in the LSO and MNTB neurons suggests that in certain neuronal types, functional KCC2 might require post-translational modifications to exert its physiological effect on E_{Cl} value (Balakrishnan et al., 2003). Until recently, there has been no research demonstrating mechanisms which are developmentally up- or down- regulated in parallel to the gradual shift of E_{Cl} in a hyperpolarizing direction during development. Molecular identification of this mechanism might help to further understand the regulation of KCC2 activity as well as its functional implications.

In this study, I used a *beta*-actin promoter and CMV enhancer to drive KCC2 expression in a neuronal enriched culture system. Although the *beta*-actin promoter drives heterogenous gene expression in every cell type including glia and astrocytes, in this experimental system, most of the examined cells were neurons since neuronal cells could be distinguished by their morphology in *in-vitro* culture systems. However, in order to investigate the role of excitatory GABA/glycine *in- vivo*, it is necessary to use a neuron specific gene expression system, since *in-vivo* KCC2 is expressed in neurons only (Karadsheh and Delpire, 2001).

In summary, from my dissertation study, I used KCC2-KD mice to investigate how neural circuits develop in the absence of the developmental switch of hyperpolarizational GABA/glycine responses and the possible physiological interpretation. In the future, it will be necessary to extend our knowledge on how circuits develop in the reversed condition, i.e. in the absence of depolarizing GABA/glycinergic responses during development. Based on the results presented in Chapter 4, it is possible to address this future question *in-vivo* when KCC2 overexpression is employed in a transgenic mouse model (Appendix).

6.0 APPENDIX: GENERATION OF KCC2 OVEREXPRESSION MICE

6.1 INTRODUCTION

The involvement of GABAergic excitation during perinatal development has been intensely studied due to the ability of GABA-mediated depolarization to cause the increase in $[Ca^{2+}]_i$. At early developmental stages, rises in $[Ca^{2+}]_i$ have been implicated in proliferation, migration and differentiation (Owens and Kriegstein, 2002). At embryonic day 19 (E19), application of GABA in the ventricular zone decreases the number of cells synthesizing DNA, suggesting that GABA stimulates neurons to progress from proliferating to differentiating stages (Lo Turco et al., 1995). In migrating neurons, block of GABA activity with the $GABA_A$ specific antagonist bicuculline caused an increase in the number of neurons found in the cortical plate (CP), while block of GABA activity through the GABAB specific antagonist saclofen caused a reduction in the number of neurons reaching the CP (Behar et al., 2000). These results suggest that GABA is involved in several different mechanisms regulating neuronal migration. Furthermore, GABA also promotes neurites outgrowth during the differentiation stage. Dissociated hippocampal cultures (E17) displayed an increased number of neurons with neurites, when $GABA_A$ activity was increased by muscimol, implying more neurons are forming neurites following GABAergic $[Ca^{2+}]_i$ (Marty et al., 1996). Excitatory GABA responses can also occur in mature circuits due to reduced KCC2 function in, for example, epilepsy (Palma et al. 2006), spinal cord injury (Coull et al., 2003), axotomy (Nabekura et al., 2002), ischemic injury (Galeffi et al., 2004), etc.

Recently, there have been efforts to more directly investigate the role of excitatory (and depolarizing) GABAergic responses and the subsequent increase in $[Ca^{2+}]_i$. When normal

GABAergic excitatory responses were disturbed during development (Chudotvorova et al., 2005; Akerman and Cline, 2006), inhibitory synapses were strengthened; at the same time, excitatory synapses were weakened (Akerman and Cline, 2006). Even in the adult brain, excitatory GABAergic responses in newly born neurons seem to be important for their incorporation into an existing network (Ge et a., 2006). Also, without normal GABAergic excitation, neuronal morphology became atrophic with shorter dendritic branches in cortex (Cancedda et al., 2007). However, many answers have remained elusive, especially concerning how disturbed excitatory GABAergic responses might affect the development of neuronal circuits, including the balance between inhibitory and excitatory pathways. In the auditory brainstem, GABA/glycinergic projections from the MNTB to the LSO undergo tonotopic map refinement through synaptic silencing and elimination, resulting in a reduction of the area of the MNTB providing functional input to a single LSO neuron (Kim and Kandler, 2003). This refinement of presynaptic input area occurs during the first postnatal week, when LSO responses to GABAergic inputs from the MNTB are depolarizing (Kandler and Friauf, 1995; Kullman and Kandler, 2001). This lead to the hypothesis that increases in $[Ca^{2+}]_i$ mediated by depolarizing responses to GABA/glycine is critical for functional maturation of inhibitory synapses and circuits (Kandler, 2004).

Since the *in-vitro* data presented in Chapter III show that premature KCC2 overexpression can abolish GABAergic depolarization and increases in $[Ca^{2+}]_i$, the generation of a transgenic mouse in which KCC2 can be overexpressed conditionally (**KCC2OVER mice**) will provide a unique experimental paradigm to study the role of GABA/glycinergic-mediated increases in intracellular calcium in a developmentally specific manner. Investigations of neural circuit development and function in KCC2OVER mice will also provide an important breakthrough in our understanding of the more general role of depolarizing GABA/glycinergic responses during development *in- vivo*, in conjunction with behavioral consequences.

6.2 MATERIALS AND METHOD

6.2.1 cDNA construct for inducible- and neuron-specific expression of hKCC2

The Thy1.2 mouse expression cassette was a gift from Dr. Pico Caroni (Friedrich Miescher Institute, Basel Switzerland) and the pBS302 construct was a gift from Dr. Brian Sauer (Stower Institute, Kansas). The "floxedP-STOP" sequence from the pBS302 construct was combined with KCC2-IRES-EGFP using the EcoRI site in the pMES vector (Fig 5.1. A). The 6.1 Kb loxP-STOP-loxP-KCC2-IRES-EGFP fragment was subcloned into the Thy1.2 expression cassette using the XhoI site (blunt end ligation using T4 polymerase). The final construct, #9, contained Thy1.2 promoter -loxp-STOP-loxp- hKCC2:IRES:EGFP (~13.6 Kb). The KCC2 sequence within the #9 construct was sequenced in both sense and anti-sense directions.

In order to test the Cre-LoxP system, the following constructs were also generated: pMES-STOP, Thy1.2-hKCC2, pMES-STOP-hKCC2, pMES/Crej1 (with EGFP), and pCAX/Crej1 (without EGFP).

6.2.2 Generation and genotyping for transgenic mice.

The #9 construct was linearized with EcoRI and NdeI (13.6 Kb). Pronuclear injection was conducted in a transgenic mouse facility at Vanderbilt University resulting in the production of KCC2OVER mice. KCC2OVER founder mice (F1 progeny) were screened by PCR. Primer sets were as follows: KCC2-#7; 5'-GCA GGA GCC ATG TAC ATC CT-3', KCC2-#9; 5'-ACT GGA CCC TCT CCT TCC TG-3', KCC2-R1; 5'-ACA CCA CAG TGG CCA TGC A-3', EGFP-ANS; 5'-AAC TCC AGC AGG ACC ATG TGA T-3', Thy-SNS ; 5'-TCT CTG AGT GGC AAA GGA CC-3', STOP-R1; 5'-TGG CAG CAG ATC TAA CGG-3'. DNA was isolated from tails using the PUREgene kit (Gentra Corp.).

Cre-ERTM mice were purchased from Jackson Laboratory (Tg(Cre-Esr1)5AMC; catalog number: 004682, Main, USA). Primers for genotyping Cre-ERTM mice were "CAgg"; 5'-CTC TAG AGC CTC TGC TAA CC-3' and "CRE"; 5'- CCT GGC GAT CCC TGA ACA

TGT CC-3'. Genotyping of mouse GAPDH (glyceraldehyde-3-phosphate dehydrogenase) was used as a control; sense-5'-ATT GTC AGC AAT GCA TCC TGC A-3' and anti-sense-5'-AGA CAA CCT GGT CCT CAG TGT A-3'.

6.2.3 Transfection of COS7 cells and cortical neurons

These procedures were conducted as described in Chapter III.

6.2.4 Immunoblotting and immunocytochemistry of cultured cells.

These procedures were conducted as described in Chapter III. Cytosolic fractions were immunoblotted for *beta*-actin and membrane fractions were immunoblotted for KCC2. Monoclonal *beta*-actin antibody was diluted 1:5000 (Sigma-Aldrich, USA) and horseradish peroxidase conjugated goat-anti-mouse antibody was diluted 1:3000.

6.2.5 EGFP antibody staining of sectioned tissue.

Animals were perfused transcardially with 0.1 M PBS followed by 4% paraformaldehyde (PFA). Isolated brains were cryoprotected in 30% sucrose. Coronal brain sections were cut into 50 μm thickness using a sliding microtome, starting at the brainstem at the level of the cochlear nucleus and continuing through the auditory cortex (rhinal fissure). Every 3rd slice was selected for EGFP staining. After blocking for 4 hours, slices were incubated with primary antibody (rabbit anti-GFP (Invitrogen, USA), 1:2000 dilution) for 2 hrs at room temperature (RT) and at 4°C overnight. The following day, slices were stained with secondary antibody (Goat-anti-Rabbit biotinylated (Vectorlabs)1:200) for 2 hrs at RT. Immunoreactivity was visualized through diaminobenzidine (DAB) – hydrogen peroxide reaction.

6.2.6 KCC2 gene induction *in- vivo* from double transgenic mice (KCC2OVER$^+$/Cre$^+$)

Tamoxifen (Sigma T-5648) was dissolved in sterile-filtered vegetable oil to make a 2 mg / ml stock. Stock solutions were aliquoted and frozen at (- 20 ˚C). Before use, aliquots were sonicated for 15 minutes. Approximately 0.01~0.02 µl of Tamoxifen solution was mouth-fed to neonatal pups for 5 to 6 consecutive days, starting from postnatal day 2 (P2).

6.2.7 Acetylcholinesterase (AChE) histochemistry

AChE staining was performed as described in Tago et al (1986). Fixed brain sections fixed in 4% PFA (50 µm thickness) and were incubated in 0.1M Acetate Buffer (pH.6.0) for 30 min and then transferred into sonicated pre-reaction solution containing 18-36µM Acetylthiocholine iodide (A-5751, Sigma), 5 µM $K_3Fe(CN)_6$, 30 µM CuSO4, 50 µM Sodium citrate•$2H_20$ in 0.1M Acetate Buffer (pH 6.0), and iso-OMPA (tetraisopropyl pyrophosphoramide)(T-1505, Sigma). After 2~3 hours of pre-reaction solution incubation, slices were washed 5 times with 50 mM Tris-HCl (pH 7.6). Signal was amplified for 10 minutes in 0.04% DAB and 0.3% Nickel ammonium sulfate in 50 mM Tris-HCl (pH 7.6). Visualizaiton was performed by adding 0.003% H_2O_2 for 5 minutes and stopped by washing off with 50 mM Tris-HCl (pH 7.6).

6.3 RESULTS

6.3.1 Design of neuron-specific and inducible KCC2 gene expression

I intended to generate a transgenic mouse in which KCC2 can be overexpressed specifically in neuronal cells, thus avoiding abnormal glia function or neuron-glia interaction which could result from aberrant KCC2 overexpression in glial cell (Payne et al., 1996; Lu et al., 1999; Li et al., 2002; Barres and Barde; 2000). In addition, heterologous KCC2 expression should be strong enough to overcome inward chloride pumps such as NKCC1 that are expressed by immature neurons (Chapter III). Because of these reasons, I choose to use the Thy1.2 mouse expression cassette (Thy1.2). Thy1.2 has been widely used in the study of adult neuronal diseases such as Alzheimer's and neuronal cancer because it is capable of a strong, neuron specific, heterogenous expression (Aigner L et al., 1995). Although it was originally reported that Thy 1.2 drives gene expression as early as P6 (Caroni P 1997), however, it was later shown that gene expression can be detected as early as embryonic day 11 (Campsall et al., 2002), thus initiating gene expression not only in post-mitotic neurons, but also in proliferating neurons.

At the same time, it was also necessary to prevent KCC2 overexpression in proliferating neurons, because GABA depolarization can exert a trophic effect (Represa and Ben-Ari, 2005), as well as synaptic plasticity (Gaiarsa et al., 2002). In order to regulate KCC2 gene expression during a restricted developmental period, the "floxed P-STOP cassette" was positioned in front of KCC2 (Fig 6.1. A). The "floxed P-STOP cassette" is a DNA sequence which prevents downstream gene expression (Sauer, 1993). In the presence of the "floxed P-STOP cassette", KCC2 (and EGFP) expression will be suppressed, resulting in "silent KCC2OVER" mice. "Silent KCC2OVER" mice will be turn into "active KCC2OVER" mice if cells express the protein Cre. According to the Cre-loxP system, Cre protein binds to the loxP site and excises the STOP sequence (Lakso et al., 1992; Tsien et al., 1996), thus allowing Thy1.2 to drive KCC2 gene expression (Fig 6.1. C).

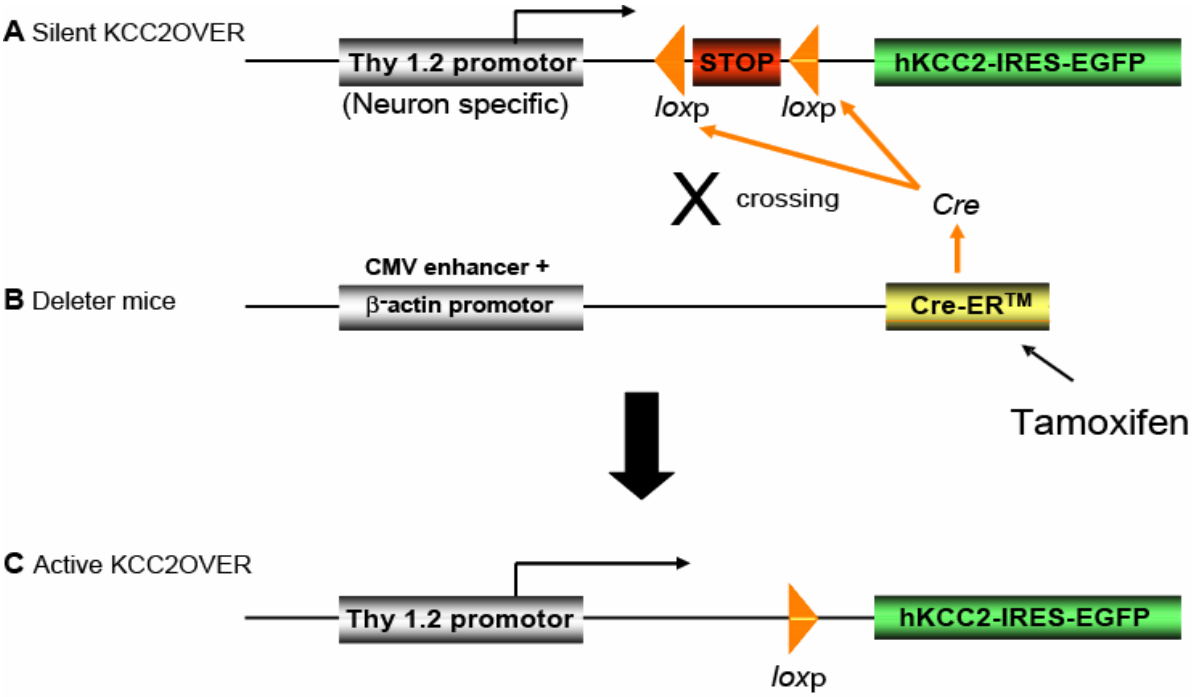

Figure 6.1. Schematic representation of inducible KCC2OVER mice

(A) *Silent KCC2OVER:* The Thy1.2 mouse expression cassette contains the Thy1.2 promoter which regulates neuron-specific gene expression. KCC2-IRES-EGFP is positioned downstream of the floxedSTOP cassette, which suppress downstream gene expression. **(B)** *Deleter mouse;* Cre expression is induced by tamoxifen. CMV enhancer and *beta*-actin pomoter drives strong CRE expression in every cell, including neurons. **(C)** *Active KCC2OVER mouse;* Offsprings from mating between Silent KCC2OVER mice **(A)** and Deleter mice **(B)**. Tamoxifen-induced Cre excised STOP, allowing the Thy1.2 promoter to drive the gene expression of hKCC2-IRES-EGFP.

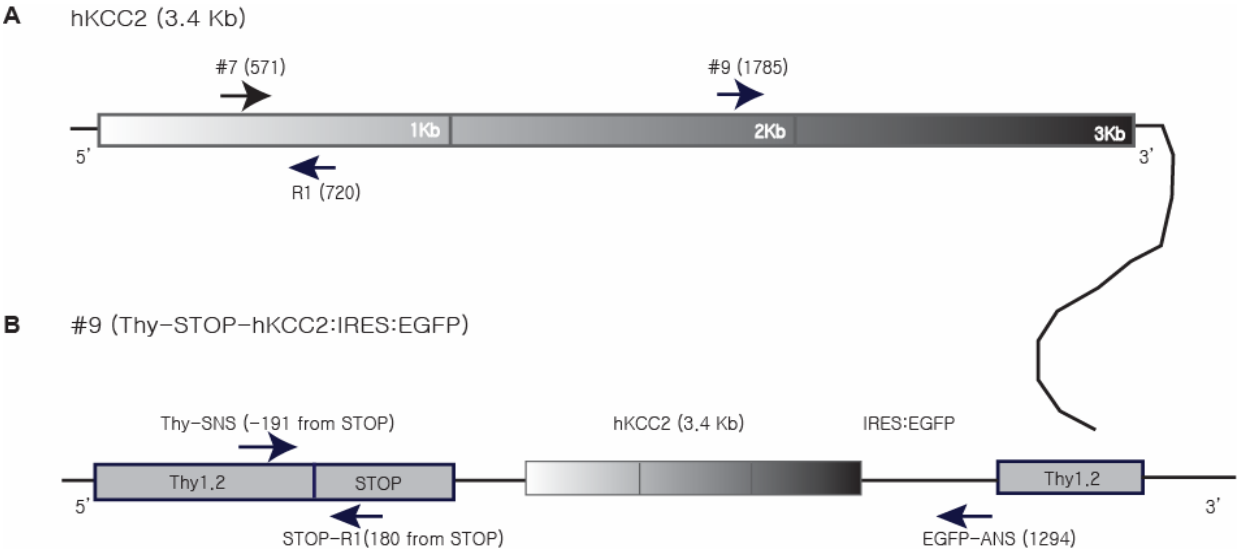

Figure 6.2. Diagram of the #9 construct (Thy1.2-loxP-STOP-loxP-KCC2-IRES-EGFP).

Arrows represent primer locations used for F1 genotyping; #7, #9, #Thy-SNS, Anti sense primers; #R1, #EGFP-ANS, KCC2-R1, Four combinations of primers (estimated size for PCR product): #7+R1 (149 base pair(bp)), #9+EGFP-ANS (3Kb), Thy-SNS+R1 (370 bp), Thy-SNS+STOP-R1 (270 bp) (primer sequence in materials and method section). Specific location for each primer within sequence map (bp) is indicated.

At last, in order to up-regulate Cre expression in a short period of time, I chose to use the Cre-ER^{TM} mouse line because in these mice tamoxifen application can quickly induce strong Cre expression pattern during the differentiation period as well as the proliferation period (Hayahsi and McMahon, 2002) (Fig 6.1. B). Using the #9 construct, containing Thy1.2 promoter-loxP-STOP-loxP-hKCC2:IRES:EGFP (Fig 6.2.), I generated "silent KCC2OVER" mice with inducible and spatially-regulated KCC2 overexpression.

6.3.2 *In-vitro* test for Cre/loxP site-specific recombination system

Before pronuclear injection of the linearized #9 construct, I tested:

A) if the STOP sequence would be sufficient to prevent KCC2 expression,
B) if Thy1.2 would render neuron specific expression, without leakage expression in a non-neuronal cells, and
C) if the Cre-LoxP system would provide inducible expression.

I tested (A) - (C) using immunoblots and immunocytochemistry.

Immunoblot: COS7 cells were transfected with 1) pMES-hKCC2, 2) pMES-STOP-hKCC2, 3) Thy1.2-hKCC2, 4) pMES-STOP-hKCC2 + pMES/Crej1 5) pMES-STOP-hKCC2 + pCAX/Crej1 and the KCC2 expression was detected in five lanes (Fig 6. 3.). In lane 1, there was a strong band at the appropriate molecular weight of KCC2, indicating KCC2 expression in cells transfected with pMES-hKCC2. This band was absent in lane 2, demonstrating that the STOP sequence effectively prevented KCC2 expression. In lane 3, KCC2 protein was not detected either, in line with Thy1.2 being a neuron specific expression cassette. Finally, in lanes 4 and 5, where pMES-STOP-KCC2 was co-transfected with Cre constructs, KCC2 expression was similar to lane 1, demonstrating the Cre/loxP site-specific recombination system is working as described elsewhere.

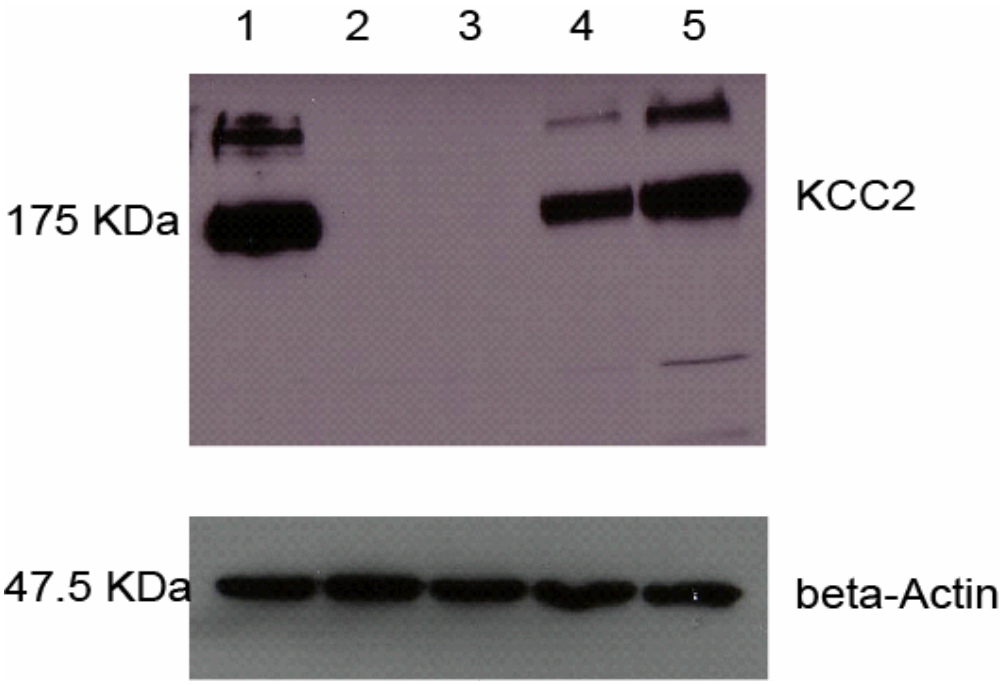

Figure 6.3. Cre/loxP site-specific recombination system tested by immunoblot.

COS7 cells transfected with pMES-hKCC2 (lane 1), pMES-STOP-hKCC2 (lane 2), Thy-hKCC2 (lane 3), pMES-STOP-hKCC2 + pMES/Crej1 (lane 4), pMES-STOP-hKCC2 + pCAX/Crej1 (lane 5). Lane 1; High level of hKCC2 expression was detected. Lane2; KCC2 expression was suppressed due to STOP cassette. Lane 3; Thy1.2 did not drive hKCC2 expression in COS7 cells. Lanes 4 & 5; Suppressed expression of KCC2 in pMES-STOP-hKCC2 was restored when a Cre vector was co-transfected. Protein amount was normalized to *beta*-actin (~45 KDa).

Immunocytochemistry: The #9 construct was transfected into immature cortical neurons in primary culture (E17 + 3DIV) and KCC2 overexpression was examined 2-3 days after transfection. When the #9 construct was transfected alone, no KCC2 overexpression was observed. However, with increased laser power, homogeneous background level of KCC2 was detected (Fig 6. 4., A, B), most likely representing low amount of endogenously expressed KCC2. When the #9 construct was co-transfected with a Cre construct (pCAX/Crej1), several neurons showed strong expression of KCC2 (Fig 6. 4 (C) ~ (D)), consistent with the results from the immunoblots (Fig 6. 3.).

Based on the above *in-vitro* test, I confirmed that the #9 construct is an optimal construct to be used for Cre/loxP site-specific recombination system *in- vivo*. At the transgenic facility at the Vanderbilt University, the #9 construct was linearized and injected into pseudo-pregnant mice for transgenic mice generation, from which 64 offsprings were born as candidate for transgenic mice. In order to screen for transgene insertion into genomic DNA, I conducted sequencing of DNA isolated from tails using the primer sets described in Fig 6.2. Primer sets generated 149 bp (#7 + R1), 3 Kbp (#9 + EGFP-ANS), 370 bp (Thy-SNS + R1), and 270 bp (Thy-SNS + STOP-R1) fragments (data not shown). Finally, I confirmed there were five different mice lines that incorporated the #9 construct into their genome ($KCC2OVER^{+}$). $KCC2OVER^{+}$ mice were mated to Cre-ER^{TM}. The offspring were genotyped with #7 + R1 thereafter. Among these, I characterized two mouse lines for KCC2 overexpression through EGFP detection: K8 and K7.

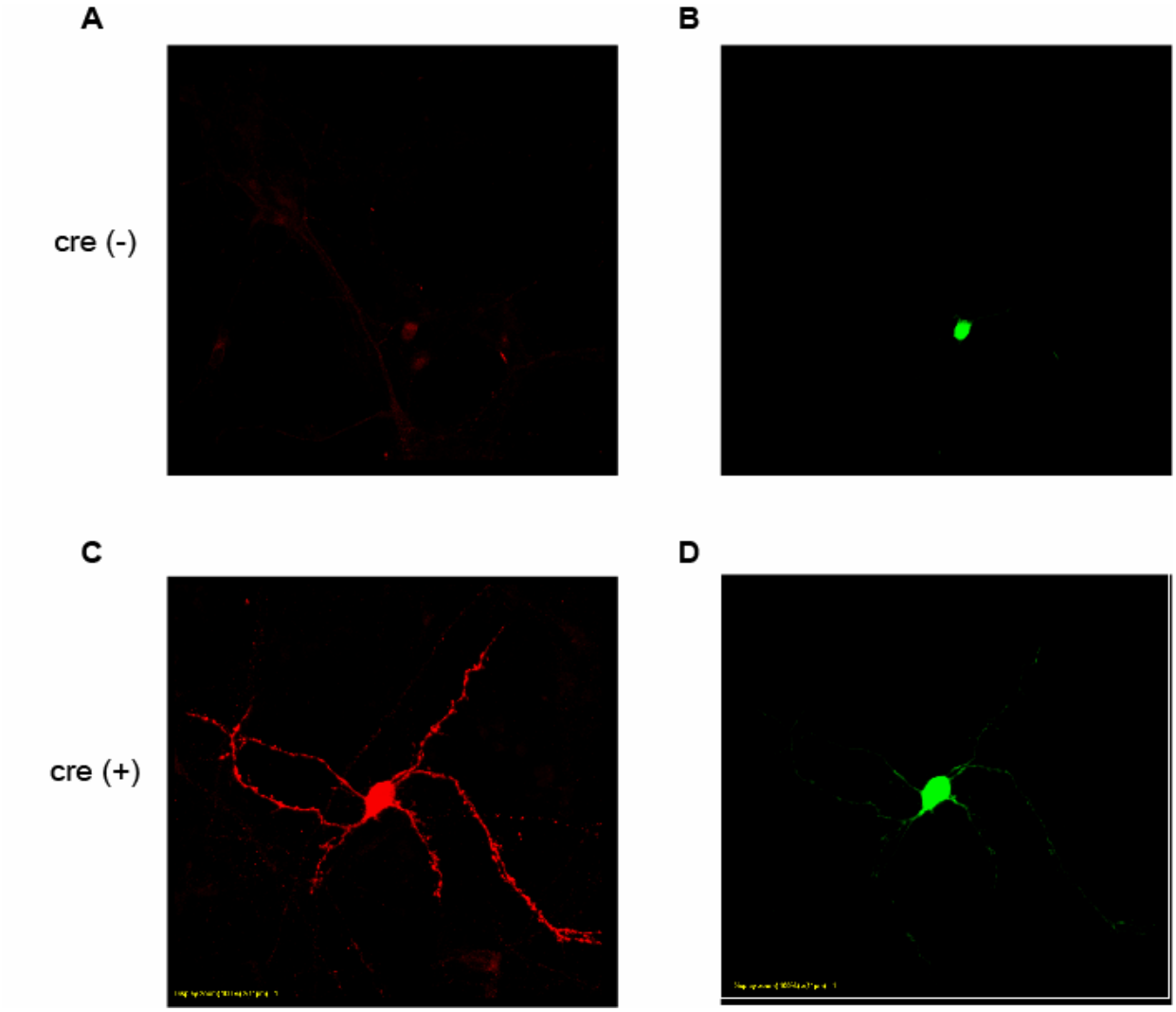

Figure 6.4. Expression of #9 construct (Thy1.2-loxp-STOP-loxp-hKCC2-IRES-EGFP) in primary cultured neurons and the test for the Cre/loxP site-specific recombination system by Immunocytochemistry.

Confocal images of KCC2 (**A** and **C**) and EGFP (**B** and **D**) expression. **(A)** & **(B)** the #9 construct was transfected alone. Neither KCC2 overexpression nor EGFP fluorescence was detected. PMT for **(A)** and **(B)** were considerably increased to observed background fluorescence. **(C)** ~ **(D)** The #9 construct and pCAX/Crej1 were co-transfected. KCC2 overexpression was readily detected in neurons exhibiting EGFP expression. pCAX/Crej1 does not contain EGFP.

6.3.3 KCC2 overexpression patterns *in-vivo*; EGFP immunoreactivity

K8-Line: The earliest age I characterized EGFP induction was P8 (offspring from the mating with Cre-ER-TM were fed Tamoxifen from P2 to P6). As presented in Fig 6.5., EGFP expression was detected in large pyramidal neurons in the cortex and hippocampal region. In the hippocampus, pyramidal neurons in CA1, CA2 and CA3 showed strong EGFP expression. In the cortex, such as visual, auditory and somatosensory areas, strong EGFP expression was restricted to layer V only. There was little EGFP expression in upper layers (layer II/III), layer VI, or subplate. No layer IV neurons expressed EGFP (Fig 6.5. A-C). Prefrontal cortex also showed strong EGFP expression in large pyramidal neurons (data not shown). In the cerebellum, EGFP expression was observed in small cells within the white matter. Based on their morphology, they did not appear to be neuronal cells, but further characterization is necessary to clarify this point (Fig 6.5. D). In the brain stem, EGFP was observed only in the facial nucleus and hypoglossal nuclei. Specifically, no EGFP expression was observed in any auditory brainstem regions, the inferior colliculus, or the thalamus. EGFP expression was not examined in spinal cord. Other than the cerebellar white matter, where subsequent characterization is needed, I did not observe EGFP expression in non-neuronal cells.

K7-Line: The earliest age at which I characterized for EGFP induction was P7 (offspring from the mating with Cre-ER-TM were fed Tamoxifen from P2 to P6). As presented in figure 6.6, large pyramidal neurons in the cortex and hippocampus expressed EGFP. Neurons in the dentate gyrus also showed strong EGFP expression (Fig 6.6. F). The K7 line showed strong EGFP expression in upper layers (layer II/III), layer VI and subplate. EGFP expression was not observed in Layer IV. The auditory brainstem region did not show EGFP expression nor did the inferior colliculus. Gene expression pattern in other brain areas has not been characterized. I did not observe EGFP expression in non-neuronal cells of the K7 mice.

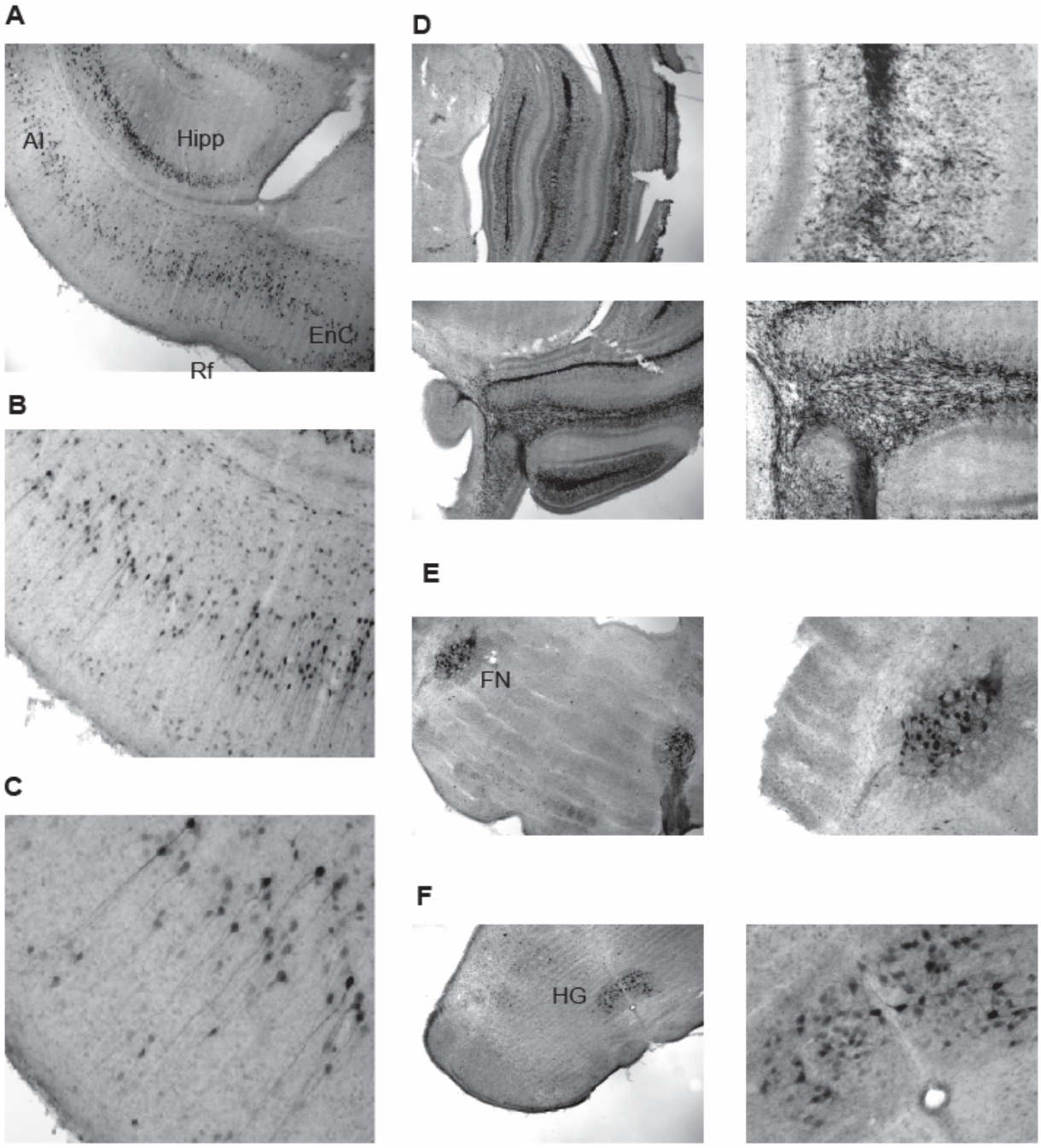

Figure 6.5.

Figure 6.5. KCC2 overexpression patterns in the K8 line at age P8 as detected by EGFP **(A)** Auditory cortex and hippocampus (including entorhinal cortex). Within auditory cortex, EGFP overexpression was prominent in layer V pyramidal neurons. Very little expression was detected in supergranular upper layers (layer II/III) and in layer VI or subplate. Also, hippocampal neurons showed EGFP overexpression in hippocampus. X10 Rf; rhinal fissure **(B)** Enlarged image for auditory cortex X20 **(C)** Enlarged image for layer V pyramidal neurons X40. **(D)** Cerebellum; Within cerebellum, EGFP overexpression was observed in non-neuronal cells (Further characterization is necessary.). X10 (left), X20 (right). **(E)** and **(F)** nuclei within brainstem also overexpressed EGFP in pyramidal neurons. **(E)** Facial Nucleus; X10 (left), X20 (right) **(F)** Hypoglossal; X10 (left), X20 (right)

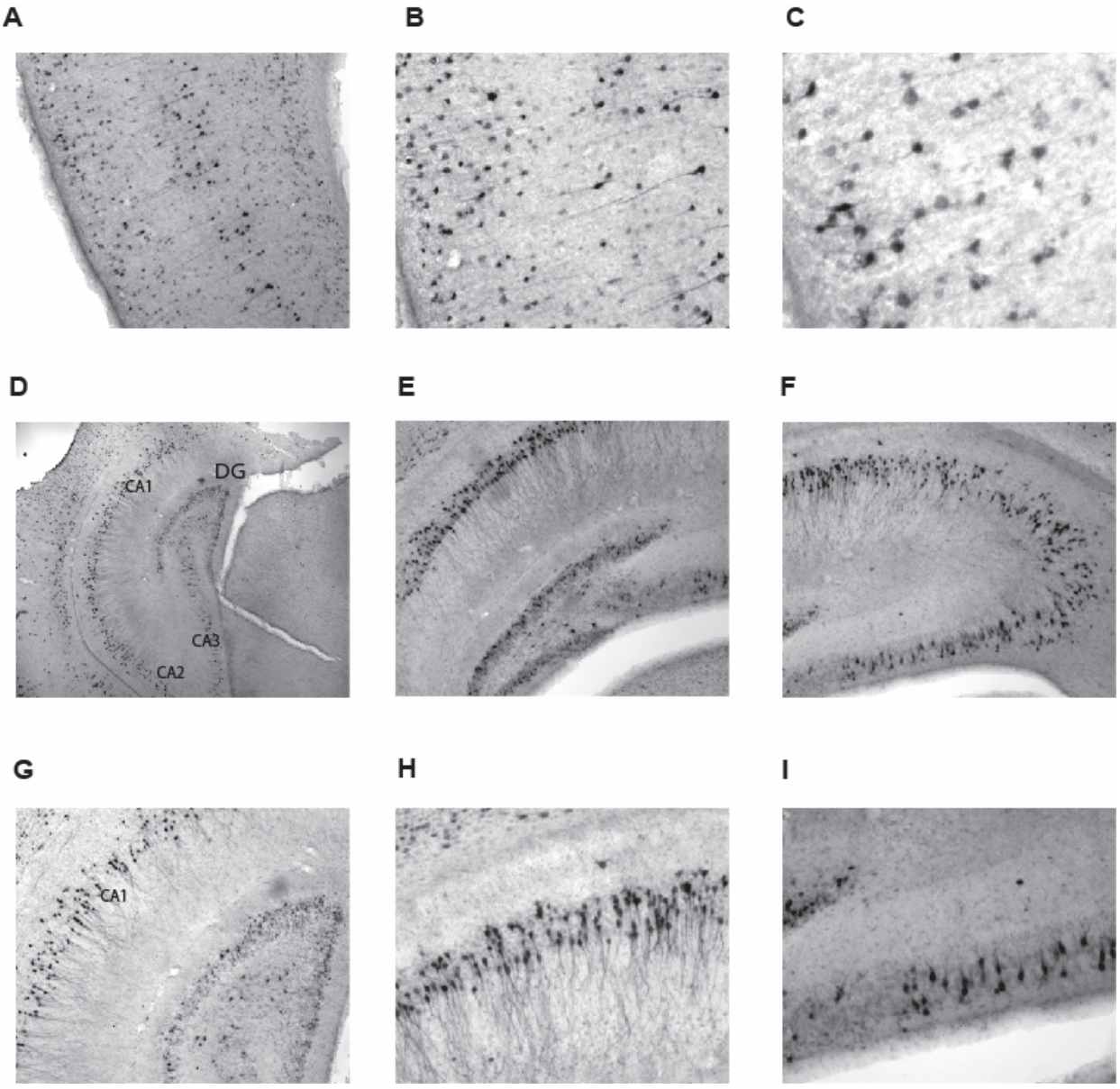

Figure 6.6.

Figure 6.6. KCC2 overexpression pattern in the K7 line at age P7 detected by EGFP.
(A)-(C) auditory cortex. Within the auditory cortex; EGFP overexpression was detected in layer V pyramidal neurons. Also, EGFP overexpression was detected in upper layer (layer II/III) and layer VI and subplate. **(D)~(F)** Hippocampus; CA1, CA2, CA3 and dentate gyrus. Large pyramidal neurons express high level of EGFP.

6.3.4 Auditory cortex detection using AChE staining method; K8

In both K7 and K8 mouse line KCC2 could be overexpressed in cortical areas which may include the primary auditory cortex. In a coronal brain slice, the location of the auditory cortex can be ambiguous due to its proximity to the visual cortex and somatosensory cortex. Therefore, I confirmed the relative location of the auditory cortex in a coronal section using acetylcholine esterase histochemistry (Modified from Tago et al., 1986). Also, I wanted to investigate if the auditory cortex does in fact exist in KCC2OVER mice since premature KCC2 overexpression could have an effect on the circuit wiring during the synapse refinement period. Previous studies showed that development, AChE is transiently expressed the auditory cortex of rats, with peak expression occurring around the second postnatal week (Aramakis and Matherate, 1998). Consistent to what was observed in rat auditory cortex, in KCC2OVER mice, the AChE staining within cortical area was detected next to the rhinal fissure (Fig 6.7. A), a region which corresponds to the auditory cortex (Ref: Mouse brain atlas). In enlarged images, the layer IV-specific staining of AChE was evident (Fig 6.7. B). The length of the auditory area in rostral-caudal direction is around 600-700 μm. Also, there was high level of AChE in the thalamus and prefrontal cortical areas.

In conclusion, I generated transgenic mice where KCC2overexpression can be achieved in a neuron-specific and in a timely regulated manner. These mice can be used in future studies to investigate how neural circuit matures in the absence of GABA/glycinergic depolarization.

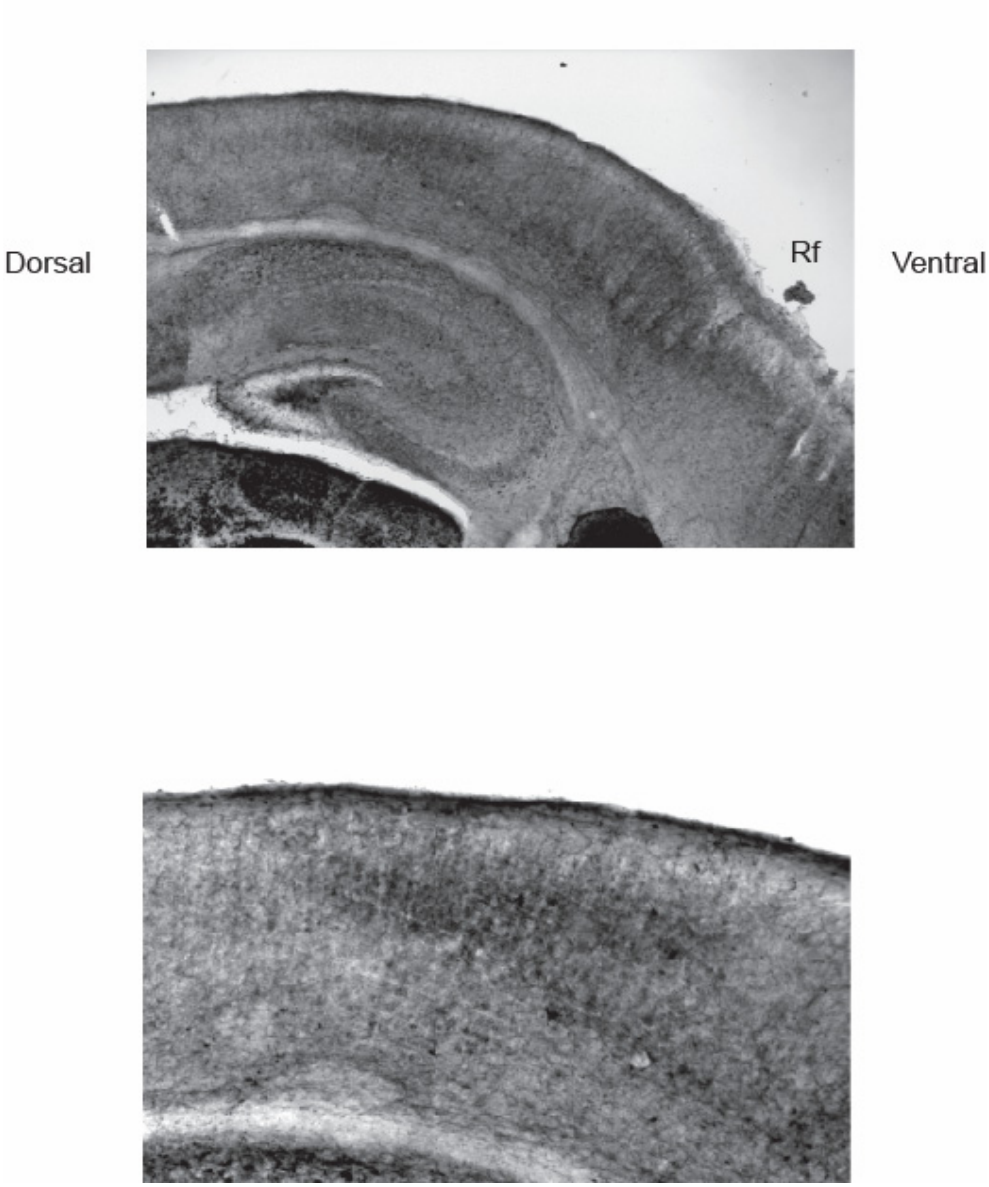

Figure 6.7. AChE staining in cortical slice of K8.

AChE staining in cortical slice of K8. Auditory cortex was detected using acetylcholine esterase histochemistry method. **(A)** Specific staining (darker area within cortex) was observed in layer IV in dorsal direction next to the Rf. Thalamus showed the strongest staining. Hippocampus also showed high expression of acetylcholine esterase. X10 **(B)** enlarged image of auditory cortex. Specific staining within layer IV was clear. X40

6.4 DISCUSSION

By using the Cre/loxP site-specific recombination system (Sauer, 1993), I demonstrated that KCC2 could be overexpressed conditionally *in-vivo*. Tamoxifen-induced EGFP expression was observed primarily in large pyramidal neurons within cortex and hippocampus in both K7 and K8. However, the EGFP expression pattern between K7 and K8 varied, even though the incorporated regulatory elements, Thy1.2 mice expression cassette (Caroni, 1997), were identical. This variation in expression of EGFP between K7 and K8 is consistent with previous observations in transgenic mice, in which Thy promoter drove various expression patterns of incorporated XFP (red, green, yellow and cyan) protein (Feng et al., 2000), suggesting that Thy1.2 might exert its control over gene expression variably depending on the specific condition encountered *in-vivo* during its incorporation into a genomic DNA.

K8 is of particular interest since it showed specific expression only in cortical layer V. Layer V is the major source of output to the thalamus (Turner et al., 2005), intercortex (Alitto and Usrey, 2003), and inferior colliculus (Bajo and Moore, 2005), after combining synaptic input from the upper cortical layers. Therefore, these mice could be useful in investigating how layer V pyramidal neurons interact with upper cortical layers to process inhibitory and excitatory synaptic inputs in the absence of normal GABAergic excitatory responses during early postnatal development.

In K7, interestingly, neurons within all cortical layers except layer IV express EGFP. This line could be useful in addressing the role of inhibitory synapse maturation in the development of layer-specific columnar structure, which would be formed through interactions between layers. For example, previous studies have shown that the subplate governs maturation of inhibition within the cortex, which is crucial for the formation of ocular dominance columns in visual cortex (Kanold and Shatz, 2006). This study might suggest that interaction between

cortical layers is important to regulate refined structure within the cortex. The previous study employed ablation into the layer VI, which resulted in the down regulation of KCC2 in layer IV. In my case, it would be interesting to address how layer IV neurons (output layer which did not express EGFP) would respond to the earlier switch to GABA/glycinergic hyperpolarization in upper layers (layer II/III, input layer which expressed EGFP) or ablation within layer IV and its effect on layer II/III in the presence or absence of KCC2overexpression during perinatal development. This further study would extend our knowledge on if GABA/glycinergic response polarity in specific layer(s) would be important for the refinement of cortical circuit.

In the KCC2OVER mice characterized in this study, EGFP expression was not observed in LSO neurons, implying that GABA/glycinergic response polarity would remain normal in these neurons during development in KCC2OVER mice. Thus, it could not be tested whether the functional refinement of the MNTB-LSO pathway is mediated through depolarizing GABA/glycinergic responses during the first postnatal week in LSO neurons (Kim and Kandler, 2003). Still, KCC2OVER mice will provide a valuable *in-vivo* model where the importance of GABA/glycinergic excitatory responses can be addressed in neural circuit development. However, whether KCC2 protein overexpressed *in- vivo* is functional, capable of shifting E_{Cl} to a more hyperpolarized and prematurely terminating the depolarizing GABA/glycinergic responses, remains to be addressed. In addition, it is important to know how early KCC2 overexpression can be induced in KCC2OVER mice. K7 and K8 mice survive to later developmental ages if KCC2 is overexpressed by Tamoxifen application during the first postnatal week (Personal observation made up to 3 weeks of age in KCC2-KD mice). Thus, it would also be interesting to investigate whether genetic modifications during early developmental stage would cause abnormal circuit development or behavioral modifications to arise during later development.

7.0 BIBLIOGRAPHY

Aamodt SM, Constantine-Paton M. (1999) The role of neural activity in synaptic development and its implications for adult brain function. Adv Neurol 79:133-44.

Aguado F, Carmona MA, Pozas E, Aguilo A, Martinez-Guijarro FJ, Alcantara S, Borrell V, Yuste R, Ibanez CF, Soriano E. (2003) BDNF regulates spontaneous correlated activity at early developmental stages by increasing synaptogenesis and expression of the K+/Cl- co-transporter KCC2. Development., 130:1267-80.

Akerman CJ, Cline HT. (2006) Depolarizing GABAergic conductances regulate the balance of excitation to inhibition in the developing retinotectal circuit in vivo. J Neurosci., 26:5117-30.

Aigner L, Arber S, Kapfhammer JP, Laux T, Schneider C, Botteri F, Brenner HR, Caroni P. (1995) Overexpression of the neural growth-associated protein GAP-43 induces nerve sprouting in the adult nervous system of transgenic mice. Cell. 83:269-78.

Ali DW, Drapeau P, Legendre P. (2000) Development of spontaneous glycinergic currents in the Mauthner neuron of the zebrafish embryo. J Neurophysiol. 84:1726-36.

Alitto HJ, Usrey WM. (2003) Corticothalamic feedback and sensory processing. Curr Opin Neurobiol. 13:440-5.

Andrasfalvy BK, Magee JC. (2001) Distance-dependent increase in AMPA receptor number in the dendrites of adult hippocampal CA1 pyramidal neurons. J Neurosci. 21:9151-9.

Aramakis VB, Metherate R. (1998) Nicotine selectively enhances NMDA receptor-mediated synaptic transmission during postnatal development in sensory neocortex. J Neurosci. 18:8485-95.

Arvidsson A, Kokaia Z, Lindvall O. (2001) N-methyl-D-aspartate receptor-mediated increase of neurogenesis in adult rat dentate gyrus following stroke. Eur J Neurosci. 14:10-8.

Awatramani GB, Turecek R, Trussell LO. (2005) Staggered development of GABAergic and glycinergic transmission in the MNTB. J Neurophysiol. 93:819-28.

Bajo VM, Moore DR. (2005) Descending projections from the auditory cortex to the inferior colliculus in the gerbil, Meriones unguiculatus. J Comp Neurol. 486:101-16.

Balakrishnan V, Becker M, Lohrke S, Nothwang HG, Guresir E, Friauf E. (2003) Expression and Function of Chloride Transporters during Development of Inhibitory Neurotransmission in the Auditory Brainstem. J Neurosci. 23:4134-4145.

Baldelli P, Novara M, Carabelli V, Hernandez-Guijo JM, Carbone E. (2002) BDNF up-regulates evoked GABAergic transmission in developing hippocampus by potentiating presynaptic N- and P/Q-type Ca2+ channels signalling. Eur J Neurosci. 16:2297-310.

Balice-Gordon RJ, Lichtman JW. (1994) Long-term synapse loss induced by focal blockade of postsynaptic receptors. Nature. 372:519-24.

Barnes-Davies M, Forsythe ID. (1995) Pre- and postsynaptic glutamate receptors at a giant excitatory synapse in rat auditory brainstem slices. J Physiol. 488:387-406.

Barres BA, Barde Y. (2000) Neuronal and glial cell biology. Curr Opin Neurobiol. 10:642-8.

Bedford, F.K., Kittler, J.T., Muller, E., Thomas, P., Uren, J.M., Merlo, D., Wisden, W., Triller, A., Smart, T.G. and Moss, S.J. (2001) GABAA receptor cell surface number and subunit stability are regulated by the ubiquitin-like protein Plic-1. Nat. Neurosci. 4: 908–916

Behar TN, Li YX, Tran HT, Ma W, Dunlap V, Scott C, Barker JL. (1996) GABA stimulates chemotaxis and chemokinesis of embryonic cortical neurons via calcium-dependent mechanisms. J Neurosci. 16:1808-18.

Behar TN, Schaffner AE, Scott CA, Greene CL, Barker JL. GABA receptor antagonists modulate postmitotic cell migration in slice cultures of embryonic rat cortex. (2000) Cereb Cortex. 10:899-909.

Ben Ari, Y. (2002) Excitatory actions of gaba during development: the nature of the nurture. Nature Rev. Neurosci., 3, 728–739.

Ben Ari, Y., Khazipov, R., Leinekugel, X., Caillard, O. & Gaiarsa, J.L. (1997) GABAA, NMDA and AMPA receptors: a developmentally regulated 'menage a trois'. TINS, 20, 523–529.

Billups B, Graham BP, Wong AY, Forsythe ID. (2005) Unmasking group III metabotropic glutamate autoreceptor function at excitatory synapses in the rat CNS. J Physiol. 565:885-96.

Bonislawski DP, Schwarzbach EP, Cohen AS. Brain injury impairs dentate gyrus inhibitory efficacy. (2007) Neurobiol Dis. 25:163-9.

Bormann, J., Hamill, O.P. & Sakmann, B. (1987) Mechanism of anion permeation through channels gated by glycine and gamma-aminobutyric acid in mouse cultured spinal neurones. J. Physiol. (Lond.), 385, 243–286.

Borodinsky LN, Root CM, Cronin JA, Sann SB, Gu X, Spitzer NC. (2004) Activity-dependent homeostatic specification of transmitter expression in embryonic neurons. Nature. 429:523-30

Boudreau JC, Tsuchitani C (1968) Binaural interaction in the cat superior olive S segment. J Neurophysiol 31: 442-454.

Breitwieser, G.E., Altamirano, A.A. & Russell, J.M. (1990) Osmotic stimulation of Na(+)-K(+)-Cl cotransport in squid giant axon is $[Cl]_i$ dependent. Am. J. Physiol., 258, C749–C753.

Brunig I, Penschuck S, Berninger B, Benson J, Fritschy JM. (2001) BDNF reduces miniature inhibitory postsynaptic currents by rapid downregulation of GABA(A) receptor surface expression. Eur J Neurosci. 13:1320-8.

Campsall KD, Mazerolle CJ, De Repentingy Y, Kothary R, Wallace VA. (2002) Characterization of transgene expression and Cre recombinase activity in a panel of Thy-1 promoter-Cre transgenic mice. Dev Dyn. 224:135-43.

Cancedda L, Fiumelli H, Chen K, Poo MM. (2007) Excitatory GABA action is essential for morphological maturation of cortical neurons *in-vivo.* J Neurosci. 27:5224-35.

Caroni P (1997) Overexpression of growth-associated proteins in the neurons of adult transgenic mice. J Neurosci Methods. 71:3-9.

Chang EH, Kotak VC, Sanes DH. (2003) Long-term depression of synaptic inhibition is expressed postsynaptically in the developing auditory system. J Neurophysiol. 90:1479-88.

Chen C, Regehr WG. (2000) Developmental remodeling of the retinogeniculate synapse. Neuron. 28:955-66.

Chih B, Engelman H, Scheiffele P. (2005) Control of excitatory and inhibitory synapse formation by neuroligins. Science. 307:1324-8.

Chudotvorova I, Ivanov A, Rama S, Hubner CA, Pellegrino C, Ben-Ari Y, Medina I. (2005) Early expression of KCC2 in rat hippocampal cultures augments expression of functional GABA synapses. J Physiol. 566:671-9.

Clayton, G.H., Owens, G.C., Wolff, J.S. & Smith, R.L. (1998) Ontogeny of cation-Cl cotransporter expression in rat neocortex. Brain Res. Dev. Brain Res., 109, 281–292.

Colman H, Nabekura J, Lichtman JW. (1997) Alterations in synaptic strength preceding axon withdrawal. Science. 275:356-61.

Colonnese MT, Zhao JP, Constantine-Paton M. (2005) NMDA receptor currents suppress synapse formation on sprouting axons *in- vivo*. J Neurosci. 25:1291-303.

Colonnese MT, Constantine-Paton M. (2006) Developmental period for N-methyl-D-aspartate (NMDA) receptor-dependent synapse elimination correlated with visuotopic map refinement. J Comp Neurol. 494:738-51.

Connor, J.A., Tseng, H.Y. & Hockberger, P.E. (1987) Depolarization- and transmitter-induced changes in intracellular Ca^{2+} of rat cerebellar granule cells in explant cultures. J. Neurosci., 7, 1384–1400

Coull, J.A.M., Boudreau, D., Bachand, K., Prescott, S.A., Nault, F., Sik, A., De Koninck, P. & De Koninck, Y. (2003) Trans-synaptic shift in anion gradient in spinal lamina I neurons as a mechanism of neuropathic pain. Nature, 424, 938–942

Craven SE, Bredt DS. (1998) PDZ proteins organize synaptic signaling pathways. Cell. 93:495-8.

Dames W, Joo F, Feher O, Toldi J, Wolff JR. (1985) gamma-Aminobutyric acid enables synaptogenesis in the intact superior cervical ganglion of the adult rat. Neurosci Lett. 54:159-64.

Dani VS, Chang Q, Maffei A, Turrigiano GG, Jaenisch R, Nelson SB. (2005) Reduced cortical activity due to a shift in the balance between excitation and inhibition in a mouse model of Rett syndrome. Proc Natl Acad Sci U S A. 102:12560-5

DeFazio, R.A., Keros, S., Quick, M.W., Hablitz, J.J. (2000) Potassium-coupled chloride cotransport controls intracellular chloride in rat neocortical pyramidal neurons. Journal of Neuroscience 20: 8069-8076

De Koninck Y. (2007) Altered chloride homeostasis in neurological disorders: a new target. Curr Opin Pharmacol. 7:93-9.

Delpire E, Mount DB. (2002) Human and murine phenotypes associated with defects in cation-chloride cotransport. Annu Rev Physiol. 64:803-843

Desai NS, Cudmore RH, Nelson SB, Turrigiano GG. (2002) Critical periods for experience-dependent synaptic scaling in visual cortex. Nat Neurosci. 5:783-9.

Durham D, Rubel EW, Steel KP. (1989) Cochlear ablation in deafness mutant mice: 2-deoxyglucose analysis suggests no spontaneous activity of cochlear origin. Hear Res. 43:39-46.

Ehret G, Romand R. (1992) Development of tone response thresholds, latencies and tuning in the mouse inferior colliculus. Brain Res Dev Brain Res. 67:317-26.

Ehrlich, I., Lohrke, S. & Friauf, E. (1999) Shift from depolarizing to hyperpolarizing glycine action in rat auditory neurones is due to age-dependent Cl regulation. J. Physiol. (Lond.), 520, 121–137.

Ehrlich I, Malinow R. (2004) Postsynaptic density 95 controls AMPA receptor incorporation during long-term potentiation and experience-driven synaptic plasticity. J Neurosci. 24:916-27.

Ehlers MD. (2000) Reinsertion or degradation of AMPA receptors determined by activity-dependent endocytic sorting. Neuron. 28:511-25.

Ehret G, Romand R. (1992) Development of tone response thresholds, latencies and tuning in the mouse inferior colliculus. Brain Res Dev Brain Res. 67:317-26.

Elgoyhen AB, Johnson DS, Boulter J, Vetter DE, Heinemann S. (1994) Alpha 9: an acetylcholine receptor with novel pharmacological properties expressed in rat cochlear hair cells. Cell. 79:705-15.

El-Husseini AE, Schnell E, Chetkovich DM, Nicoll RA, Bredt DS. (2000) PSD-95 involvement in maturation of excitatory synapses. Science. 290:1364-8.

Ene FA, Kalmbach A, Kandler K. (2007) Metabotropic glutamate receptors in the lateral superior olive activate TRP-like channels: Age and experience-dependent regulation. J Neurophysiol. 97:3365-75

Ene FA, Kullmann PH, Gillespie DC, Kandler K. (2003) Glutamatergic calcium responses in the developing lateral superior olive: receptor types and their specific activation by synaptic activity patterns. J Neurophysiol. 90:2581-91.

Erazo-Fischer E, Striessnig J, Taschenberger H. (2007) The role of physiological afferent nerve activity during *in- vivo* maturation of the calyx of Held synapse. J Neurosci. 27: 1725-37.

Essrich, C., M. Lorez, J.A. Benson, J.M. Fritschy, and B. Luscher. (1998) Postsynaptic clustering of major GABAA receptor subtypes requires the gamma 2 subunit and gephyrin. *Nat. Neurosci.* 1:563–571

Feller MB, Butts DA, Aaron HL, Rokhsar DS, Shatz CJ. (1997) Dynamic processes shape spatiotemporal properties of retinal waves. Neuron. 19:293-306.

Feng G, Mellor RH, Bernstein M, Keller-Peck C, Nguyen QT, Wallace M, Nerbonne JM, Lichtman JW, Sanes JR. (2000) Imaging neuronal subsets in transgenic mice expressing multiple spectral variants of GFP. Neuron 28:41-51.

Fiszman ML, Schousboe A. (2004) Role of calcium and kinases on the neurotrophic effect induced by gamma-aminobutyric acid. J Neurosci Res. 76:435-41.

Fiumelli H, Cancedda L, Poo MM. (2005) Modulation of GABAergic transmission by activity via postsynaptic Ca2+-dependent regulation of KCC2 function. Neuron. 48:773-86.

Fiumelli H, Woodin MA. (2007) Role of activity-dependent regulation of neuronal chloride homeostasis in development. Curr Opin Neurobiol. 17:81-6.

Forsythe ID, Clements JD. (1990) Presynaptic glutamate receptors depress excitatory monosynaptic transmission between mouse hippocampal neurones. J Physiol. 429:1-16.

Franks KM, Isaacson JS. (2005) Synapse-specific downregulation of NMDA receptors by early experience: a critical period for plasticity of sensory input to olfactory cortex. Neuron. 47:101-14.

Frerking M, Borges S, Wilson M. (1995) Variation in GABA mini amplitude is the consequence of variation in transmitter concentration. Neuron. 15:885-95.

Fritschy JM, Meskenaite V, Weinmann O, Honer M, Benke D, Mohler H. (1999) GABAB-receptor splice variants GB1a and GB1b in rat brain: developmental regulation, cellular distribution and extrasynaptic localization. Eur J Neurosci. 11:761-8.

Futai K, Okada M, Matsuyama K, Takahashi T. (2001) High-fidelity transmission acquired via a developmental decrease in NMDA receptor expression at an auditory synapse. J Neurosci. 21:3342-9.

Gaiarsa JL, Caillard O, Ben-Ari Y. (2002) Long-term plasticity at GABAergic and glycinergic synapses: mechanisms and functional significance. Trends Neurosci. 25:564-70.

Galanopoulou, A.S., Kyrozis, A., Claudio, O.I., Stanton, P.K. & Moshe, S.L. (2003) Sex-specific KCC2 expression and GABA(A) receptor function in rat substantia nigra. Exp. Neurol., 183, 628–637.

Galeffi F, Sah R, Pond BB, George A, Schwartz-Bloom RD. (2004) Changes in intracellular chloride after oxygen-glucose deprivation of the adult hippocampal slice: effect of diazepam. J Neurosci. 24:4478-88.

Ganguly K, Schinder AF, Wong ST, Poo M. (2001) GABA itself promotes the developmental switch of neuronal GABAergic responses from excitation to inhibition. Cell. 105:521-32.

Gao BX, Stricker C, Ziskind-Conhaim L. (2001) Transition from GABAergic to glycinergic synaptic transmission in newly formed spinal networks. J Neurophysiol. 86:492-502.

Ge S, Goh EL, Sailor KA, Kitabatake Y, Ming GL, Song H. (2006) GABA regulates synaptic integration of newly generated neurons in the adult brain. Nature. 439:589-93.

Geiger JR, Melcher T, Koh DS, Sakmann B, Seeburg PH, Jonas P, Monyer H. (1995) Relative abundance of subunit mRNAs determines gating and Ca2+ permeability of AMPA receptors in principal neurons and interneurons in rat CNS. Neuron. 15:193-204.

Glaum SR, Brooks PA. (1996) Tetanus-induced sustained potentiation of monosynaptic inhibitory transmission in the rat medulla: evidence for a presynaptic locus. J. Neurophysiol. 76:30–38.

Glowatzki E, Fuchs PA. (2000) Cholinergic synaptic inhibition of inner hair cells in the neonatal mammalian cochlea. Science. 288:2366-8.

Gonzalez-Islas C, Wenner P. (2006) Spontaneous network activity in the embryonic spinal cord regulates AMPAergic and GABAergic synaptic strength. Neuron. 49:563-75.

Goodman CS, Shatz CJ. (1993) Developmental mechanisms that generate precise patterns of neuronal connectivity. Cell. 72:77-98.

Hamann M, Billups B, Forsythe ID. (2003) Non-calyceal excitatory inputs mediate low fidelity synaptic transmission in rat auditory brainstem slices. Eur J Neurosci. 18:2899-902.

Hanover JL, Huang ZJ, Tonegawa S, Stryker MP. (1999) Brain-derived neurotrophic factor overexpression induces precocious critical period in mouse visual cortex. J Neurosci. 19:RC40.

Hartman KN, Pal SK, Burrone J, Murthy VN. (2006) Activity-dependent regulation of inhibitory synaptic transmission in hippocampal neurons. Nat Neurosci. 9:642-9.

Hartnett, K.A., Stout, A.K., Rajdev, S., Rosenberg, P.A., Reynolds, I.J. & Aizenman, E. (1997) NMDA receptor-mediated neurotoxicity: a paradoxical requirement for extracellular Mg^{2+} in Na^{+}/Ca^{2+}-free solutions in rat cortical neurons *in- vitro*. J. Neurochem., 68, 1836–1845.

Hayashi S, McMahon AP. (2002) Efficient recombination in diverse tissues by a tamoxifen-inducible form of Cre: a tool for temporally regulated gene activation/inactivation in the mouse. Dev Biol 244:305-318

Hayashi Y, Shi SH, Esteban JA, Piccini A, Poncer JC, Malinow R. (2000) Driving AMPA receptors into synapses by LTP and CaMKII: requirement for GluR1 and PDZ domain interaction. Science. 287:2262-7.

Hendry SH, Jones EG. (1986) Reduction in number of immunostained GABAergic neurones in deprived-eye dominance columns of monkey area 17. Nature. 320:750-3.

Hensch TK, Fagiolini M, Mataga N, Stryker MP, Baekkeskov S, Kash SF. (1998) Local GABA circuit control of experience-dependent plasticity in developing visual cortex. Science. 282:1504-8.

Hoffpauir BK, Grimes JL, Mathers PH, Spirou GA. (2006) Synaptogenesis of the calyx of Held: rapid onset of function and one-to-one morphological innervation. J Neurosci. 26:5511-23.

Hollmann M, Hartley M, Heinemann S. (1991) Ca2+ permeability of KA-AMPA--gated glutamate receptor channels depends on subunit composition. Science. 252:851-3.

Huang ZJ, Kirkwood A, Pizzorusso T, Porciatti V, Morales B, Bear MF, Maffei L, Tonegawa S. (1999) BDNF regulates the maturation of inhibition and the critical period of plasticity in mouse visual cortex. Cell. 98:739-55.

Hubner CA, Stein V, Hermans-Borgmeyer I, Meyer T, Ballanyi K, Jentsch TJ. (2001) Disruption of KCC2 reveals an essential role of K-Cl cotransport already in early synaptic inhibition. Neuron. 30:515-24

Hull C, von Gersdorff H. (2004) Fast endocytosis is inhibited by GABA-mediated chloride influx at a presynaptic terminal. Neuron. 44:469-82.

Inoue K, Yamada J, Ueno S, Fukuda A. (2006) Brain-type creatine kinase activates neuron-specific K+-Cl- co-transporter KCC2. J Neurochem. 96:598-608.

Isaacson JS. (1998) GABAB receptor-mediated modulation of presynaptic currents and excitatory transmission at a fast central synapse. J Neurophysiol. 80:1571-6.

Isaacson JS, Solis JM, Nicoll RA. (1993) Local and diffuse synaptic actions of GABA in the hippocampus. Neuron. 10:165-75.

Isokawa M. (1996) Decrement of GABAA receptor-mediated inhibitory postsynaptic currents in dentate granule cells in epileptic hippocampus. J Neurophysiol. 75:1901-8

Iwasaki S, Takahashi T. (2001) Developmental regulation of transmitter release at the calyx of Held in rat auditory brainstem. J Physiol. 534:861-71.

Jiao Y, Zhang C, Yanagawa Y, Sun QQ. (2006) Major effects of sensory experiences on the neocortical inhibitory circuits. J Neurosci. 26:8691-701.

Joshi I, Wang LY. (2002) Developmental profiles of glutamate receptors and synaptic transmission at a single synapse in the mouse auditory brainstem, Journal of Physiology 540: 861-873

Joshi I, Shokralla S, Titis P, Wang LY. (2004) The role of AMPA receptor gating in the development of high-fidelity neurotransmission at the calyx of Held synapse. J Neurosci. 24:183-96.

Kamiya K, Takahashi K, Kitamura K, Momoi T, Yoshikawa Y. (2001) Mitosis and apoptosis in postnatal auditory system of the C3H/He strain. Brain Res. 901:296-302.

Kandler K. (2004) Activity-dependent organization of inhibitory circuits: lessons from the auditory system. Curr Opin Neurobiol. 14:96-104.

Kandler K and Friauf F (1993) Pre- and postnatal development of efferent connections of the cochlear nucleus in the rat. J. Comp. Neurol. 328:161-184.

Kandler K, Friauf E. (1995) Development of glycinergic and glutamatergic synaptic transmission in the auditory brainstem of perinatal rats. J Neurosci. 15:6890-904.

Kandler, K and Gillespie, DC (2005) Developmental refinement of inhibitory sound-localization circuits. TINS 28: 290-296

Kandler, K., Kullmann, P.H.M., Ene, F.A. & Kim, G. (2002) Excitatory action of an immature glycinergic/GABAergic sound localization pathway. Physiol. Behav., 77:583–587.

Kanold PO, Shatz CJ. (2006) Subplate neurons regulate maturation of cortical inhibition and outcome of ocular dominance plasticity. Neuron. 51:627-38.

Kapfer C, Seidl AH, Schweizer H, Grothe B. (2002) Experience-dependent refinement of inhibitory inputs to auditory coincidence-detector neurons. Nat Neurosci. 5:247-53.

Karadsheh MF, Delpire E. (2001) Neuronal restrictive silencing element is found in the KCC2 gene: molecular basis for KCC2-specific expression in neurons. J Neurophysiol. 85:995-7.

Katz LC, Shatz CJ. (1996) Synaptic activity and the construction of cortical circuits. Science. 274:1133-8.

Kelsch, W., Hormuzdi, S., Straube, E., Lewen, A., Monyer, H. & Misgeld, U. (2001) Insulin-like growth factor 1 and a cytosolic tyrosine kinase activate chloride outward transport during maturation of hippocampal neurons. J. Neurosci., 21, 8339–8347.

Khazipov R, Congar P, Ben-Ari Y. (1995) Hippocampal CA1 lacunosum-moleculare interneurons: comparison of effects of anoxia on excitatory and inhibitory postsynaptic currents. J Neurophysiol. 74:2138-49.

Kilman V, van Rossum MC, Turrigiano GG. (2002) Activity deprivation reduces miniature IPSC amplitude by decreasing the number of postsynaptic GABA(A) receptors clustered at neocortical synapses. J Neurosci. 22:1328-37.

Kim G and Kandler K (2003) Functional elimination and strengthening of glycinergic/GABAergic connections during formation of a tonotopic map. Nature Neuroscience, 6:282-290.

Kim G and Kandler K (2006) Role of Cholinergic Feedback to Cochlea in Organizing an Inhibitory Sound Localization Circuit. Society for Neuroscience., (204.5) R

Kirsch J and Betz H. (1998) Glycine-receptor activation is required for receptor clustering in spinal neurons. Nature. 392: 717-720.

Kirsch J, Wolters I, Triller A, Betz H. (1993) Gephyrin antisense oligonucleotides prevent glycine receptor clustering in spinal neurons. Nature. 366:745-8.

Klausberger T, Magill PJ, Marton LF, Roberts JD, Cobden PM, Buzsaki G, Somogyi P. (2003) Brain-state- and cell-type-specific firing of hippocampal interneurons *in- vivo*. Nature. 421:844-8.

Kokaia Z, Kokaia M. (2001) Changes in GABA(B) receptor immunoreactivity after recurrent seizures in rats. Neurosci Lett. 315:85-8.

Kneussel M, Betz H. (2000) Clustering of inhibitory neurotransmitter receptors at developing postsynaptic sites: the membrane activation model. Trends Neurosci. 23:429-35.

Kneussel M, Brandstätter JH, Laube B, Stahl S, Müller U, Betz H. (1999) Loss of postsynaptic GABA(A) receptor clustering in gephyrin-deficient mice. J Neurosci. 19:9289-97.

Kneussel M, Loebrich S. (2007) Trafficking and synaptic anchoring of ionotropic inhibitory neurotransmitter receptors. Biol Cell. 99:297-309.

Koike-Tani M, Saitoh N, Takahashi T. (2005) Mechanisms underlying developmental speeding in AMPA-EPSC decay time at the calyx of Held. J Neurosci. 25:199-207.

Komatsu Y, Iwakiri M. (1991) Postnatal development of neuronal connections in cat visual cortex studied by intracellular recording in slice preparation. Brain Res. 540:14-24.

Komatsu Y, Iwakiri M. (1993) Long-term modification of inhibitory synaptic transmission in developing visual cortex. Neuroreport. 4:907-10.

Kotak VC, Korada S, Schwartz IR, Sanes DH. (1998) A developmental shift from GABAergic to glycinergic transmission in the central auditory system. J Neurosci. 18:4646-55.

Kotak VC, Sanes DH. (1995) Synaptically evoked prolonged depolarizations in the developing auditory system. J Neurophysiol. 74:1611-20.

Kotak VC, Sanes DH. (1996) Developmental influence of glycinergic transmission: regulation of NMDA receptor-mediated EPSPs. J Neurosci. 16:1836-43.

Kotak VC, Sanes DH. (2003) Gain adjustment of inhibitory synapses in the auditory system. Biol Cybern. 89:363-70.

Kriegstein AR, Owens DF. (2001) GABA may act as a self-limiting trophic factor at developing synapses. Sci STKE. 14:PE1.

Kullmann PHM, Ene F. Aura, and Kandler K (2002) Glycinergic and GABAergic calcium responses in the developing lateral superior olive. Europ. J. Neurosci. 15:1093-1104.

Kullmann PHM and Kandler K (2001) Glycinergic/GABAergic synapses in the lateral superior olive are excitatory in neonatal C57Bl/6J mice. Dev Brain Res. 131:143-147.

Kumar SS, Wen X, Yang Y, Buckmaster PS. (2006) GABAA receptor-mediated IPSCs and alpha1 subunit expression are not reduced in the substantia nigra pars reticulata of gerbils with inherited epilepsy. J Neurophysiol. 95:2446-55.

Kyrozis, A. & Reichling, D.B. (1995) Perforated-patch recording with gramicidin avoids artifactual changes in intracellular chloride concentration. J. Neurosci. Meth., 57, 27–35.

Lakso M, Sauer B, Mosinger B Jr, Lee EJ, Manning RW, Yu SH, Mulder KL, Westphal H. Targeted oncogene activation by site-specific recombination in transgenic mice. (1992) Proc Natl Acad Sci U S A. 89:6232-6.

Lee H, Chen CX, Liu YJ, Aizenman E, Kandler K. (2005) KCC2 expression in immature rat cortical neurons is sufficient to switch the polarity of GABA responses. Eur J Neurosci. 21:2593-9.

Leao RN, Oleskevich S, Sun H, Bautista M, Fyffe RE, Walmsley B. (2004) Differences in

glycinergic mIPSCs in the auditory brain stem of normal and congenitally deaf neonatal mice. J Neurophysiol. 91:1006-12.

Leinekugel X, Medina I, Khalilov I, Ben-Ari Y, Khazipov R. (1997) Ca2+ oscillations mediated by the synergistic excitatory actions of GABA(A) and NMDA receptors in the neonatal hippocampus. Neuron. 18:243-55.

Levi S, Chesnoy-Marchais D, Sieghart W, Triller A. (1999) Synaptic control of glycine and GABA(A) receptors and gephyrin expression in cultured motoneurons. J Neurosci. 19:7434-49.

Li H, Tornberg J, Kaila K, Airaksinen MS, Rivera C. (2002) Patterns of cation-chloride cotransporter expression during embryonic rodent CNS development. Eur J Neurosci. 16:2358-70.

Liao D, Zhang X, O'Brien R, Ehlers MD, Huganir RL. (1999) Regulation of morphological postsynaptic silent synapses in developing hippocampal neurons. Nat. Neurosci. 2: 37– 43

Lichtman JW, Colman H. (2000) Synapse elimination and indelible memory. Neuron. 25:269-78.

Lippe WR. (1994) Rhythmic spontaneous activity in the developing avian auditory system. J Neurosci. 14:1486-95.

Lissin DV, Carroll RC, Nicoll RA, Malenka RC, von Zastrow M. (1999) Rapid, activation-induced redistribution of ionotropic glutamate receptors in cultured hippocampal neurons. J Neurosci.19:1263-72.

Lissin DV, Gomperts SN, Carroll RC, Christine CW, Kalman D, et al. (1998) Activity differentially regulates the surface expression of synaptic AMPA and NMDA glutamate receptors. Proc. Natl. Acad. Sci. USA 95: 7097– 102

Llano I, Gonzalez J, Caputo C, Lai FA, Blayney LM, Tan YP, Marty A. (2000) Presynaptic

calcium stores underlie large-amplitude miniature IPSCs and spontaneous calcium transients. Nat Neurosci. 3:1256-65.

López-Bendito G, Shigemoto R, Kulik A, Vida I, Fairén A, Luján R. (2004) Distribution of metabotropic GABA receptor subunits GABAB1a/b and GABAB2 in the rat hippocampus during prenatal and postnatal development. Hippocampus. 14:836-48.

LoTurco, J.J., Owens, D.F., Heath, M.J.S., Davis, M.B.E. & Kriegstein, A.R. (1995) GABA and glutamate depolarize cortical progenitor cells and inhibit DNA synthesis. Neuron. 15:1287–1298.

Lu, J., Karadsheh, M. & Delpire, E. (1999) Developmental regulation of the neuronal-specific isoform of K-Cl cotransporter KCC2 in postnatal rat brains. J. Neurobiol., 39, 558–568.

Luhmann, H.J. & Prince, D.A. (1991) Postnatal maturation of the GABAergic system in rat neocortex. J. Neurophysiol., 65, 247–263.

Luk KC, Kennedy TE, Sadikot AF. (2003) Glutamate promotes proliferation of striatal neuronal progenitors by an NMDA receptor-mediated mechanism. J Neurosci. 23:2239-50.

Maas C, Tagnaouti N, Loebrich S, Behrend B, Lappe-Siefke C, Kneussel M. (2006) Neuronal cotransport of glycine receptor and the scaffold protein gephyrin. J Cell Biol. 172:441-51.

Maccaferri G, Roberts JD, Szucs P, Cottingham CA, Somogyi P. (2000) Cell surface domain specific postsynaptic currents evoked by identified GABAergic neurones in rat hippocampus *in-vitro*. J Physiol. 524 :91-116.

Maffei A, Nelson SB, Turrigiano GG. (2004) Selective reconfiguration of layer 4 visual cortical circuitry by visual deprivation. Nat Neurosci. 7:1353-9.

Maffei A, Nataraj K, Nelson SB, Turrigiano GG. (2006) Potentiation of cortical inhibition by visual deprivation. Nature. 443(7107):81-4.

Magnusson AK, Kapfer C, Grothe B, Koch U. (2005) Maturation of glycinergic inhibition in the gerbil medial superior olive after hearing onset. J Physiol. 568:497-512.

Malenka RC, Nicoll RA. (1993) NMDA-receptor-dependent synaptic plasticity: multiple forms and mechanisms. Trends Neurosci. 16:521-7.

Malitschek B, Rüegg D, Heid J, Kaupmann K, Bittiger H, Fröstl W, Bettler B, Kuhn R. (1998) Developmental changes of agonist affinity at GABABR1 receptor variants in rat brain. Mol Cell Neurosci. 12:56-64.

Maric D, Liu QY, Maric I, Chaudry S, Chang YH, Smith SV, Sieghart W, Fritschy JM, Barker JL. GABA expression dominates neuronal lineage progression in the embryonic rat neocortex and facilitates neurite outgrowth via GABA(A) autoreceptor/Cl- channels. (2001) J Neurosci. 21:2343-60

Marcotti W, Erven A, Johnson SL, Steel KP, Kros CJ. (2006) Tmc1 is necessary for normal functional maturation and survival of inner and outer hair cells in the mouse cochlea. J Physiol. 574:677-98.

Markram H, Toledo-Rodriguez M, Wang Y, Gupta A, Silberberg G, Wu C. (2004) Interneurons of the neocortical inhibitory system. Nat Rev Neurosci. 5:793-807.

Marty S, Berninger B, Carroll P, Thoenen H. (1996) GABAergic stimulation regulates the phenotype of hippocampal interneurons through the regulation of brain-derived neurotrophic factor. Neuron. 16:565-70.

Marty S, Wehrle R, Sotelo C. (2000) Neuronal activity and brain-derived neurotrophic factor regulate the density of inhibitory synapses in organotypic slice cultures of postnatal hippocampus. J Neurosci. 20:8087-95.

Marty S, Wehrle R, Fritschy JM, Sotelo C. (2004) Quantitative effects produced by modifications of neuronal activity on the size of GABAA receptor clusters in hippocampal slice cultures. Eur J Neurosci. 20:427-40.

McLean HA, Caillard O, Ben-Ari Y, Gaiarsa JL. (1996) Bidirectional plasticity expressed by GABAergic synapses in the neonatal rat hippocampus. J Physiol. 496:471-7.

Miles R, Toth K, Gulyas AI, Hajos N, Freund TF. (1996) Differences between somatic and dendritic inhibition in the hippocampus. Neuron. 16:815-23.

Morales B, Choi SY, Kirkwood A. (2002) Dark rearing alters the development of GABAergic transmission in visual cortex. J Neurosci. 22:8084-90.

Morishita W, Sastry BR. (1996) Postsynaptic mechanisms underlying long-term depression of GABAergic transmission in neurons of the deep cerebellar nuclei. J Neurophysiol. 76:59-68.

Nabekura J, Ueno T, Okabe A, Furuta A, Iwaki T, Shimizu-Okabe C, Fukuda A, Akaike N. (2002) Reduction of KCC2 expression and GABAA receptor-mediated excitation after *in- vivo* axonal injury. J Neurosci. 22:4412-7.

Nabekura J, Katsurabayashi S, Kakazu Y, Shibata S, Matsubara A, Jinno S, Mizoguchi Y, Sasaki A, Ishibashi H. (2004) Developmental switch from GABA to glycine release in single central synaptic terminals. Nat Neurosci. 7:17-23.

O'Brien RJ, Kamboj S, Ehlers MD, Rosen KR, Fischbach GD, Huganir RL. (1998) Activity-dependent modulation of synaptic AMPA receptor accumulation. Neuron 21: 1067– 78

Oleskevich S, Walmsley B. (2002) Synaptic transmission in the auditory brainstem of normal and congenitally deaf mice. J Physiol. 540:447-55.

Oleskevich, Youssoufian, Walmsley (2004) Presynaptic plasticity at two giant auditory synapses in normal and deaf mice. J Physiol. 560: 709–719.

Otis T, Zhang S, Trussell LO. (1996) Direct measurement of AMPA receptor desensitization induced by glutamatergic synaptic transmission. J Neurosci. 16:7496-504.

Ouardouz M, Sastry BR. (2000) Mechanisms underlying LTP of inhibitory synaptic transmission in the deep cerebellar nuclei. J Neurophysiol. 84:1414-21.

Owens, D.F., Boyce, L.H., Davis, M.B.E. & Kriegstein, A.R. (1996) Excitatory GABA responses in embryonic and neonatal cortical slices demonstrated by gramicidin perforated-patch recordings and calcium imaging. J. Neurosci., 16, 6414–6423.

Owens DF, Kriegstein AR. (2002) Is there more to GABA than synaptic inhibition? Nat Rev Neurosci. 3:715-27.

Pal S, Hartnett KA, Nerbonne JM, Levitan ES, Aizenman E. (2003) Mediation of neuronal apoptosis by Kv2.1-encoded potassium channels. J Neurosci. 23:4798-802.

Palma E, Amici M, Sobrero F, Spinelli G, Di Angelantonio S, Ragozzino D, Mascia A, Scoppetta C, Esposito V, Miledi R, Eusebi F. (2006) Anomalous levels of Cl- transporters in the hippocampal subiculum from temporal lobe epilepsy patients make GABA excitatory. Proc Natl Acad Sci U S A. May 30;103(22):8465-8.

Park SK, An SJ, Hwang IK, Kim DW, Jung JY, Won MH, Choi SY, Kwon OS, Jeong YG, Kang TC. (2004) Altered GABAB receptor immunoreactivity in the gerbil hippocampus induced by baclofen and phaclofen, not seizure activity. Neurosci Res. 49:405-16.

Payne, J.A., Stevenson, T.J. & Donaldson, L.F. (1996) Molecular characterization of a putative K-Cl cotransporter in rat brain. A neuronal-specific isoform. J. Biol. Chem., 271, 16245–16252.

Payne, J.A. (1997) Functional characterization of the neuronal-specific K-Cl cotransporter: implications for $[K^+]_o$ regulation. Am. J. Physiol., 273, C1516–C1525.

Payne JA, Rivera C, Voipio J, Kaila K. (2003) Cation-chloride co-transporters in neuronal communication, development and trauma.Trends Neurosci 26:199-206.

Platzer J, Engel J, Schrott-Fischer A, Stephan K, Bova S, Chen H, Zheng H, Striessnig J. (2000) Congenital deafness and sinoatrial node dysfunction in mice lacking class D L-type Ca2+ channels. Cell. 102:89-97.

Price GD, Trussell LO. (2006) Estimate of the chloride concentration in a central glutamatergic terminal: a gramicidin perforated-patch study on the calyx of Held. J Neurosci. 26:11432-6.

Pujol R, Shnerson A, Lenoir M, Deol MS. (1983) Early degeneration of sensory and ganglion cells in the inner ear of mice with uncomplicated genetic deafness (dn): preliminary observations. Hear Res. 12:57-63.

Ravindranathan A, Donevan SD, Sugden SG, Greig A, Rao MS, Parks TN. (2000) Contrasting molecular composition and channel properties of AMPA receptors on chick auditory and brainstem motor neurons. J Physiol. 523:667-84.

Renden R, Taschenberger H, Puente N, Rusakov DA, Duvoisin R, Wang LY, Lehre KP, von Gersdorff H. (2005) Glutamate transporter studies reveal the pruning of metabotropic glutamate receptors and absence of AMPA receptor desensitization at mature calyx of held synapses. J Neurosci. 25:8482-97

Represa A, Ben-Ari Y. (2005) Trophic actions of GABA on neuronal development. Trends Neurosci. Jun;28(6):278-83.

Rietzel HJ, Friauf E. (1998) Neuron types in the rat lateral superior olive and developmental changes in the complexity of their dendritic arbors. J Comp Neurol. 390:20-40.

Rivera, C., Voipio, J., Payne, J.A., Ruusuvuori, E., Lahtinen, H., Lamsa, K., Pirvola, U., Saarma, M. & Kaila, K. (1999) The K^+/Cl co-transporter KCC2 renders GABA hyperpolarizing during neuronal maturation. Nature, 397, 251–255.

Rivera C, Li H, Thomas-Crusells J, Lahtinen H, Viitanen T, Nanobashvili A, Kokaia Z, Airaksinen MS, Voipio J, Kaila K, Saarma M. (2002) BDNF-induced TrkB activation down-regulates the K+-Cl- cotransporter KCC2 and impairs neuronal Cl- extrusion. J Cell Biol. 159:747-52.

Rivera C, Voipio J, Thomas-Crusells J, Li H, Emri Z, Sipila S, Payne JA, Minichiello L, Saarma M, Kaila K. (2004) Mechanism of activity-dependent downregulation of the neuron-specific K-Cl cotransporter KCC2. J Neurosci. 24:4683-91.

Rutherford LC, DeWan A, Lauer HM, Turrigiano GG. (1997) Brain-derived neurotrophic factor mediates the activity-dependent regulation of inhibition in neocortical cultures. J Neurosci. 17:4527-35.

Sanes DH, Chokshi P. (1992) Glycinergic transmission influences the development of dendrite shape. Neuroreport. 3:323-6.

Sanes DH, Friauf E. (2000) Development and influence of inhibition in the lateral superior olivary nucleus. Hear Res. 147:46-58.

Sanes DH, Hafidi A. (1996) Glycinergic transmission regulates dendrite size in organotypic culture. J Neurobiol. 31:503-11.

Sanes DH, Siverls V (1991) Development and specificity of inhibitory terminal arborizations in the central nervous system. J Neurobiol. 22:837-54.

Sanes DH, Song J, Tyson J. (1992) Refinement of dendritic arbors along the tonotopic axis of the

gerbil lateral superior olive. Brain Res Dev Brain Res. 67:47-55.

Sanes DH, Takacs C. (1993) Activity-dependent refinement of inhibitory connections. Eur J Neurosci. 5:570-4.

Sauer B. (1993) Manipulation of transgenes by site-specific recombination: use of Cre recombinase. Methods Enzymol. 225:890-900.

Scanziani M, Capogna M, Gahwiler BH, Thompson SM. Presynaptic inhibition of miniature excitatory synaptic currents by baclofen and adenosine in the hippocampus. (1992) Neuron 9:919-27.

Scheetz AJ, Constantine-Paton M. (1994) Modulation of NMDA receptor function: implications for vertebrate neural development. FASEB J. 8:745-52.

Schneggenburger R, Forsythe ID. (2006) The calyx of Held. Cell Tissue Res. 326:311-37.

Schomberg, S.L., Bauer, J., Kintner, D.B., Su, G., Flemmer, A., Forbush, B. & Sun, D. (2003) Cross talk between the GABA(A) receptor and the Na-K-Cl cotransporter is mediated by intracellular Cl. J. Neurophysiol., 89: 159–167.

Seil FJ, Drake-Baumann R. (1994) Reduced cortical inhibitory synaptogenesis in organotypic cerebellar cultures developing in the absence of neuronal activity. J Comp Neurol. 342:366-77.

Seil FJ, Drake-Baumann R. (2000) TrkB receptor ligands promote activity-dependent inhibitory synaptogenesis. J Neurosci. 20:5367-73.

Sen A, Martinian L, Nikolic M, Walker MC, Thom M, Increased NKCC1 expression in refractory human epilepsy.Sisodiya SM. (2007) Epilepsy Res. 74:220-7.

Shi J, Aamodt SM, Townsend M, Constantine-Paton M. (2001) Developmental depression of glutamate neurotransmission by chronic low-level activation of NMDA receptors. J Neurosci. 21:6233-44.

Shi SH, Hayashi Y, Petralia RS, Zaman SH, Wenthold RJ, Svoboda K, Malinow R. (1999) Rapid spine delivery and redistribution of AMPA receptors after synaptic NMDA receptor activation. Science. 284:1811-6.

Shibata, S., Kakazu, Y., Okabe, A., Fukuda, A. & Nabekura, J. (2004) Experience-dependent changes in intracellular Cl regulation in developing auditory neurons. Neurosci. Res. 48: 211–220.

Simon DK, Prusky GT, O'Leary DD, Constantine-Paton M. (1992) N-methyl-D-aspartate receptor antagonists disrupt the formation of a mammalian neural map. Proc Natl Acad Sci U S A. 89:10593-7.

Shnerson A, Pujol R. (1981) Age-related changes in the C57BL/6J mouse cochlea. I. Physiological findings. Brain Res. 254:65-75.

Somogyi P, Klausberger T. (2005) Defined types of cortical interneurone structure space and spike timing in the hippocampus. J Physiol. 562: 9-26.

Song, L., Mercado, A., Vazquez, N., Xie, Q., Desai, R., George, A.L. Jr, Gamba, G. & Mount, D.B. (2002) Molecular, functional, and genomic characterization of human KCC2, the neuronal K-Cl cotransporter. Brain Res. Mol. Brain Res., 103, 91–105.

Spruston, N., Jaffe, D. B., Williams, S. H. & Johnston, D. (1993). Voltage- and space-clamp errors associated with the measurement of electrotonically remote synaptic events. Journal of Neurophysiology 70, 781-802

Staley K. (1994) The role of an inwardly rectifying chloride conductance in postsynaptic

inhibition. J Neurophysiol. 72:273-84.

Staley K, Smith R, Schaack J, Wilcox C, Jentsch TJ. (1996) Alteration of GABAA receptor function following gene transfer of the CLC-2 chloride channel. Neuron. 17:543-51.

Stein, V., Hermans-Borgmeyer, I., Jentsch, T.J. & Hubner, C.A. (2004) Expression of the KCl cotransporter KCC2 parallels neuronal maturation and the emergence of low intracellular chloride. J. Comp. Neurol., 468, 57–64.

Stellwagen D, Shatz CJ. (2002) An instructive role for retinal waves in the development of retinogeniculate connectivity. Neuron. 33: 357-67.

Straessle A, Loup F, Arabadzisz D, Ohning GV, Fritschy JM. (2003) Rapid and long-term alterations of hippocampal GABAB receptors in a mouse model of temporal lobe epilepsy. Eur J Neurosci. 18:2213-26.

Strange, K., Singer, T.D., Morrison, R. & Delpire, E. (2000) Dependence of KCC2 K-Cl cotransporter activity on a conserved carboxy terminus tyrosine residue. Am. J. Physiol. Cell Physiol., 279, C860–C867.

Sun, D. & Murali, S.G. (1998) Stimulation of Na^+-K^+-$2Cl^-$ cotransporter in neuronal cells by excitatory neurotransmitter glutamate. Am. J. Physiol., 275, C772–C779

Sun, D.D. & Murali, S.G. (1999) Na^+-K^+-2Cl(–) cotransporter in immature cortical neurons: a role in intracellular Cl regulation. J. Neurophysiol., 81, 1939–1948.

Swanwick CC, Murthy NR, Mtchedlishvili Z, Sieghart W, Kapur J. (2006) Development of gamma-aminobutyric acidergic synapses in cultured hippocampal neurons. J Comp Neurol. 495: 497-510.

Swartz, M.E., Eberhart, J., Pasquale, E.B. & Krull, C.E. (2001) EphA4/ephrin-A5 interactions in muscle precursor cell migration in the avian forelimb. Development, 128, 4669–4680.

Tabb JS, Kish PE, Van Dyke R, Ueda T (1992) Glutamate transport into synaptic vesicles. Roles of membrane potential, pH gradient, and intravesicular pH. J Biol Chem 267:15412–15418.

Tago H, Kimura H, Maeda T. (1986) Visualization of detailed acetylcholinesterase fiber and neuron staining in rat brain by a sensitive histochemical procedure. J Histochem Cytochem. 34:1431-8.

Takahashi T, Kajikawa Y, Tsujimoto T. (1998) G-Protein-coupled modulation of presynaptic calcium currents and transmitter release by a GABAB receptor. J Neurosci. 18:3138-46.

Takahashi T, Svoboda K, Malinow R. (2003) Experience strengthening transmission by driving AMPA receptors into synapses. Science. 299: 1585-8.

Taschenberger H, Leao RM, Rowland KC, Spirou GA, von Gersdorff H. (2002) Optimizing synaptic architecture and efficiency for high-frequency transmission. Neuron. 36: 1127-43

Taschenberger H, von Gersdorff H. (2000) Fine-tuning an auditory synapse for speed and fidelity: developmental changes in presynaptic waveform, EPSC kinetics, and synaptic plasticity. J Neurosci. 20:9162-73.

Tollin DJ (2003) The lateral superior olive: a functional role in sound source localization. Neuroscientist. 9: 127-143.

Toyoda H, Ohno K, Yamada J, Ikeda M, Okabe A, Sato K, Hashimoto K, Fukuda A. (2003) Induction of NMDA and GABAA receptor-mediated Ca2+ oscillations with KCC2 mRNA downregulation in injured facial motoneurons. J Neurophysiol. 89:1353-62.

Trussell LO, Zhang S, Raman IM. Desensitization of AMPA receptors upon multiquantal neurotransmitter release. (1993) Neuron. 10:1185-96.

Tsien JZ, Chen DF, Gerber D, Tom C, Mercer EH, Anderson DJ, Mayford M, Kandel ER, Tonegawa S. (1996) Subregion- and cell type-restricted gene knockout in mouse brain. Cell. 87:1317-1326.

Turecek, Trussell (2001) Presynaptic glycine receptors enhance transmitter release at a mammalian central synapse. Nature. 411: 587-590

Turner JG, Hughes LF, Caspary DM. (2005) Hear Res. 202:129-40. Divergent response properties of layer-V neurons in rat primary auditory cortex.

Turrigiano GG, Leslie KR, Desai NS, Rutherford LC, Nelson SB. (1998) Activity-dependent scaling of quantal amplitude in neocortical neurons. Nature 391: 892– 96

Turrigiano GG, Nelson SB. (2004) Homeostatic plasticity in the developing nervous system. Nat Rev Neurosci. 5:97-107.

Vale C, Sanes DH. (2002) The effect of bilateral deafness on excitatory and inhibitory synaptic strength in the inferior colliculus. Eur J Neurosci. 16:2394-404.

Vale C, Schoorlemmer J, Sanes DH. (2003) Deafness disrupts chloride transporter function and inhibitory synaptic transmission. J Neurosci. 23:7516-24.

Varoqui H, Schafer MK, Zhu H, Weihe E, Erickson JD. (2002) Identification of the differentiation-associated Na+/PI transporter as a novel vesicular glutamate transporter expressed in a distinct set of glutamatergic synapses. J Neurosci. 22:142-55.

Vetter DE, Liberman MC, Mann J, Barhanin J, Boulter J, Brown MC, Saffiote-Kolman J, Heinemann SF, Elgoyhen AB. (1999) Role of alpha9 nicotinic ACh receptor subunits in the development and function of cochlear efferent innervation. Neuron. 23:93-103

Vinas AM, Drury SS, DeAngelis MM, Den Z, Huang JM, Berlin CI, Hunt JD, Batzer MA, Deininger PL, Keats BJ. (1998) The mouse deafness locus (dn) is associated with an inversion on chromosome 19. Biochim Biophys Acta. 1407:257-62.

von Gersdorff H, Borst JG. (2002) Short-term plasticity at the calyx of held. Nat Rev Neurosci. 3:53-64.

von Gersdorff H, Schneggenburger R, Weis S, Neher E. (1997) Presynaptic depression at a calyx synapse: the small contribution of metabotropic glutamate receptors. J Neurosci. 17:8137-46.

Vu TQ, Payne JA, Copenhagen DR. (2000) Localization and developmental expression patterns of the neuronal K-Cl cotransporter (KCC2) in the rat retina. J Neurosci. 20:1414-23

Walsh EJ, McGee J, McFadden SL, Liberman MC. (1998) Long-term effects of sectioning the olivocochlear bundle in neonatal cats. J Neurosci. 18:3859-69.

Wardle RA, Poo MM. (2003) Brain-derived neurotrophic factor modulation of GABAergic synapses by postsynaptic regulation of chloride transport. J Neurosci. 23:8722-32.

Williams, J.R., Sharp, J.W., Kumari, V.G., Wilson, M. & Payne, J.A. (1999) The neuron-specific K-Cl cotransporter, KCC2. Antibody development and initial characterization of the protein. J. Biol. Chem., 274, 12656–12664.

Wolff JR, Joo F, Dames W. (1978) Plasticity in dendrites shown by continuous GABA administration in superior cervical ganglion of adult rat. Nature. 274:72-4.

Wong AY, Graham BP, Billups B, Forsythe ID. (2003) Distinguishing between presynaptic and postsynaptic mechanisms of short-term depression during action potential trains. J Neurosci. 23:4868-77.

Woo, N.S., Lu, J., England, R., McClellan, R., Dufour, S., Mount, D.B., Deutch, A.Y., Lovinger, D.M. & Delpire, E. (2002) Hyperexcitability and epilepsy associated with disruption of the mouse neuronal-specific K-Cl cotransporter gene. Hippocampus, 12, 258–268.

Woodin, M.A., Ganguly, K. & Poo, M.M. (2003) Coincident pre- and postsynaptic activity modifies GABAergic synapses by postsynaptic changes in Cl transporter activity. Neuron, 39, 807–820.

Wu SH, Kelly JB. (1993) Response of neurons in the lateral superior olive and medial nucleus of the trapezoid body to repetitive stimulation: intracellular and extracellular recordings from mouse brain slice. Hear Res. 68:189-201.

Youssoufian M, Oleskevich S, Walmsley B. (2005) Development of a robust central auditory synapse in congenital deafness. J Neurophysiol. 94:3168-80.

Yuste, R. & Katz, L.C. (1991) Control of postsynaptic Ca^{2+} influx in developing neocortex by excitatory and inhibitory neurotransmitters. Neuron, 6, 333–344.

Zhou N, Parks TN. (1992) Developmental changes in the effects of drugs acting at NMDA or non-NMDA receptors on synaptic transmission in the chick cochlear nucleus (nuc. magnocellularis). Brain Res Dev Brain Res. 67:145-52.

Zhu, L., Lovinger, D. & Delpire, E. (2004) Cortical neurons lacking KCC2 expression show impaired regulation of intracellular chloride. J. Neurophysiol., 93, 1557–1568.